TOWARDS A MINIMUM INPUT BIODYNAMIC MODEL
OF MULTI-FINGERED HAND MOVEMENTS

BY

KANG LI

B. Eng., Tsinghua University, 1999
M.S., Mississippi State University, 2004

DISSERTATION

Submitted in partial fulfillment of the requirements
for the degree of Doctor of Philosophy in Mechanical Engineering
in the Graduate College of the
University of Illinois at Urbana-Champaign, 2009

Urbana, Illinois

Doctoral Committee:

Associate Professor Xudong Zhang, Chair
Assistant Professor Xin Chen
Professor Placid Ferreira
Assistant Professor Prashant Mehta
Associate Professor Vincent Duffy, Purdue University

UMI Number: 3363017

INFORMATION TO USERS

The quality of this reproduction is dependent upon the quality of the copy
submitted.   Broken or indistinct print, colored or poor quality illustrations
and photographs, print bleed-through, substandard margins, and improper
alignment can adversely affect reproduction.
In the unlikely event that the author did not send a complete manuscript
and there are missing pages, these will be noted.   Also, if unauthorized
copyright material had to be removed, a note will indicate the deletion.

UMI®

ABSTRACT

This dissertation work centers on the development of a minimum-input biodynamical model for multi-fingered hand movements. It consists of three coherent, progressively more in-depth studies.

The first study proposes a two-stage computational framework for bio-dynamic modeling of human movement. The framework decouples the conventional forward dynamic modeling process into two stages: in the first stage, two-component "agonist-antagonist" torque actuators under testable parametric control drive the forward dynamics, and the parameters are identified by an optimization-based procedure of tracking both kinematics and kinetics; the second stage completes the mapping from the muscle-tendon forces to the predicted joint torques. An empirical test using multi-finger grasping movement data demonstrates that the proposed framework allows the measured kinematics and kinetics to be faithfully and efficiently reproduced.

In the second study, the above modeling framework is applied to a hypothesis-driven comparative analysis of two different multi-fingered hand movements: cylinder-grasping and individuated flexion of the index finger ('enslaving'). The hypothesis is that a common underlying mechanism is used to control the two different multi-fingered movements. This hypothesis is supported by the findings that the two types of movement can be reproduced by the same biodynamic model with a unified control mechanism and that the numbers of invariants remain consistent in the joint and muscle-tendon dynamics. The results also show that the number of invariants in the joint dynamics is smaller than that in the muscle-tendon dynamics and the mean correlation coefficient in the joint dynamics is larger than that in the muscle-tendon dynamics, suggesting hierarchical sources for dimensionality reduction. This study thus provides evidence to support the notion that different hyper-redundant multi-fingered movement acts can be controlled by a reduced number of input commands through a common architecture.

The third study investigates the effect of the model parameter variability on the muscle-tendon force coordination and clarifies the roles of the flexors in finger movement production and control. The premise is that accommodating variability of

musculoskeletal parameters in the model would result in better population-based predictions of the muscle-tendon forces and unravel more invariant relationships in these forces. A probabilistic biodynamic model is constructed to estimate the muscle-tendon forces and shows that both flexors of the index finger contribute to sustaining the movement and the flexor digitorum superficialis (FDS) muscle is not necessarily silent. The findings, contrary to what previous deterministic models have shown but in agreement with experimental measurements, clarify the controversy surrounding the roles of the flexors in finger movement dynamics.

Taken together, these studies build a unique biomechanical science foundation for a minimum-input biodynamical model that identifies important applications, including design of next-generation hand prostheses or hand rehabilitation strategies, and advancement of digital human simulation and virtual reality technologies.

ACKNOWLEDGMENTS

This work would not have been done without the support of many people. First, I would like to convey the respect and thanks to my advisors, Dr. Xudong Zhang, for his endless support and invaluable guidance during the past four years. I would also like to thank the other members of my dissertation committee, Professor Xin Chen, Placid Ferreira, Prashant Mehta and Vincent Duffy, for serving on my committee and providing helpful comments. I must thank my colleague, Sang-Wook Lee, for sharing his valuable preliminary work with me. Thanks to the many fellow students who conducted the early experiments and contributed to my research.

Finally, thanks to my wife for lighting up my life with love and support during the long journey towards the completion of the dissertation.

TABLE OF CONTENTS

LIST OF FIGURES

LIST OF TABLES

CHAPTER I

INTRODUCTION

1.1 Significance and Research Objectives

Dexterity of the human hand is a fundamental attribute that enables one to touch, press, or manipulate objects, and to convey gestic information. It is afforded by coordinated movements of a complex and redundant biomechanical system consisting of 27 bones, 39 muscles, and over 30 degrees of freedom (DOF's), possessed mostly by the fingers (Tubiana, 1981). The fingers or digits are so vital that amputation at the metacarpophalangeal (MCP) joint is considered to be 54% impairment of an entire person (Engelberg, 1988). The number of possible motion combinations that can be created by the hand biomechanical system is overwhelming. For example, merely considering the sign of the motion (e.g., +flexion/-extension) at each of the DOF's embedded in the hand would yield millions of possibilities (Soechting and Flanders, 1997). Yet, normal individuals are able to control this complex system, with amazing ease and efficiency, in producing a vast array of deft, purposeful, and concerted hand movement acts.

The complexity concomitant of the dexterity of hand biomechanical system presents a paradox in several frontiers of biomedical engineering research and application. First is the new emerging area of digital human simulation which identifies clinical applications such as computer-assisted or virtual-reality-based surgeries. Computer simulations embedded with biologically realistic musculoskeletal representations can assist in orthopedic surgeries, particularly in the design and planning stage, by visualizing the biomechanical consequences of bone reconstruction, joint replacement, or muscle-tendon reattachment (Delp and Loan, 2000). The complexity associated with neuromusculoskeletal biodynamic modeling has been the greatest impediment in the quest for realistic ("human-like") and computationally efficient ("real-time") simulations—an inherent trade-off between physical realism and computational efficiency is hard to overcome. Naturalistic hand motion simulation models featuring a reasonable level of dexterity are currently lacking. In the meantime, however, hand-related neurological or musculoskeletal disorders (e.g., carpal tunnel syndrome) are increasingly prevalent and becoming a major source of disability and morbidity.

Second is the area of hand neuro-prosthetics. It was estimated in a 1996 report

(LePlante and Carlson, 1996) that there were more than a hundred thousand people with upper extremity amputations in US alone. The number has been growing, and significantly more rapidly since the war in Iraq began. Hand prosthesis researchers face the dilemma of coping with two conflicting goals: to maximize the functional restoration—more DOF's, more prehensile patterns for artificial hands, and at the same time to minimize or strategically simplify the control with limited residual neuron- or myo-electrical signal sources (Weir, 2003). While considerable progress has been made in multifunctional hand prosthetic mechanism design, still missing is an effective and efficient control strategy that can orchestrate multiple DOF's to produce dexterous and naturalistic finger movements (Weir, 2003; Afshar and Matsuoka, 2004; Pylatiuk et al., 2004). A third area where a similar challenge persists is the development of exoskeletons and robots resembling or compatible with hand movements for functional rehabilitation or augmentation. To use a minimum set of actuators or input commands to produce reasonably realistic hand/finger movements remains a tantalizing goal for research and device development.

One of the most fundamental problems underlying the challenge is the lack of a model that not only represents the complex hand biodynamic system but also emulates naturalistic multi-finger movement control in a computationally efficient manner. Such a model can be readily implemented as biomimetic control algorithms for devices that restore or augment hand function, and can serve as the computational engine that drives digital simulation of human movement. It may also be translated in guidelines for improved, more targeted muscle-tendon therapy in hand rehabilitation.

Therefore, the dissertation seeks to pursue two general scientific objectives: (1) to develop a biodynamic model capable of simulating multi-finger movements in a naturalistic and computationally viable manner; and (2) from data-supported model testing, to gain quantitative understanding of the dynamic coordination and coupling mechanisms that enable efficient production and control of multi-fingered hand movements.

These objectives are embodied by the following specific aims:

1) To develop a multi-finger biodynamic model that is biomechanically realistic, computationally viable, and amenable to empirical test at the system, joint, and musculo-tendon levels.

We propose a novel two-stage modeling framework: (1) a parametric-controlled torque-driven forward dynamic modeling stage amenable to hypothesis testing, and (2) a musculo-tendon force to joint torque mapping stage. The framework has an open architecture to facilitate exploring different hypothesized control strategies in search for one resulting in model-prediction best matching experimental data both kinematically and kinetically. The model is tested using an established normative database of grasping movement and is validated with the existing muscle-tendon force data available in the literature.

2) To apply the above modeling framework to examine the coordination and coupling mechanisms (the "invariants") underlying two functionally distinct multi-fingered hand movements.

We compare two different types of multi-fingered hand movement, functionally less variant (across fingers) grasping and more variant 'enslaving' movements based on an experimental database. We analyze the model-based solutions at the system, joint, and muscle-tendon levels, and identify and quantify the invariants

3) To develop a probabilistic model mapping the muscle/tendon forces to joint torque and kinematics profiles and incorporating stochasticity in musculo-tendon geometry to advance our understanding of muscle-tendon force in the finger movement and control.

We propose a probabilistic biodynamic model to predict the muscle-tendon forces during index finger flexions. We incorporate stochasticity into musculoskeletal parameters of a biodynamical model, and use a Monte-Carlo method to capture the variability of model parameters such as physiological cross sectional areas (PCSA), moment arms, passive torques, and anthropometrical measures by replacing the "average" representations with probabilistic distributions. We analyze the population-based predictions of the flexor forces and achieve better understanding of the role of flexors during the finger movement.

3

1.2 Thesis Organization

This dissertation consists of five chapters including three full-length manuscripts (Chapters II-IV) along with this introductory chapter and a concluding chapter. The three manuscripts present three coherent, progressively more in-depth studies.

Chapter II addresses the first specific aim and presents the development and validation of a computational framework for bio-dynamic modeling of human movement and its application to multi-fingered hand movement. Chapter III addresses the second specific aim. It presents a hypothesis-driven comparative analysis of two different multi-fingered hand movements: cylinder-grasping and individuated flexion of the index finger ('enslaving'), based on the modeling framework presented in Chapter II. We analyze the inter-digit dynamic couplings and coordination patterns across digits 2-5 from three levels: system control, joint and muscle-tendon dynamics. Chapter IV addresses the last specific aim. It describes a probabilistic biodynamic model for estimating the muscle-tendon forces and elucidating the roles of the flexors in finger movement production and control. Finally, Chapter V concludes the dissertation by summarizing the main contributions made by this work and recommending a few directions for future research.

1.3 References

Afshar, P., Matsuoka, Y., 2004. Neural-based control of a robotic hand: evidence for distinct muscle strategies. In the IEEE International Conference on Robotics and Automation.

Delp, S.L., Loan, J.P., 2000. A computational framework for simulating and analyzing human and animal movement. Computing in Science & Engineering 2, 46-55.

Engelberg, A.L. (1988). Guides to the evaluation of permanent impairment (3rd ed.). Chicago, IL: American Medical Association.

LePlante, M.P., Carlson, D. (1996). Disability in the United States: Prevalence and Causes, 1992. Disability Statistics Report (7): National Institute on Disability and Rehabilitation Research, US Department of Education.

Pylatiuk, C., Mounier, S., Kargov, A., Schulz, S., Bretthauer, G., 2004. Progress in the development of a multifunctional hand prosthesis. In 26th Annual International Conference of the IEEE Engineering in Medicine and Biology Society, 2004. , San Francisco, CA, USA.

Soechting, J.F., Flanders, M., 1997. Flexibility and repeatability of finger movements during typing: Analysis of multiple degrees of freedom. Journal of Computational Neuroscience 4, 29-46.

Tubiana, R. (1981). The Hand. Philadelphia: Saunders.

Weir, R.F., 2003. The great divide - the human-machine interface: Issues in the control of prostheses, manipulators, and other human machine systems. In IEEE 29th Annual Northeast Bioengineering Conference.

CHAPTER II
A NOVEL TWO-STAGE FRAMEWORK FOR MUSCULOSKELETAL DYNAMIC MODELING: AN APPLICATION TO MULTI-FINGERED HAND MOVEMENT

2.1 Abstract

In this chapter, we present a new computational framework for bio-dynamic modeling of human movement. The framework decouples the conventional dynamic modeling process into two stages: in the first stage, two-component "agonist-antagonist" torque actuators under hypothesized and testable parametric control drive the forward dynamics, and parameters are identified by tracking both kinematics and kinetics; the second stage completes the mapping from the muscle-tendon forces to the predicted joint torques. An empirical test using multi-finger grasping movement data was conducted to illustrate the application of the proposed framework, and showed that the model reproduced the measurement accurately in both kinematics and kinetics. The torque components exhibited consistent spatial-temporal patterns across joints, digits, and subjects. The muscle-tendon forces computed based on the model-predicted kinematics and kinetics had the peak values within the same order of magnitude as in vivo data reported in the literature. The potential to predict was also demonstrated as we applied the control parameters of one subject to another and achieved close matches.

2.2 Introduction

Biodynamic models are powerful means for describing the production, control, and consequences of a biological movement. Numerous models have been created to study, explain, or predict various phenomena associated with human movements (cf. review by (Erdemir et al., 2007)). These models have provided valuable insights into the causal-effect relationships between external factors, internal mechanisms of the neuro-musculo-skeletal system and outcomes of human movements at different levels. They also have transformed conventional applications and enabled emerging applications such as rehabilitation (Karlsson and Peterson, 1992; Happee, 1994; Neptune, 2000; Shelburne and Pandy, 2002; Raikova et al., 2005; Tanaka et al., 2007), product design (Rasmussen

et al., 2002; Lin et al., 2004; Chang and Wang, 2007), computer-assisted surgeries (Delp and Loan, 2000; Blemker et al., 2007), and ergonomics (Zhang, 2001).

Despite its overall success as a tool for studying the neuromusculoskeletal system, biodynamic modeling has been plagued by two major limitations. One major limitation is the inherent trade-off between model level of detail and computational tractability (Zhang and Chaffin, 2006). The human musculoskeletal system possesses more number of degrees of freedom (DOF) than what is mechanically necessary to produce a movement and more number of muscles than number of degrees of freedom being activated. The system is also highly nonlinear and often time-dependent. While simple biomechanical models may not provide adequate accuracy and sufficient insight for many of the contemporary applications, the three characteristics of a musculoskeletal dynamic system—redundancy, high nonlinearity, and time-dependence—can translate into significant computational complexity in modeling a system with even a modest level of realism. As a model evolves from oversimplified to realistic, static to dynamic, small to large scale, the variables involved in the modeling multiply, and the associated computational complexity increases exponentially—this is referred to as the 'curse of dimensionality' (Bellman, 1957). The complexity has been the greatest impediment in generating models and simulations that are both computationally efficient and biomechanically realistic. For example, it took 3.5 hours of CPU time to complete a 3-second arm motion simulation for a dynamic model consisting of 5 DOFs and 30 muscles (Yamaguchi et al., 1995),. Anderson and Pandy (Anderson and Pandy, 2001a) showed that simulation of a single gait cycle cost about 10,000 hours of CPU time to converge a solution using a human walking model that possessed 23 DOFs and 54 muscles and 810 control variables. More recent studies (Menegaldo et al., 2003; 2006) showed that simulation of raising-up movements using a 3-link planar model with 10 equivalent muscles/tendons may take 2-14 days. Such tremendous computational cost hampers the use of these models in applications requiring real-time movement animation or in model-based human movement studies involving a sizable subject pool. Use of parametric stereotyped control strategies along with torque-driven forward dynamics (Lee and Zhang, 2007) has demonstrated some promise for computationally more tractable simulation but at the expense of muscular details and insights. It appears that both stereotyped, testable

7

control strategies and anatomical details have to be incorporated into a model in order to achieve computational viability and realism in system as well as musculo-tendon dynamics.

Another major limitation is the difficulty to reconcile the inverse and forward solutions. The traditional approaches to biodynamic modeling of human movement can be classified as an inverse and a forward dynamics approach. A forward dynamics or forward solution model arguably represents the real sequence of events in movement production: from a task goal, to a varying neural drive, to muscle forces, to time-varying joint torques, to the acceleration (or deceleration) of the body segments, and then to movement (Winter, 1990). An inverse dynamics approach works in a reverse logic: it starts from observed movement kinematics, such as position, velocity and acceleration of body segments, to joint kinetics (torque, muscle forces), to neural signal or control. Although in theory both are able to estimate the intermediate state variables (e.g., joint kinetics) during movements (Zajac et al., 2002; 2003), solutions from the two approaches may depart from each other considerably (Lim et al., 2003; Buchanan et al., 2005; Menegaldo et al., 2006). Ideally, given the inverse solutions as the input of a forward simulation, the output should replicate the input of the inverse solution. Such, nevertheless, is often not the case. For example, it was shown that for a perfect inverted pendulum model, using the calculated moments from an inverse solution as input in a forward simulation without any correction usually does not result in the observed kinematics (Risher et al., 1997)—a phenomenon called inverse dynamics simulation failure (Zajac, 1993).

The difference between inverse and forward solutions therefore provokes a challenge in modeling or model-based analysis: which solution should be used? The difference, and not knowing there is a difference, could lead to divergence in interpreting the observables and understanding the underlying mechanisms. For example, Prilutsky (Prilutsky, 2000) suggested that muscle coordination features could be predicted by minimizing muscle fatigue based on the inverse dynamics approach, which is contrary to the result from the forward dynamics approach (Kautz et al., 2000). Therefore, a unifying musculoskeletal dynamic modeling framework to provide reconciled inverse and forward solutions would be critical for gaining more complete and accurate

understanding of human movement.

In this work, we propose a two-stage computational framework for bio-dynamic modeling of human movement in an attempt to alleviate or even circumvent the above described two major limitations. The framework is designed to be capable of reproducing realistic multi-joint movements while avoiding solving at once a multi-input-multi-out forward dynamics problem embedded with both kinematics redundancy (Gielen et al., 1995) and muscle redundancy (Prilutsky and Zatsiorsky, 2002). We use the modeling of multi-fingered hand movement to illustrate the application of the proposed framework. To our knowledge, no true forward dynamic model exists that can predict both kinetics and kinematics accurately.

The remainder of the chapter is organized as follows: Section II describes the general concept and structure of the two-stage modeling framework, followed by an illustrative application to the modeling of multi-fingered hand movement. In Section III, the results from the application as an empirical test of the framework are presented. Section IV recapitulates and discusses the merits of proposed framework, and analyzes the limitations of our work. Section V ends with some concluding remarks.

2.3 Methods

A. The two-stage modeling framework
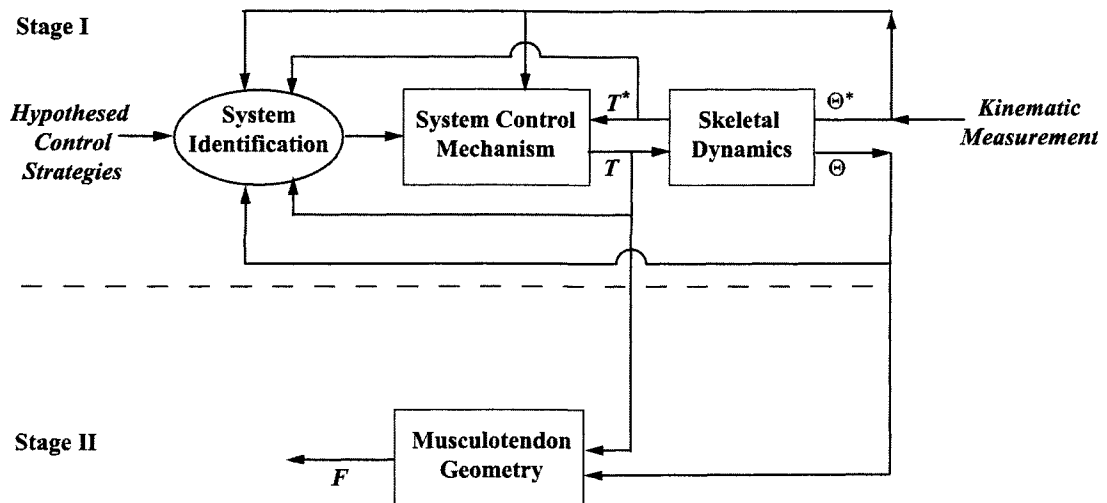
Fig. 2.1 The proposed two-stage biodynamical modeling framework. In Stage I, a control strategy is hypothesized, which once parameterized forms the system control

9

mechanism. A system identification process determines the control parameters such that the forward-simulated kinematics and kinetics best match the measured kinematics (θ^*) and measurement-derived torque (T^*). In Stage II, the muscle-tendon forces (F) are determined from the predicted torques (T), the process of which is modulated by the movement-dependent musculotendon geometry.

Fig. 2.1 illustrates the proposed two-stage modeling framework. In the first stage, a biodynamic system is modeled without the muscle-tendon components. Torque-driven forward dynamics and system identification are blended to achieve computational tractability and efficiency. A stereotyped control strategy in parametric form is first hypothesized, which controls the joint torque actuation. The controlled torques (T) drive the skeletal dynamics such that not only the predicted kinematics best match the measured ($\theta^*, \dot{\theta}^*$) but the inversely measurement-derived torques (T^*) would also be in close agreement with the controlled. The system identification to ascertain the control parameters resulting in the best matches in kinetics and kinematics is also a process of testing a hypothesis: whether the model can track the measured kinetics and kinematics accurately is indicative of the validity or plausibility of a strategy. In the second stage, the mapping from muscle-tendon forces to the joint torques is accomplished. Typically, a muscle redundancy problem is inherent in this stage: there are an infinite number of muscle-tendon force combinations that can produce the same joint torque. Optimization with various forms of cost function or performance criterion, depending on the nature or the goal of a movement (Seireg and Arvikar, 1975; Dul et al., 1984; van der Helm, 1994; Brook et al., 1995), can be used to solve the redundancy.

By decoupling the entire dynamic modeling process into two stages, the proposed framework decomposes an otherwise computationally costly or even intractable problem into two simpler problems while ensuring the key intermediate connecting variables (here the joint torques) are trustworthy. Solutions to the two problems can render forward dynamic simulation efficiently and preserve the details and possible insights at the musculo-tendon junction. In addition, the proposed framework offers an open architecture allowing various hypotheses to be formulated and tested at the motor control

level as well as the musculo-tendon force level.

B. Stage I: parametric-controlled torque-driven forward dynamic modeling

The dynamics of a general 3-segment, 3-DOF linkage system without considering gravity at time t can be represented by the following equations of motion:

$$M(\theta(t))\ddot{\theta}(t) = V(\theta(t),\dot{\theta}(t)) + \tau(t), \tag{2.1}$$

where $\theta(t) \in \Re^{3\times1}$, $\dot{\theta}(t) \in \Re^{3\times1}, \ddot{\theta}(t) \in \Re^{3\times1}$ are the angle, angular velocity, and angular acceleration vectors, $M(\theta(t)) \in \Re^{3\times3}$ is a positive definite mass matrix, $V(\theta(t),\dot{\theta}(t)) \in \Re^{3\times1}$ is the centrifugal (square of joint velocity) and Coriolis force, $\tau(t) \in \Re^{3\times1}$ is the torque vector at the joints. In the first stage of our modeling framework, we hypothesize that the torque actuator of each joint has two components: one component $\tau_{flexor}(t)$ represents the flexor action and the other $\tau_{extensor}(t)$ represents the extensor action at time t. Both torque actuators are controlled by proportional-derivative (PD) controllers and modulated by distribution functions that emulate muscle contractile mechanics. This novel stereotyped control scheme can be described by the following equations.

$$\tau(t) = \tau_{flexor}(t) + \tau_{extensor}(t) \tag{2.2}$$

$$\tau_{flexor}(t) = -q(t)[K^p_{flexor}\Delta\theta(t) + K^d_{flexor}\Delta\dot{\theta}(t)] \tag{2.3}$$

$$\tau_{extensor}(t) = -s(t)[K^p_{extensor}\Delta\theta(t) + K^d_{extensor}\Delta\dot{\theta}(t)] \tag{2.4}$$

$$q(t) = 1.0 - (1.0 - \alpha_q t + \frac{\alpha_q}{2}t^2)e^{-\alpha_q t} \tag{2.5}$$

$$s(t) = \frac{s_0}{B(\beta_s,1)}t^{\beta_s-1} = \frac{s_0}{\int_0^1 t^{\beta_s-1}dt}t^{\beta_s-1} \tag{2.6}$$

where $\Delta\theta(t) \in \Re^{3\times1}, \Delta\dot{\theta}(t) \in \Re^{3\times1}$ are the angle and angular velocity differences between current time t and the ending time t_{end}; $K^p_{flexor} \in \Re^{3\times1}$, $K^p_{extensor} \in \Re^{3\times1}$, and $K^d_{flexor} \in \Re^{3\times1}$, $K^d_{extensor} \in \Re^{3\times1}$ are the associated proportional and derivative gains; $q(t)$ is a gamma distribution function; $s(t)$ is a beta distribution function; α_q is the scale factor of the gamma distribution, and β_s is the shape parameter of the beta distribution function. Note that the parameters, $K^p_{flexor}, K^p_{extensor}$, K^d_{flexor}, $K^d_{extensor}$, α_q, and β_s are time-

11

independent.

The hypothesized two-component torque actuator originated from the observation that the agonist and antagonist muscles exhibit different spatial-temporal patterns as recorded by electromyography (EMG) during single-joint movements (Hallett et al., 1975; Hallett and Marsden, 1979; Hannaford and Stark, 1985; Schmidt et al., 1988; Sherwood et al., 1988; Almeida et al., 1995; Gottlieb, 1998; Irlbacher et al., 2006). It has been found that the EMG activity of single-joint movements consists of two or three phases. The first one is the initial agonist burst, which starts the movement and accelerates the segment towards its target position. During this phase, the EMG activity of agonist muscles first increases quickly. After reaching its peak, it decreases gradually. The second phase is the antagonist burst, which decelerates the segment. In this phase, the EMG activity of antagonist muscles exhibits similar envelop as that of agonist muscles in the first phase but has a delay of several hundred milliseconds, referred to as the antagonist latency (Gottlieb et al., 1989). A possible third phase is the second agonist burst, which could prevent possible oscillations of the segment and lock it on the target, which may not be observable in all single-joint movements. The pattern of EMG activities usually has the best correlation with the generation of muscle torques (Lacquaniti and Soechting, 1986; Marconi et al., 2006), supporting the use of an EMG-pattern-based torque-driven model to produce human movements. Our two-component 'agonist-antagonist' torque actuators are intended to capture the bi-phasic muscle co-contraction dynamics. The antagonist latency was implemented using two distribution functions with different temporal characteristics. By doing so, smooth net torque profile can be obtained since the onsets of the two torque components can be chosen as the same, and two torque actuators can be set to start simultaneously. These two distributions are also effective in simulating the kinetics profile during initial stage of the joint movement. The function of the second agonist burst—that is, to decelerate the motion, is jointly implemented by the flexor and extensor torque components.

With the proposed control scheme, an optimization problem to identify the system parameters by tracking both kinematics and kinetics can be formulated as follows:

$$\underset{\{K^p_{flexor}, K^d_{flexor}, K^p_{extensor}, K^d_{extensor}, \alpha_p, \beta_s\}}{\text{minimize}} \quad \int_0^{t_{max}} (\theta(t) - \theta^*(t))^2 \, dt \tag{2.7}$$

12

subject to
$$M(\theta(t))\ddot{\theta}(t) = V(\theta(t),\dot{\theta}(t)) + \tau(t)$$

$$\tau(t) = \tau_{\text{flexor}}(t) + \tau_{\text{extensor}}(t)$$

$$\tau_{\text{flexor}}(t) = -q(t)[K^p_{\text{flexor}}\Delta\theta(t) + K^d_{\text{flexor}}\Delta\dot{\theta}(t)]$$

$$\tau_{\text{extensor}}(t) = -s(t)[K^p_{\text{extensor}}\Delta\theta(t) + K^d_{\text{extensor}}\Delta\dot{\theta}(t)]$$

$$\frac{\dfrac{1}{t_{\max}}\displaystyle\int_0^{t_{max}} (\tau(t)-\tau^*(t))^2\, dt}{\dfrac{1}{t_{\max}}\displaystyle\int_0^{t_{max}} (\tau^*(t))^2\, dt} < tol$$

where $\theta(t)$, $\dot{\theta}(t)$, and $\ddot{\theta}(t)$ are the model-predicted angle, angular velocity, and angular acceleration vector at time t; $\theta^*(t)$ is the measured kinematics; $\tau(t)$ is the torque vector at time t; and $\tau_{\text{flexor}}(t)$, $\tau_{\text{extensor}}(t)$ are the flexor and extensor torque components; $\tau^*(t)$ is the torque derived using inverse dynamics at time t; tol is the tolerance expressed as the normalized mean-square difference between measured and model-predicted torque profiles.

C. Stage II: mapping of muscle-tendon forces to joint torques

Once the joint torque $\tau(t)$ at time t is known and ensured to be physiologically realistic, the muscle force can be estimated as follows. Assume that n muscles are involved in the movement of the 3-segment 3-DOF system, the moment arm values at time t is $M(t) = \left[m_{jk}(t)\right] \in \Re^{3 \times n}$ where $m_{jk}(t)$ is moment arm of muscle/tendon force k with respect to joint j at time t, the moment equilibrium conditions can be described by the equation:

$$\tau(t) = M(t) \cdot F(t) \tag{2.8}$$

where $F(t) = [F_k] \in \Re^{n \times 1}$ is muscle-tendon force vector at time t and F_k is a muscle-tendon force. For each time point, usually the number of muscles is greater than the number of equations, or number of degrees of freedom to be activated, which is referred to as muscle redundancy. This muscle redundancy problem can be solved using linear or nonlinear optimization techniques by minimizing an objective function $J(F(t))$ (Erdemir et al., 2007), which, depending on the nature or the goal of a movement, could be muscle force, muscle stress, intensity-compression, muscle activation, and etc. A

general formulation is as follows.

minimize $\quad\quad\quad\quad\quad J(F(t))$ $\quad\quad\quad\quad\quad\quad\quad\quad\quad\quad\quad\quad\quad$ (2.9)

subject to $\quad\quad\quad\quad\quad M(t) \cdot F(t) = \tau(t)$

$$F_{min} \leq F(t) \leq F_{max}$$

$$g(F(t), \theta(t)) = 0$$

$$h(F(t), \theta(t)) \leq 0$$

where F_{max} and F_{min} are the maximum and minim um physiological forces; g and h are the additional constraints depending on the anatomical structure of the joint under investigation and/or the muscle dynamics.

D. An application to modeling of multi-fingered hand movement

The above modeling framework was tested by applying it to multi-finger grasp movement data. Data for 19 trials performed by 19 subjects were selected from a database previously established in our laboratory. One major selection criterion was that the movement must be 'well-coordinated', as characterized by the bell-shaped joint velocity and double-peaked joint acceleration profiles. These trials satisfied this criterion without significant missing data (due to surface marker drop-outs in measurement) were used to test this modeling framework. The multi-finger kinematics were measured and derived using a well-published experimental and processing protocol (Zhang et al., 2003; Lee and Zhang, 2005; Lee and Zhang, 2007). Reflective markers were placed on the dorsum of the subjects' right hands and the three-dimensional (3D) marker coordinates were recorded by a five-camera Vicon 250 system (Oxford Metrics, UK) at a sampling frequency of 120 Hz. The angular profiles were then derived from the marker coordinates.

The finger model in this application represents each of digits 2-5 as an open chain of three segments-distal phanlanx (DP), middle phanlanx (MP), and proxiamal phalanx (PP), connected by three 1-DOF revolute joints—distal interphalangeal (DIP), proximal interphalangeal (PIP) and metacarpophalangeal (MCP) joints (see Fig. 2.2(a)). The segments are modeled as conical cylinders with a density of $1.1 g/cm^3$ (Dempster, 1955) and the length and thickness of each segment were modeled as functions of the hand length (Lee and Zhang, 2007). It was assumed that all the joints (DIP, PIP, and MCP) of

14

digits 2-5 were controlled by the two-component torque actuator proposed in the previous section.

The tendons and intrinsic muscles crossing these joints as each of the four fingers on the three joints considered in the model are listed in Table 2.1. For these four fingers (see Fig. 2.2(b)), the flexor digitorum profundus (FDP) and flexor digitorum superficialis (FDS) are the flexors of the fingers, inserting at the bases of DP and MP, respectively (Brand and Hollister, 1999; Gonzalez et al., 2005). The extensor mechanism itself is an intricate network of tendons connecting muscle tendons and tendon bands: the extensor digitorum communis (EDC) trifurcates over PP into extensor slip (ES) and two lateral bands (LB and UB); the former inserts onto the MP while the latter two re-connect and merge into the terminal tensor (TE) inserting onto DP. Besides the EDC, the extensor indicis proprius (EIP) inserts on the ulnar/radial side of EDC in the index finger and the extensor digiti quinti (EDQ) is on the ulnar side of the EDC in the little finger. Of note is that we do not consider the scenario that the EDC has no tendon inserting into the little finger in the current work. The intrinsic muscles add further complexity to the system: the lumbrical (LUM) muscle is the only muscle in the human body that originates from a tendon (of FDP) and inserts on a tendon (the lateral bands of extensor), both of which themselves span multiple joints; the interosseous muscles, radial or ulnar, originate from the lateral aspects of the MCP and insert on either side of the extensor hood. The little finger does not have an interosseous muscle on its ulnar side. Instead, the adductor digiti quinti (ADQ) muscle serves for abducting the finger. It is assumed that ADQ has the same properties as the UI. Note that two 'virtual' muscles were introduced into the middle and fingers (Table 2.1) to allow the model to be generic for all the digits.

Table 2.1

Tendons and intrinsic muscles of fingers

Joint	Index (Dig 2)	Middle (Dig 3)	Ring (Dig 4)	Little (Dig 5)
DIP	1.FDP	1. FDP	1. FDP	1. FDP
	3.TE	3. TE	3. TE	3. TE
PIP	1.FDP	1. FDP	1. FDP	1. FDP
	2.FDS	2. FDS	2. FDS	2. FDS
	4.ES	4. ES	4. ES	4. ES
	5.UB	5. UB	5. UB	5. UB
	6.RB	6. RB	6. RB	6. RB
MCP	1.FDP	1. FDP	1. FDP	1. FDP
	2.FDS	2. FDS	2. FDS	2. FDS
	7.LUM	7. LUM	7. LUM	7. LUM
	8.RI	8. RI	8. RI	8. RI
	9.UI	9. UI	9. UI	9. ADQ
	10. EDC	10. EDC	10. EDC	10. EDC
	11. EIP	11. (virtual)	11. (virtual)	11. EDQ
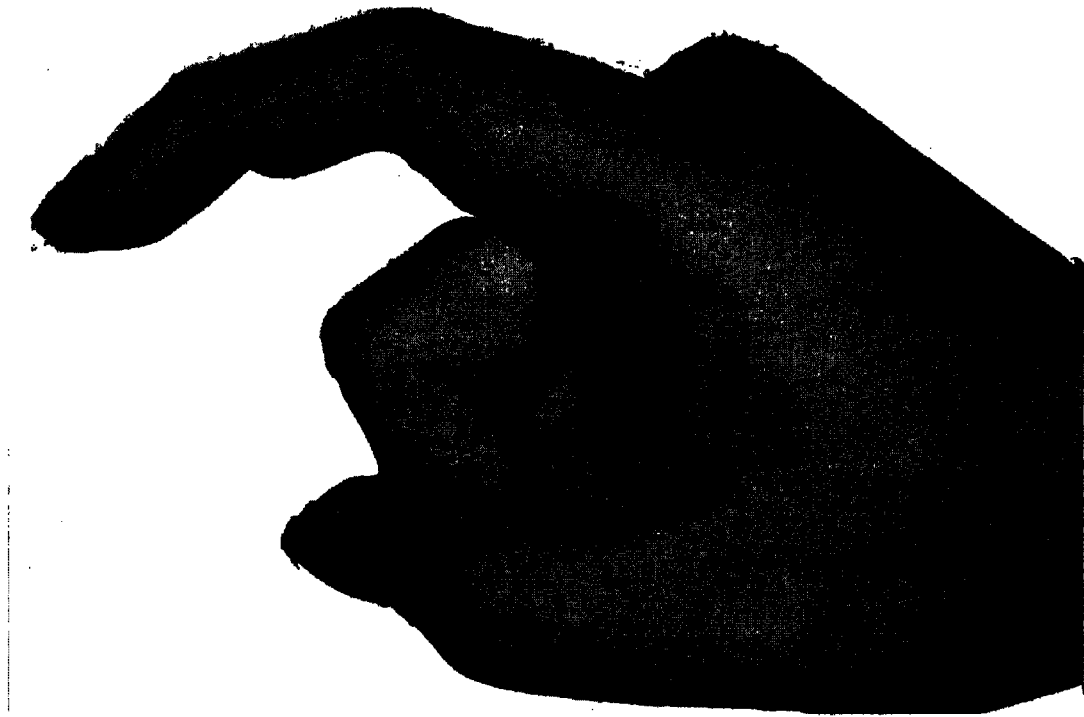
Fig. 2.2. (a) a 3-segment linkage model without musculotendon components

DIP: Distal Phalangeal
PIP: Proximal Phalangeal
MCP: Metacarpophalangeal

EDC: Extensor Digitorum Cummunis
ES: Extensor Slip
FDP: Flexor Digitorum Profundus
FDS: Flexor Digitorum Superficialis
LUM: Lumbrical
RI: Radial Interosseous
TE: Terminal Extensor
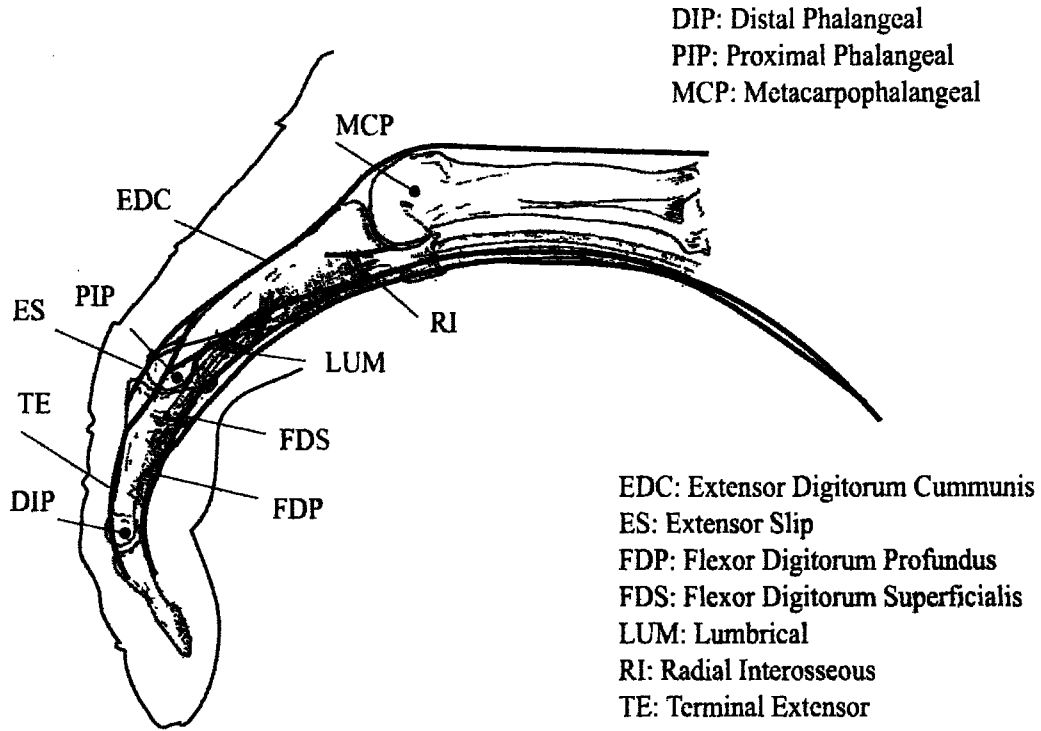
Fig. 2.2 (b) muscles and tendons added to the model

Fig. 2.2. The finger models in two development stages: (a) a torque-driven 3-segment, 3-DOF linkage model without musculotendon components; (b) muscles and tendons added to the model (RB, UB ,UI, ADQ, EIP and EDQ are not shown).

Thus for each individual finger, the moment equilibrium conditions can be described by the following equation:

$$\tau = M \cdot F \tag{2.10}$$

where

$$\tau = [\tau_1 \ \tau_2 \ \tau_3]^T, \quad F = [F_1 \ F_2 \ ... F_{11}]^T, M = \begin{bmatrix} m_{11} & 0 & m_{13} & & & & & & & & \\ m_{21} & m_{22} & & m_{24} & m_{25} & m_{26} & & & & & \\ m_{31} & m_{32} & & & & & m_{37} & m_{38} & m_{39} & m_{3,10} & m_{3,11} \end{bmatrix};$$

m_{jk} is moment arm of muscle/tendon force k with respect to joint j. The moment arms of the index finger are estimated by the method proposed by Brook et al. (1995). The moment arms of the remaining fingers are scaled by the ratios of respective finger

18

lengths to the index finger length. It is also assumed that no abduction-adduction occurs in the MCP joints during primarily flexion-extension finger movments. Therefore, we have another moment equilibrium equation:

$$M_4 \cdot F = 0 \tag{2.11}$$

where $M_4 = [m_{41} \quad m_{42} \quad 0 \quad 0 \quad 0 \quad 0 \quad m_{47} \quad m_{48} \quad m_{49} \quad m_{4,10} \quad m_{4,11}]$ and m_{4k} is the moment arm of muscle-tendon force k with respect to the MCP joint for abduction and adduction movements.

There are also force constraint equations as described by Brook et al. (1995):

$$F_3 = \chi_{RB} F_6 + \chi_{UB} F_5 \tag{2.12}$$

$$F_4 = (1 - \alpha_{UI}) F_9 + (1 - \alpha_{LUM}) F_7 + (1 - 2\alpha_{LE}) F_{10} + K(\varepsilon_{UB} + \varepsilon_{RB}) \tag{2.13}$$

$$F_5 = \alpha_{LE} (F_{10} + F_{11}) + \alpha_{LUM} F_7 - K\varepsilon_{UB} \tag{2.14}$$

$$F_6 = \alpha_{LE} (F_{10} + F_{11}) + \alpha_{LUM} F_7 - K\varepsilon_{RB} \tag{2.15}$$

where χ_{RB} and χ_{UB} are two cosine terms, which account for the convergence angles of the RB and UB onto the TE; ε_{RB} and ε_{UB} account for the relative motion between the ES and the RB and UB, respectively. The α coefficients are additional unknowns, which are determined in the subsequent nonlinear optimization. K is the tendon elasticity coefficient. Given that the moment arm values in M are known for each individual finger, the moment equilibrium system contains 11 unknown muscle/tendon forces and 3 unknown α coefficients in 8 equations. Note that F, τ and M are all time-dependent. To estimate the muscle force, a nonlinear optimization technique is employed with the objective function of minimizing the muscle stress which is defined as the quotient of the muscle force divided by its physiological cross sectional area (PCSA). The objective function is defined as:

$$J = \sum_{i \in A} (\frac{F_i}{PCSA_i})^2, \text{A} = \{1, 2, 7, 8, 9, 11\} \tag{2.16}$$

It is assumed that the same muscles of the four fingers have identical PCSA values presented in Chao and An (1978). The PCSA's of the three virtual muscles are set to be a very small but nonzero number to ensure that the virtual muscles are 'silent'. The muscle stress would be extremely large and be out of the optimal value if the virtual muscles underwent any force values, given that the objective function in the model is the

19

muscle stress.   The model was implemented using MATLAB® programs (The MathWorks, Boston, MA) and the MATLAB optimization toolbox.

2.3 Results

With the two-stage modeling framework, the model-predicted grasping movement was successfully replicating the experimental kinetics (see Fig. 2.3) and kinematics (see Fig. 2.4 and 2.5).   In contrast, directly applying the torque inverse solutions via conventional forward simulation (inverse simulation) based on the 4th-order Runge-Kutta method caused inverse dynamics simulation failure (see Fig. 2.6).   The root-mean-square error (RMSE) values for the pair-wise difference between the model-predicted and measured angular profile for each joint ranged from 1.56° to 3.73° (see Table 2.2).   The grand mean of the RMSE values across 19 trials was 2.32°.

The flexor and extensor torque components have consistent spatial-temporal patterns across joints, digits (see Fig. 2.7), and subjects (not shown here).   These patterns resembled the EMG patterns of the agonist and antagonist muscles observed during single-joint movements.   The model also demonstrated its potential for prediction, as we applied the control parameters of one subject to another and achieved close matches (Figure 2.8).

Table 2.2

Mean and standard deviation of RMSE values (unit: °)

Joint	Digit			
	2	3	4	5
DIP	2.86(0.87)	3.73(0.66)	3.16(0.99)	2.76(1.08)
PIP	1.93(1.04)	2.21(1.01)	2.12(1.06)	1.60(0.78)
MCP	1.56(0.57)	1.65(0.69)	1.64(0.61)	1.48(0.75)
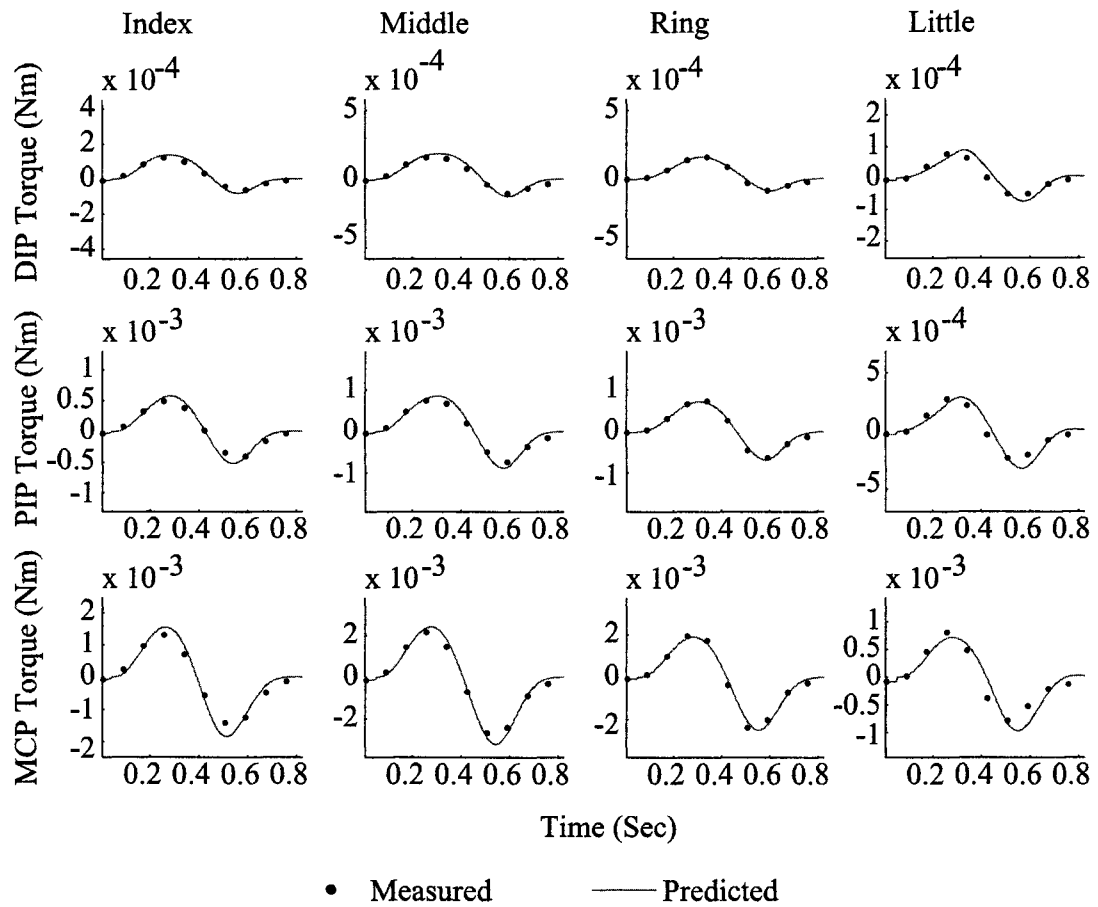
Fig. 2.3. Model-predicted (solid line) and inversely (measurement) derived net joint torques (dots) at 12 joints as functions of time t for a representative case. Note that the selected measured data points (dots) are sampled at 12Hz to better discriminate the model-prediction and measurement.
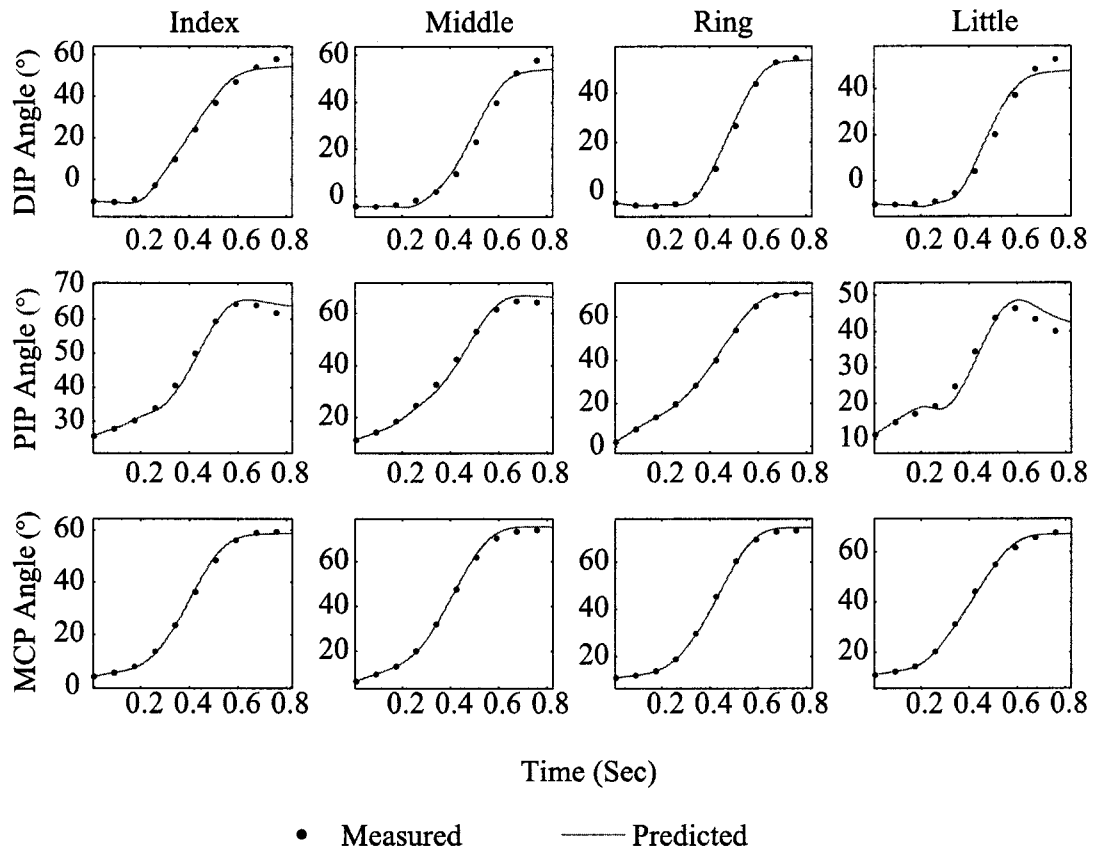
Fig. 2.4. Model-predicted and measured joint kinematics at 12 joints as functions of time t for the same representative case presented in Fig. 2.3. The RMSE values ranged from 0.72° to 3.60°, which are comparable to the statistical median of RMSEs across all cases.

22
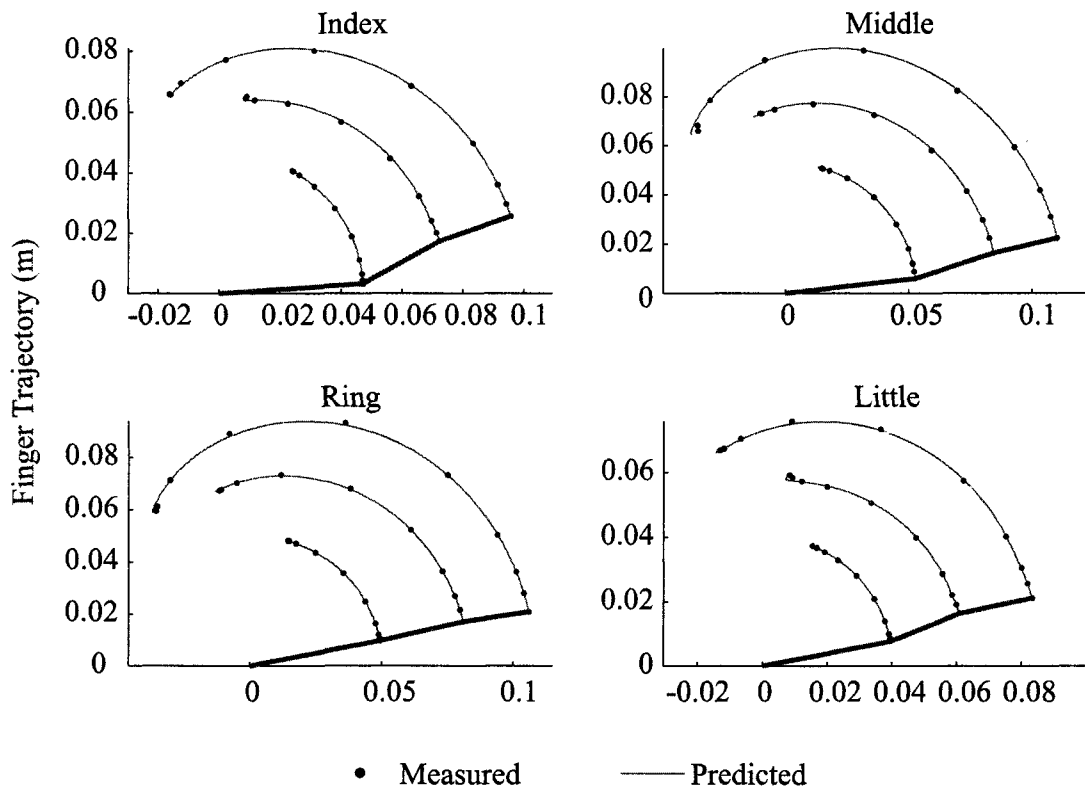
Fig. 2.5. Model-predicted and measured finger trajectories in flexion-extension planes of digits 2-5 for the same representative case presented in Fig. 2.3. The three-segment linkage (thick solid line) represents the initial finger posture with the origin being the MCP joint.
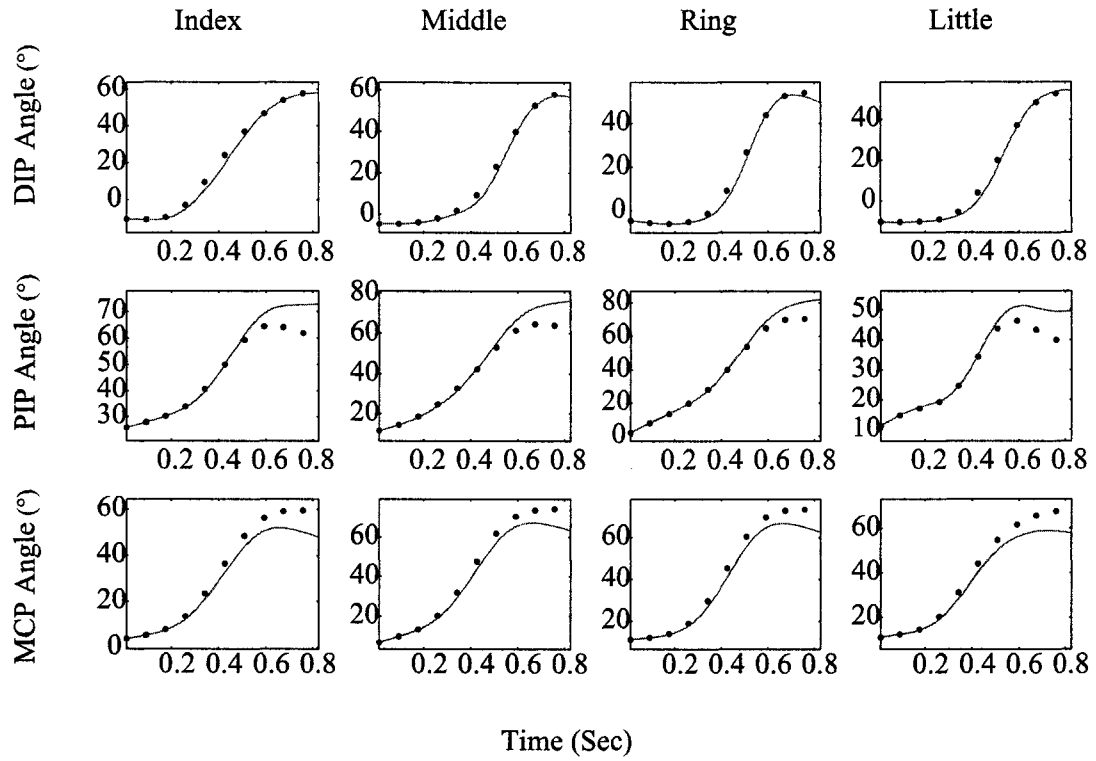
Fig. 2.6. Joint kinematics predicted by a forward simulation using a conventional inverse dynamic solution based on the 4th-order Runge-Kutta method (solid line) and measured kinematics for the same representative case presented in Fig.2.3. The RMSE values ranged from 1.3° to 5.50°.
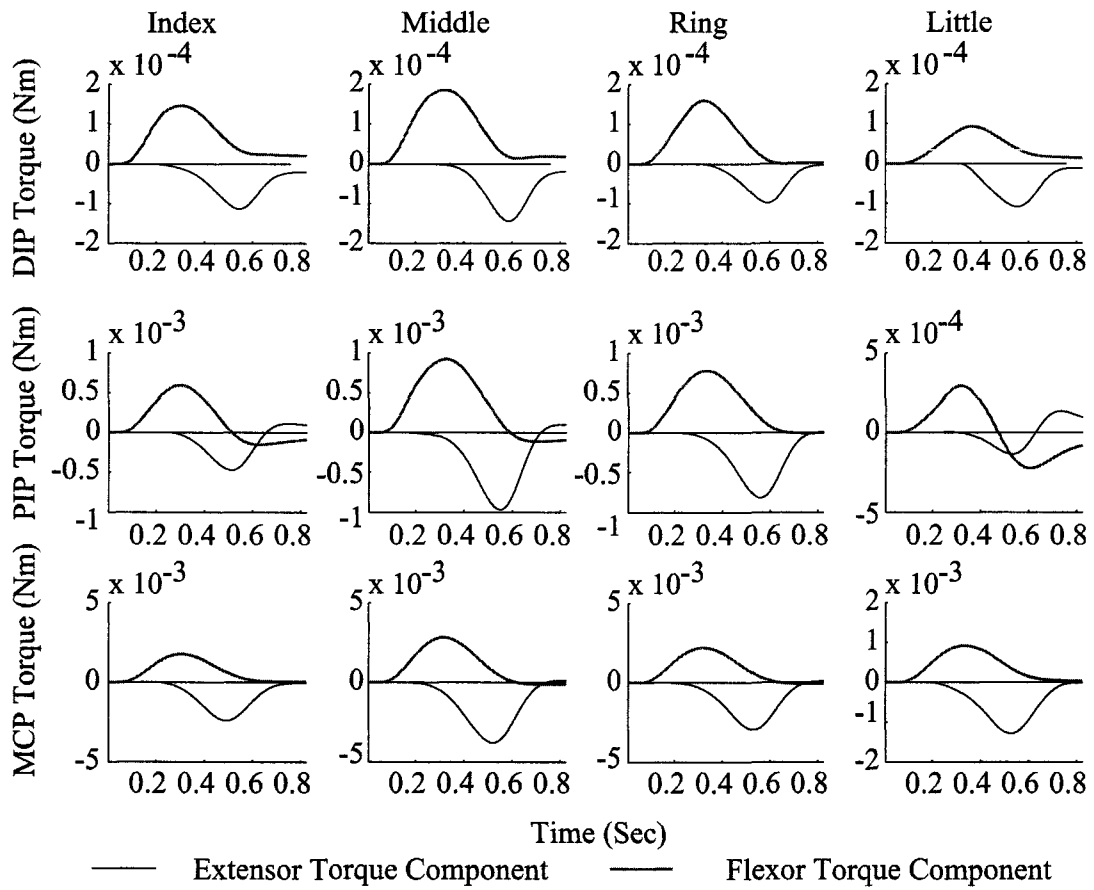
Fig. 2.7. Torque components across joints and digits for the same representative case presented in Fig. 2.3. The flexor (red line) and extensor (black) torque components demonstrated consistent spatial-temporal patterns across joints, digits. These patterns are similar to the spatial-temporal patterns of the agonist and antagonist muscle activities during single-joint movements as recorded by electromyography (EMG) in the literature (Hallett et al., 1975; Hallett and Marsden, 1979; Hannaford and Stark, 1985; Schmidt et al., 1988; Sherwood et al., 1988; Almeida et al., 1995; Gottlieb, 1998; Irlbacher et al., 2006). Note that the summation of the two components is the predicted net joint torque presented in Fig. 2.3.
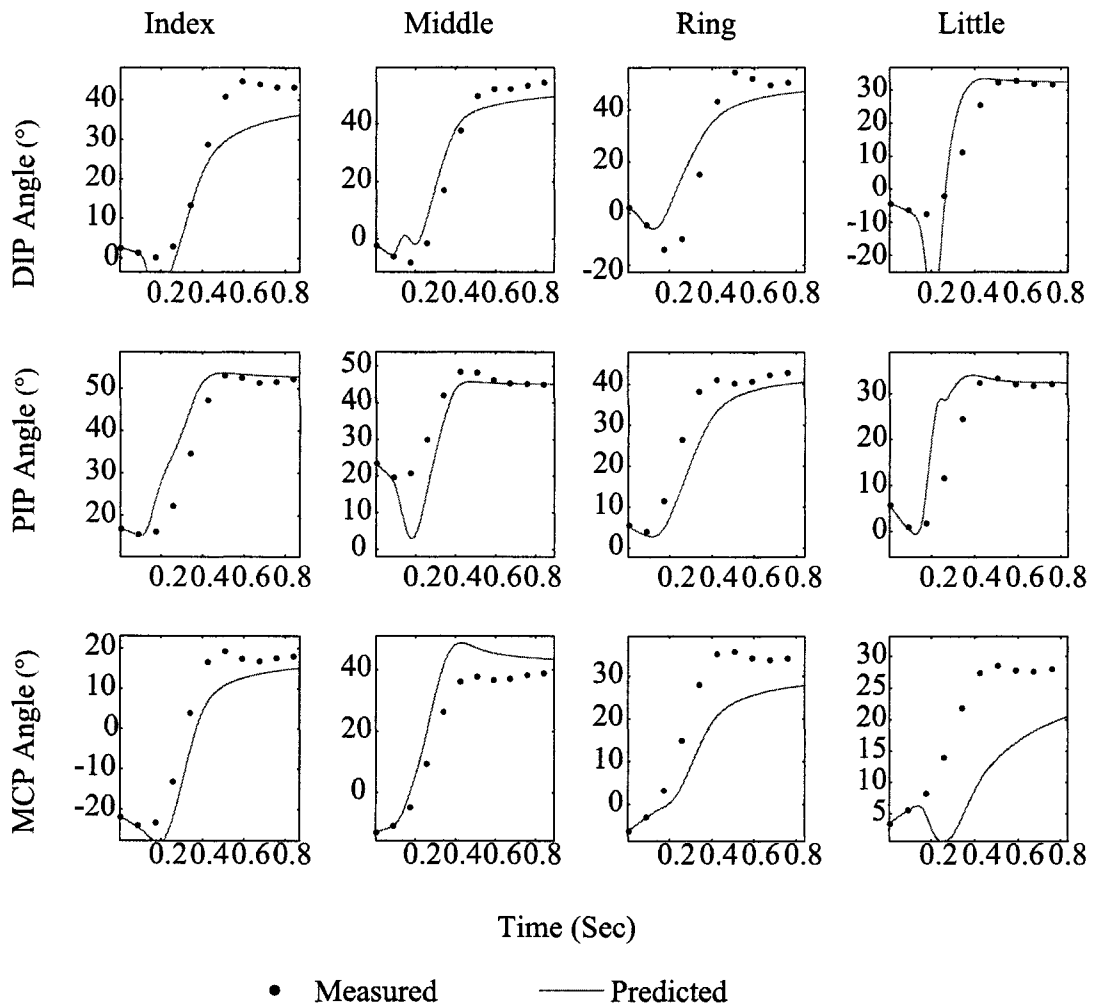
Fig. 2.8. An illustrative example of model's predictive potential: kinematics of one subject predicted by using the control parameters of another subject (solid line), in comparison with measured kinematics (dots).

The muscle-tendon forces computed based on the model-predicted kinematics and kinetics (Fig. 2.9) had the peak flexor forces within the same order of magnitude as measured in vivo by previous studies (Dennerlein et al., 1999; Kursa et al., 2006; Nikanjam et al., 2007). Both in vivo measurements and our prediction suggested that the peak forces of the FDP and FDS were less than 10N during flexion for an index finger. Such an agreement to some extent supports the plausibility of the estimated muscle-tendon forces. It should be recognized that the in vivo finger muscle-tendon force data

26

available in the literature were very limited and that the movements measured were not the same as though not fundamentally different from (e.g., no external force applied to the finger) the cylinder-grasp movements we studied in this work. In addition, the FDS force was larger than the FDP in the initial phase of the movement and then decreased to zero while the FDP force initially was small and then increased to sustain the motion. These observations appear to be in agreement with the literature data (Bendz, 1980; Nikanjarn et al., 2007). It was also observed that the combined extensor force was always greater than the combined flexor force, which confirms what was found by an in vivo study (Kuo et al., 2006). Besides the flexors and extensors, the intrinsic muscle forces also agreed with the muscle activities measured in vivo (Kuo et al., 2006). Both studies converged on the finding that the LUM should be almost silent during flexion/extension.
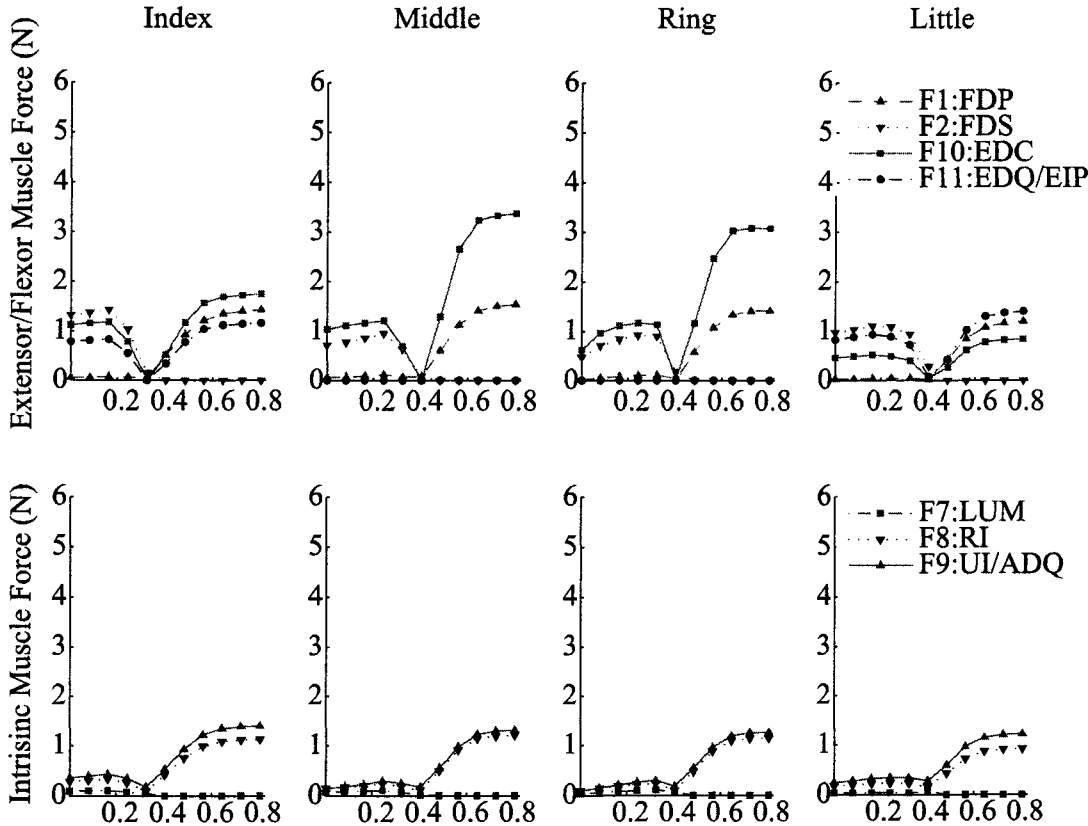
Fig. 2.9. The muscle-tendon force profiles based on the model-predicted kinematics and kinetics for the same representative case presented in Fig. 3 and Fig. 4.

2.4 Discussion

The current study developed a two-stage computational framework for biodynamical modeling and illustrated it by an application to modeling of multi-fingered hand movements. It was demonstrated that the computational framework was able to address two chief concerns plaguing musculoskeletal biodynamical modeling: the realism-efficiency trade-off and the irreconcilability of the inverse and forward solutions. The computational efficiency of our modeling framework was embodied by the significantly shortened time for complete integration of the state equations (<1 second) in forward simulation and reduced number of the integrations during control parameter identification (ranged from 10-500). Unlike most forward dynamic models with musculo-tendon components, this framework does not incur a computational demand that increases exponentially with the model variables (DOFs and muscle-tendon forces). Instead, the parameters of the stereotyped control scheme are identified in a static optimization process; once they are determined, the kinematics and muscle-tendon forces are predicted expeditiously. Further, the framework does not require estimation of any muscle activation pattern, which cannot be done reliably with the existing technology and has been acknowledged as a major drawback of the conventional forward dynamics approaches (Buchanan et al., 2005).

Reconciliation between inverse and forward solutions was also achieved with the proposed framework. The irreconcilability of the inverse and forward solutions may have its root causes from both inverse and forward dynamics approaches. First, both inverse and forward solutions themselves could be susceptible to significant errors. When joint torques are estimated, inverse solutions are highly sensitive to a variety of factors such as measurement noise, accuracy of anatomical parameters, and veracity of a segment model (Desjardins et al., 1998; Kuo, 1998; Hatze, 2002; Silva and Ambrosio, 2004; Alonso et al., 2007; Riemer et al., 2007). A forward approach could suffer from compromised validity of the biomechanical model (Zajac et al., 2002), and inaccuracy in model parameter estimation (Lim et al., 2003). These could result in non-physiological joint moments and muscle forces (Buchanan et al., 2005; Erdemir et al., 2007; Lee and Zhang, 2007), inaccurate ground reaction forces (Buczek et al., 2006), and unrealistic acceleration and power (Zajac et al., 2002). Second, even when inverse solutions are

28

derived free of model parameter estimation errors, they could still result in inverse dynamics simulation failures in practice due to numerical integration errors (Tashman, 1992), mismatches between inverse and forward dynamics models (Zajac, 1993), or insufficient control signal dimensionality (Risher et al., 1997).

The irreconcilable difference could lead to conflicts or debates in interpreting movement mechanism and impede comprehensive understanding of underlying mechanisms. It has been recognized that understanding of human movement demands integrative studies across disciplines, ranging from biomechanics, physiology, neuroscience to engineering, psychology, sport, medicine (Nishikawa et al., 2007; Stuart, 2007). Both inverse and forward solutions have been widely utilized in these disciplines. Generally, inverse solutions are preferred by experimentalists and clinical practitioners in physiology, biomechanics, motor control, and neuroscience due to its low computational cost, while forward solutions are favored by computational scientists and theorists in these fields. Without a unified solution across different disciplines or fields, it would be a tremendous challenge to seamlessly integrate multidisciplinary knowledge for understanding human movement. It has been suggested that inverse solutions should be used when accurate experimental data and appropriate time-independent performance criteria are available for muscle force estimation (Anderson and Pandy, 2001b) or the aim is to predict how a change of one moment of force affects another moment of force and the movement (Otten, 2003). Forward solutions should be used when the goal is to predict a novel movement (Anderson and Pandy, 2001b) or to investigate the effect of the body structure change on function and performance of a motor task (Pandy, 2001). Yet, these suggestions do not necessarily provide a solution to reconcile the difference. Our framework addressed this problem and generated a reconciled solution in a single musculoskeletal modeling framework. The proposed framework therefore could potentially serve as a unifying approach across disciplines and facilitate a more coherent understanding about how people move.

Our modeling framework also displayed a great potential to predict across digits and subjects, although no systematic evaluation of the prediction power was done in the current study. When we randomly applied the control parameters from one digit to another, or from one subject to another, close matches were found between observed and

predicted kinetics and kinematics. This potential predictive power can be evidence supporting a common stereotypical control strategy, and is important for applications such as computer-aided design, ergonomics (Zhang and Chaffin, 2006), and surgical planning (Menegaldo et al., 2006).

In addition, the proposed framework could facilitate inferring the internal models humans employ to coordinate the complex musculoskeletal system. Using traditional forward dynamics approach may not render insight into why the central nervous system is coordinating muscles the way it does (Zajac, 1993). A stiffness control mechanism based co-contraction of flexor and extensor muscles could be a way to simplify multi-joint motion control (Darling et al., 1994). The observed resemblance in spatial-temporal patterns between the EMG activities of the agonist and antagonist muscles during single-joint movements and the flexor and extensor torque components inspired the notion that our hypothesized control strategy could be a possible internal model at the motor control level.

It is acknowledged that the proposed framework was only tested with 'well-coordinated' cylinder-grasping motions. Whether it is applicable for other types of hand movement and other multi-segmental body movements remains unexplored. We expect that the distribution functions dictating the stereotyped movement control will have some dependence on the movement type. One of the advantages of the framework is that it has the open architecture allowing various control schemes or distribution functions to be hypothesized and empirically tested.

2.5 Conclusion

We proposed a novel modeling framework and demonstrated its ability to produce multi-fingered movement predictions that are realistic in both kinematics and kinetics. This is the first forward dynamic model we are aware of that can achieve such biomechanical realism at a relatively low computational cost. The model also provides a solution to alleviate the inverse dynamics failure problem that has been a persisting challenge in computational biomechanics. Our future work will focus on further improvement of this model, quantifying the correlations or invariants in the stereotyped patterns in joint torques, muscle/tendon forces both within and across individual digits,

30

and examining the effect of model parameter variability.

2.6 References

Almeida, G.L., Hong, D.A., Corcos, D., Gottlieb, G.L., 1995. Organizing principles for voluntary movement: extending single-joint rules. Journal of Neurophysiology 74, 1374-1381.

Alonso, F.J., Del Castillo, J.M., Pintado, P., 2007. Motion data processing and wobbling mass modelling in the inverse dynamics of skeletal models. Mechanism and Machine Theory 42, 1153-1169.

Anderson, F.C., Pandy, M.G., 2001a. Dynamic optimization of human walking. Journal of Biomechanical Engineering-Transactions of the ASME 123, 381-390.

Anderson, F.C., Pandy, M.G., 2001b. Static and dynamic optimization solutions for gait are practically equivalent. Journal of Biomechanics 34, 153-161.

Bellman, R.E. (1957). Dynamic Programming. Princeton, NJ: Princeton University Press.

Bendz, P., 1980. The motor balance of the fingers of the open hand. An experimental study using a gonio-electromyographic technique. Scandinavian journal of rehabilitation medicine 12, 115-121.

Blemker, S.S., Asakawa, D.S., Gold, G.E., Delp, S.L., 2007. Image-based musculoskeletal modeling: Applications, advances, and future opportunities. Journal of Magnetic Resonance Imaging 25, 441-451.

Brand, P.W., Hollister, A.M. (1999). Clinical mechanics of the hand (3rd ed.). St. Louis, MO: Mosby-Year Book, Inc.

Brook, N., Mizrahi, J., Shoham, M., Dayan, J., 1995. A biomechanical model of index finger dyanmics. Medical Engineering & Physics 17, 54-63.

Buchanan, T.S., Lloyd, D.G., Manal, K., Besier, T.F., 2005. Estimation of muscle forces and joint moments using a forward-inverse dynamics model. Medicine and Science in Sports and Exercise 37, 1911-1916.

Buczek, F.L., Cooney, K.M., Walker, M.R., Rainbow, M.J., Concha, M.C., Sanders, J.O., 2006. Performance of an inverted pendulum model directly applied to normal human gait. Clinical Biomechanics (Bristol, Avon) 21, 288-296.

Chang, S.W., Wang, M.J.J., 2007. Digital human modeling and workplace evaluation: Using an automobile assembly task as an example. Human Factors and Ergonomics in Manufacturing 17, 445-455.

Chao, E.Y., An, K.N., 1978. Graphical interpretation of the solution to the redundant problem in biomechanics. Journal of Biomechanical Engineering 100, 159-167.

Darling, W.G., Cole, K.J., Miller, G.F., 1994. Coordination of index finger movements. Journal of Biomechanics 27, 479-491.

Delp, S.L., Loan, J.P., 2000. A computational framework for simulating and analyzing human and animal movement. Computing in Science & Engineering 2, 46-55.

Dempster, W.T. (1955). Space requirements of the seated operator (No. WADC-TR-55-159). Wright-patterson Air Force Base, OH: Aerospace Medical Research Laboratories.

Dennerlein, J.T., Diao, E., Mote, C.D., Rempel, D.M., 1999. In vivo finger flexor tendon force while tapping on a keyswitch. Journal of Orthopaedic Research 17, 178-184.

Desjardins, P., Plamondon, A., Gagnon, M., 1998. Sensitivity analysis of segment models to estimate the net reaction moments at the L5/S1 joint in lifting. Medical Engineering & Physics 20, 153-158.

Dul, J., Townsend, M.A., Shiavi, R., Johnson, G.E., 1984. Muscular Synergism .1. On Criteria for Load Sharing between Synergistic Muscles. Journal of Biomechanics 17, 663-673.

Erdemir, A., McLean, S., Herzog, W., van den Bogert, A.J., 2007. Model-based estimation of muscle forces exerted during movements. Clinical Biomechanics 22, 131-154.

Gielen, C.C.A.M., Vanbolhuis, B.M., Theeuwen, M., 1995. On the control of biologically and kinematically redundant manipulators. Human Movement Science 14, 487-509.

Gonzalez, M., Mohan, V., Elhassan, B., Amirouche, F., 2005. Biomechanics of the digit. Journal of the American Society for Surgery of the Hand 5, 48-60.

Gottlieb, G.L., 1998. Muscle activation patterns during two types of voluntary single-joint movement. Journal of Neurophysiology 80, 1860-1867.

Gottlieb, G.L., Corcos, D.M., Agarwal, G.C., 1989. Organizing principles for single-joint movements. I. A speed-insensitive strategy. Journal of Neurophysiology 62, 342-357.

Hallett, M., Marsden, C.D., 1979. Ballistic flexion movements of the human thumb. Journal of Physiology 294, 33-50.

Hallett, M., Shahani, B.T., Young, R.R., 1975. EMG analysis of stereotyped voluntary movements in man. Journal of Neurology, Neurosurgery, and Psychiatry 38, 1154-1162.

Hannaford, B., Stark, L., 1985. Roles of the elements of the triphasic control signal. Experimental Neurology 90, 619-634.

Happee, R., 1994. Inverse Dynamic Optimization Including Muscular Dynamics, a New Simulation Method Applied to Goal-Directed Movements. Journal of Biomechanics 27, 953-960.

Hatze, H., 2002. The fundamental problem of myoskeletal inverse dynamics and its implications. J Biomech 35, 109-115.

Irlbacher, K., Voss, M., Meyer, B.U., Rothwell, J.C., 2006. Influence of ipsilateral transcranial magnetic stimulation on the triphasic EMG pattern accompanying fast ballistic movements in humans. Journal of Physiology 574, 917-928.

Karlsson, D., Peterson, B., 1992. Towards a Model for Force Predictions in the Human Shoulder. Journal of Biomechanics 25, 189-199.

Kautz, S.A., Neptune, R.R., Zajac, F.E., 2000. General coordination principles elucidated by forward dynamics: minimum fatigue does not explain muscle excitation in dynamic tasks. Motor Control 4, 75-80; discussion 97-116.

Kuo, A.D., 1998. A least-squares estimation approach to improving the precision of inverse dynamics computations. Journal of Biomechanical Engineering-Transactions of the ASME 120, 148-159.

Kuo, P.L., Lee, D.L., Jindrich, D.L., Dennerlein, J.T., 2006. Finger joint coordination during tapping. Journal of Biomechanics 39, 2934-2942.

Kursa, K., Lattanza, L., Diao, E., Rempel, D., 2006. In vivo flexor tendon forces increase with finger and wrist flexion during active finger flexion and extension. Journal of Orthopaedic Research 24, 763-769.

Lacquaniti, F., Soechting, J.F., 1986. EMG responses to load perturbations of the upper limb: effect of dynamic coupling between shoulder and elbow motion. Experimental Brain Research 61, 482-496.

Lee, S.W., Zhang, X., 2005. Development and evaluation of an optimization-based model for power-grip posture prediction. Journal of Biomechanics 38, 1591-1597.

Lee, S.W., Zhang, X., 2007. Biodynamic modeling, system identification, and variability of multi-finger movements. Journal of biomechanics 40, 3215-3222.

Lim, C.L., Jones, N.B., Spurgeon, S.K., Scott, J.J.A., 2003. Reconstruction of human neuromuscular control signals using a sliding mode control technique. Simulation Modelling Practice and Theory 11, 223-235.

Lin, H.T., Su, F.C., Wu, H.W., An, K.N., 2004. Muscle forces analysis in the shoulder mechanism during wheelchair propulsion. Proceedings of the Institution of Mechanical Engineers, Part H: Journal of Engineering in Medicine 218, 213-221.

Marconi, N.F., Almeida, G.L., Gottlieb, G.L., 2006. Electromyographic and kinetic strategies to control movements. Revista Brasileira de Fisioterapia 10, 1-8.

Menegaldo, L.L., Fleury, A.D., Weber, H.I., 2003. Biomechanical modeling and optimal control of human posture. Journal of Biomechanics 36, 1701-1712.

Menegaldo, L.L., Fleury, A.D., Weber, H.I., 2006. A 'cheap' optimal control approach to estimate muscle forces in musculoskeletal systems. Journal of Biomechanics 39, 1787-1795.

Neptune, R.R., 2000. Computer modeling and simulation of human movement. Applications in sport and rehabilitation. Physical medicine and rehabilitation clinics of North America 11, 417-434.

Nikanjarn, M., Kursa, K., Lehman, S., Lattanza, L., Diao, E., Rempel, D., 2007. Finger flexor motor control patterns during active flexion: An in vivo tendon force study. Human Movement Science 26, 1-10.

Nishikawa, K., Biewener, A.A., Aerts, P., Ahn, A.N., Chiel, H.J., Daley, M.A., Daniel, T.L., Full, R.J., Hale, M.E., Hedrick, T.L., Lappin, A.K., Nichols, T.R., Quinn, R.D., Satterlie, R.A., Szymik, B., 2007. Neuromechanics: an integrative approach for understanding motor control. Integrative and Comparative Biology 47, 16-54.

Otten, E., 2003. Inverse and forward dynamics: models of multi-body systems. Philosophical Transactions of the Royal Society of London Series B-Biological Sciences 358, 1493-1500.

Pandy, M.G., 2001. Computer modeling and simulation of human movement. Annual Review of Biomedical Engineering 3, 245-273.

Prilutsky, B.I., 2000. Coordination of two- and one-joint muscles: Functional consequences and implications for motor control. Motor Control 4, 1-44.

Prilutsky, B.I., Zatsiorsky, V.M., 2002. Optimization-based models of muscle coordination. Exercise and Sport Sciences Reviews 30, 32-38.

Raikova, R.T., Gabriel, D.A., Aladjov, H.T., 2005. Experimental and modelling investigation of learning a fast elbow flexion in the horizontal plane. Journal of Biomechanics 38, 2070-2077.

Rasmussen, J., Damsgaard, M., Christensen, S.T., Surma, E., 2002. Design optimization with respect to ergonomic properties. Structural and Multidisciplinary Optimization 24, 89-97.

Riemer, R., Hsiao-Wecksler, E.T., Zhang, X., 2007. Uncertainties in inverse dynamics solutions: A comprehensive analysis and an application to gait. Gait & Posture.

Risher, D.W., Schutte, L.M., Runge, C.F., 1997. The use of inverse dynamics solutions in direct dynamics simulations. Journal of Biomechanical Engineering-Transactions of the ASME 119, 417-422.

Schmidt, R.A., Sherwood, D.E., Walter, C.B., 1988. Rapid movements with reversals in direction. I. The control of movement time. Experimental Brain Research 69, 344-354.

Seireg, A., Arvikar, R.J., 1975. Prediction of Muscular Load Sharing and Joint Forces in Lower-Extremities during Walking. Journal of Biomechanics 8, 89-102.

Shelburne, K.B., Pandy, M.G., 2002. A dynamic model of the knee and lower limb for simulating rising movements. Computer Methods in Biomechanics and Biomedical Engineering 5, 149-159.

Sherwood, D.E., Schmidt, R.A., Walter, C.B., 1988. Rapid movements with reversals in direction. II. Control of movement amplitude and inertial load. Experimental Brain Research 69, 355-367.

Silva, M.P., Ambrosio, J.A., 2004. Sensitivity of the results produced by the inverse dynamic analysis of a human stride to perturbed input data. Gait & Posture 19, 35-49.

Stuart, D.G., 2007. Reflections on integrative and comparative movement neuroscience. Integrative and Comparative Biology 47, 482-504.

Tanaka, S., Wada, T., Kawakita, K., 2007. Determination of human motion for rehabilitation based on time-scale transformation. In Mechatronics and Automation, 2007. ICMA 2007. International Conference on.

Tashman, S. (1992). Experimental Analysis and Computer Modeling of Paraplegic Ambulation in a Reciprocating Gait Orthosis: Implications for the Desgin of Hybrid FNS/Orthotic Systems. Unpublished Ph.D Dissertation, CA, Stanford.

van der Helm, F.C.T., 1994. A Finite-Element Musculoskeletal Model of the Shoulder Mechanism. Journal of Biomechanics 27, 551-569.

Winter, D.A. (1990). Biomechanics and motor control of human movement. New York: John Wiley & Sons.

Yamaguchi, G.T., Moran, D.W., Si, J., 1995. A Computationally Efficient Method for Solving the Redundant Problem in Biomechanics. Journal of Biomechanics 28, 999-1005.

Zajac, F.E., 1993. Muscle Coordination of Movement - a Perspective. Journal of Biomechanics 26, 109-124.

Zajac, F.E., Neptune, R.R., Kautz, S.A., 2002. Biomechanics and muscle coordination of human walking - Part I: Introduction to concepts, power transfer, dynamics and simulations. Gait & Posture 16, 215-232.

Zajac, F.E., Neptune, R.R., Kautz, S.A., 2003. Biomechanics and muscle coordination of human walking Part II: Lessons from dynamical simulations and clinical implications. Gait & Posture 17, 1-17.

Zhang, X. 2001. Biomechanical Realism Versus Algorithmic Efficiency: A Trade-off in Human Motion Simulation Modeling. Paper presented at the Proceedings of 4th Digital Human Modeling for Design and Engineering Conference.

Zhang, X., Chaffin, D.B. (2006). Digital human modeling for computer-aided ergonomics. In Karwowski, W. & Marras, W. S. (Eds.), *Handbook of Occupational Ergonomics*: Taylor & Francis CRC Press.

Zhang, X., Lee, S.-W., Braido, P., 2003. Determining finger segmental centers of rotation in flexion-extension based on surface marker measurement. Journal of Biomechanics 36, 1097-1102.

CHAPTER III
IDENTIFYING MULTI-LEVEL INVARIANTS UNDERLYING MULTI-FINGERED HAND MOTIONS VIA BIODYNAMIC MODELING

3.1 Abstract

This study explored whether common mechanisms are deployed to control functionally different multi-finger movements: cylinder-grasping and individuated flexion of the index finger ('enslaving'). A two-stage biodynamical computational framework was used to model the joint dynamics of the two types of multi-fingered movements (eleven trials for each type) and to estimate the muscle-tendon forces during these movements. The numbers of invariants or effective degrees of freedom in the joint and muscle-tendon dynamics of these movements were then identified using principal components analysis (PCA). The results showed that the two types of movement were faithfully reproduced by the same biodynamic model with a unified control mechanism and that the numbers of invariants remained consistent across movement types in both the joint and muscle-tendon dynamics. The grand means of the root-mean-square error (RMSE) values for grasping and 'enslaving' movements were $2.25°$ and $1.24°$, respectively. The identified numbers of invariants were about one in the joint dynamics and three in the muscle-tendon dynamics. The distributions of the percent variance accounted for (PAVF) across movements remained largely constant at the joint angle and muscle-tendon force levels. These results provided evidence to support the commonality of control mechanisms underlying different multi-finger movements, and hierarchical sources for dimensionality reduction in the control. Insights gained from the study can guide or inspire applications including the design of next-generation hand neuro-prosthetics and exoskeletons or hand rehabilitation strategies.

3.2 Introduction

The human hand provides superior dexterity with its 27 bones, 39 muscles, and over 20 degrees of freedom (DOF's). How such a complex biomechanical system is orchestrated to produce a vast array of deft, purposeful, and concerted hand movements remains an open question that continues to perplex researchers. Much research effort

has been devoted to tackling this question and several mechanisms have been hypothesized from different perspectives. One mechanism is that the anatomy structure of the hand performs anatomical computation (Valero-Cuevas et al., 2007). It has been suggested that the hand anatomical structure itself is able to regulate muscle-tendon tensions, joint torques, and joint function across different joints through complex interacting between tendons during movement (Valero-Cuevas et al., 2007; Benjamin et al., 2008) while the whole tendon network acts like a single functional entity (Benjamin et al., 2008). Thus, the anatomical structure of the hand enables 'non-neural somatic logic' (Valero-Cuevas et al., 2007) and allows the hand to undergo information-processing tasks spontaneously. This mechanism functions within fingers and can only partially alleviate the computational burden of the central nervous system (CNS).

Another mechanism hypothesized from kinematic point of view is that the hand movements are produced by activating combinations of a small set of task-independent synergic hand motions or "kinematics synergies." This mechanism is supported by the observation that human exhibits highly coordinative kinematics within and across fingers (Cole and Abbs, 1987; Fish and Soechting, 1992; Soechting and Flanders, 1997; Hager-Ross and Schieber, 2000; Mason et al., 2001; Santello et al., 2002; Braido and Zhang, 2004; Li et al., 2004; Li, 2006; Thakur et al., 2008) during hand movements. It also has been evidenced by a phenomenon referred to as "enslaving:" the voluntary motion or force production of one digit is companied by unintentional motion or force production of other digits (Zatsiorsky et al., 1998; 2000; Braido and Zhang, 2004; Li et al., 2004). A recent study done by Ishida et al. (2007) has reported that a limited number of muscle synergies can explain most of the observed muscle activation patterns, implying a third mechanism that the motor system organizes the muscle elements into controllable units with different spatial-temporal patterns and generates actions or movements by activating combinations of these muscle synergies. All these observations suggested that all the joints and fingers are not completely independent but synergized as controllable units (Cole and Abbs, 1987) and thus the mechanical DOF's of the hand can be simplified into a much reduced number of functional DOF's (Li, 2006).

Nevertheless, these past studies were conducted at discrete levels, examining either kinematics, or EMG-based muscle activation, or muscle-tendon forces. The findings are

38

thus more or less disconnected and may also be contradictory on issues such as at which levels or to what extent at each level the control simplification or dimensionality reduction occurs. There has not been a well integrated study examining from multiple levels the synergies in production and control of multi-fingered hand movements. This may be attributable to the lack of a multi-finger biodynamic model that can connect musculotendon forces to joint torque and kinematics and do so without some of the long-persisting limitations of dynamic simulation, including excessive computational cost (Anderson and Pandy, 2001; Menegaldo et al., 2003; 2006) and inverse dynamics simulation failure (Risher et al., 1997). The latter refers to the phenomenon that inverse dynamics solutions fail to reproduce measured kinematics via forward dynamics based on an identical model, thus casting doubt on the validity of the joint torques and muscle-tendon forces derived.

This study aimed to investigate the synergies or invariants underlying multi-fingered hand movements at multiple levels—the system control, joint and muscle-tendon dynamics. We employed a newly developed biodynamic model (Li and Zhang, 2008) that can overcome the above noted limitations. Our central hypothesis is that the mechanisms to control functionally different multi-finger movements remain consistent. We tested this hypothesis by examining (1) whether two functionally different multi-finger hand movements, power grasp and individuated flexion of index finger ('enslaving'), can be accurately reproduced by our biodynamic model with a unified control mechanism; and (2) whether the inter-digit dynamic couplings and coordination patterns underlying these multi-fingered movements are generally consistent.

3.3 Methods

Experimental Data

The experimental data of both cylinder-grasping and individuated flexion of index finger ('enslaving') movements were from a database previously established in our laboratory (Braido and Zhang, 2004). During the cylinder-grasping movements, the subjects grasped a vertical cylindrical handle (45 mm in diameter) by voluntarily flexing digits 2-5 in a concurrent way while they only voluntarily flexed digit 2 without consciously controlling involuntary joint flexion of other digits during the individuated

39

flexion of index finger movements.   Eleven trials performed by eleven subjects for each type of movement were selected using the selection criterion that the movements of the active finger must be 'well-coordinated', as characterized by bell-shaped joint velocity profiles and single- or double-peaked joint acceleration profiles.   Trials satisfying this criterion without significant missing data (due to surface marker dropouts in measurement) were used.   The multi-finger kinematics was measured and derived using a well-published experimental and processing protocol (Zhang et al., 2003; Lee and Zhang, 2005).

Biodynamical Model

A recently developed biodynamical computational framework (Li and Zhang, 2008) was used to model the two types of multi-fingered hand movements and elicit system control parameters, joint and muscle-tendon dynamics measures.   This framework decoupled the conventional forward dynamic modeling process into two stages.   In the first stage, each of digits 2-5 was represented as an open chain of three segments-distal phanlanx (DP), middle phanlanx (MP), and proxiamal phalanx (PP), connected by three 1-DOF revolute joints—distal interphalangeal (DIP), proximal interphalangeal (PIP) and metacarpophalangeal (MCP) joints.   The forward dynamics of the finger system was assumed to be driven by a physiologically based two-component ("agonist-antagonist") torque actuators.   The torque at each joint of digits 2-5 was modeled as:

$$\tau(t) = \tau_{\text{flexor}}(t) + \tau_{\text{extensor}}(t) \tag{3.1}$$

$$\tau_{\text{flexor}}(t) = -q(t)[K^p_{\text{flexor}}\Delta\theta(t) + K^d_{\text{flexor}}\Delta\dot{\theta}(t)] \tag{3.2}$$

$$\tau_{\text{extensor}}(t) = -s(t)[K^p_{\text{extensor}}\Delta\theta(t) + K^d_{\text{extensor}}\Delta\dot{\theta}(t)] \tag{3.3}$$

$$q(t) = 1.0 - (1.0 - \alpha_q t + \frac{\alpha_q}{2}t^2)e^{-\alpha_q t} \tag{3.4}$$

$$s(t) = \frac{s_0}{B(\beta_s, 1)}t^{\beta_s - 1} = \frac{s_0}{\int_0^1 t^{\beta_s - 1} dt}t^{\beta_s - 1} \tag{3.5}$$

where $\tau_{\text{flexor}}(t)$ represents the flexor action and $\tau_{\text{extensor}}(t)$ represents the extensor action at time t; $K^p_{\text{flexor}} \in \Re^{3\times1}$, $K^p_{\text{extensor}} \in \Re^{3\times1}$, and $K^d_{\text{flexor}} \in \Re^{3\times1}$, $K^d_{\text{extensor}} \in \Re^{3\times1}$ are the associated proportional and derivative gains; $\Delta\theta(t) \in \Re^{3\times1}$, $\Delta\dot{\theta}(t) \in \Re^{3\times1}$ are the angle and angular velocity changes; $q(t)$ is a gamma distribution function; $s(t)$ is a beta

distribution function; α_q is the scale factor of the gamma distribution, and β_s is the shape parameter of the beta distribution function. The system parameters were identified in an optimization-based procedure that best matched the model-prediction and measurement in both kinematics and joint torque dynamics of the multi-fingered movements. The procedure was able to overcome the inverse dynamics failure problem in forward dynamic simulation, and ensured that the inversely measurement-derived torque was faithfully reproduced by the model.

In the second stage, the muscle-tendon forces were computed from the joint torques $\tau(t)$ predicted in the first stage. Eleven tendons and muscles for each of digits 2-5 were considered in the model, including two 'virtual' muscles (the extensor indicis proprius (EIP) muscles for the middle and ringer fingers) which allowed a generic formulation for all the digits. The moment arms of the muscles and tendons of the index finger were estimated by the method proposed by Brook et al. (1995). The moment arms of the remaining fingers were scaled by the ratios of respective finger lengths to the index finger length.

For each individual finger, the muscle-tendon forces were estimated by solving a nonlinear optimization problem with the objective function of minimizing the muscle stress. Here, the muscle stress was defined as the quotient of the muscle force divided by its physiological cross sectional area (PCSA) and the objective function was defined as:

$$J = \sum_i (\frac{F_i}{PCSA_i})^2 \tag{3.7}$$

where i is the index of the muscles. The PCSA values of the index finger were from Chao and An (1978). The other fingers were assumed to have the same PCSA values as the index finger. A sufficiently small but nonzero number was assigned to the PCSA values of the virtual muscles to ensure that the virtual muscles are 'silent.'

Data Analysis

The joint angles and muscle-tendon forces acquired through the two-stage biodynamical modeling process formed 12- and 44-dimension data sets, respectively, and served as the inputs of the subsequent data analyses. Principal component analysis (PCA) (Dunteman, 1989) was used to examine the synergistic behaviors and to quantify

41

the spatiotemporal characteristics across the two types of movements.

The PCA is capable of discovering linear degrees of freedom underlying complex hand movements and checking whether and to what extent the high-dimensional hand movements can be reconstructed with low-dimensional data (less degree of freedom). The percent variance accounted for (PVAF) by the ith component, DF_i ($i = 1, ..., k$, where k is the total number of joints or the total number of musculo-tendon forces) can be computed as,

$$PVAF_i = \frac{Var(DF_i)}{Var(DF_1) + ... + Var(DF_k)} \cdot 100 \,. \tag{3.8}$$

The residual variance RV_i was defined as $1 - \sum_{j=1}^{i} PVAF_j$, which is a monotonically decreasing function of i.   The number of invariants or the functional degrees of freedom was then estimated by finding the i where a 'knee' (slope reduction point) (Daffertshofer et al., 2004) was observed in the linear-log plot of the RV_i curve.   All the preceding computations were implemented using MATLAB® programs (The MathWorks, Boston, MA).

An analysis of variance (ANOVA) was then conducted to examine the effects of movement type and subject on the $PVAF_i$ and the number of invariants using the General Linear Model procedure in SAS software program (SAS Institute, Cary, NC).

3.4 Results

Both grasping and 'enslaving' movements were closely reproduced in kinematics (Fig. 3.1 and Fig. 3.2) and kinetics (Fig. 3.3) by the model.   The root-mean-square error (RMSE) values for the pair-wise difference between the model-predicted and measured angular profiles for each joint ranged from 1.50° to 3.62° for grasping movements and from 0.58° to 2.95° for 'enslaving' movements (see Table 3.1).   The grand means of the RMSE values for grasping and 'enslaving' movements were 2.25° and 1.24°, respectively. Based on the model-predicted kinematics and joint torque, the muscle-tendon forces were predicted (Fig. 3.4); the peak flexor forces were found to have the same order of magnitude as values reported in the literature (Dennerlein et al., 1999; Kursa et al., 2006; Nikanjam et al., 2007).   The results also indicate that all the joints during grasping

movements underwent significant movements whereas the DIP joint only presented minimal movements during 'enslaving' movements (Fig. 3.1). Further, it can be observed that the FDP dominated grasping movements while the FDS dominated 'enslaving' movements (Fig. 3.4).

Table 3.1

Mean and standard deviation of the RMSE values for the pair-wise difference between the model-predicted and measured angular profiles for each joint for both grasping and 'enslaving' movements (unit: °)

Movement	Joint	Digit			
		2	3	4	5
grasping(n=11)					
	DIP	2.82(1.05)	3.62(0.67)	3.36(1.02)	2.86(1.23)
	PIP	1.92(1.26)	2.09(0.89)	2.06(0.97)	1.71(0.93)
	MCP	1.50(0.47)	1.68(0.64)	1.72(0.62)	1.61(0.88)
enslaving (n=11)					
	DIP	2.05(0.94)	0.86(0.51)	0.79(0.45)	0.67(0.20)
	PIP	2.94(1.13)	1.44(1.50)	1.00(0.98)	0.61(0.46)
	MCP	1.85(0.67)	1.31(0.64)	0.75(0.45)	0.58(0.46)
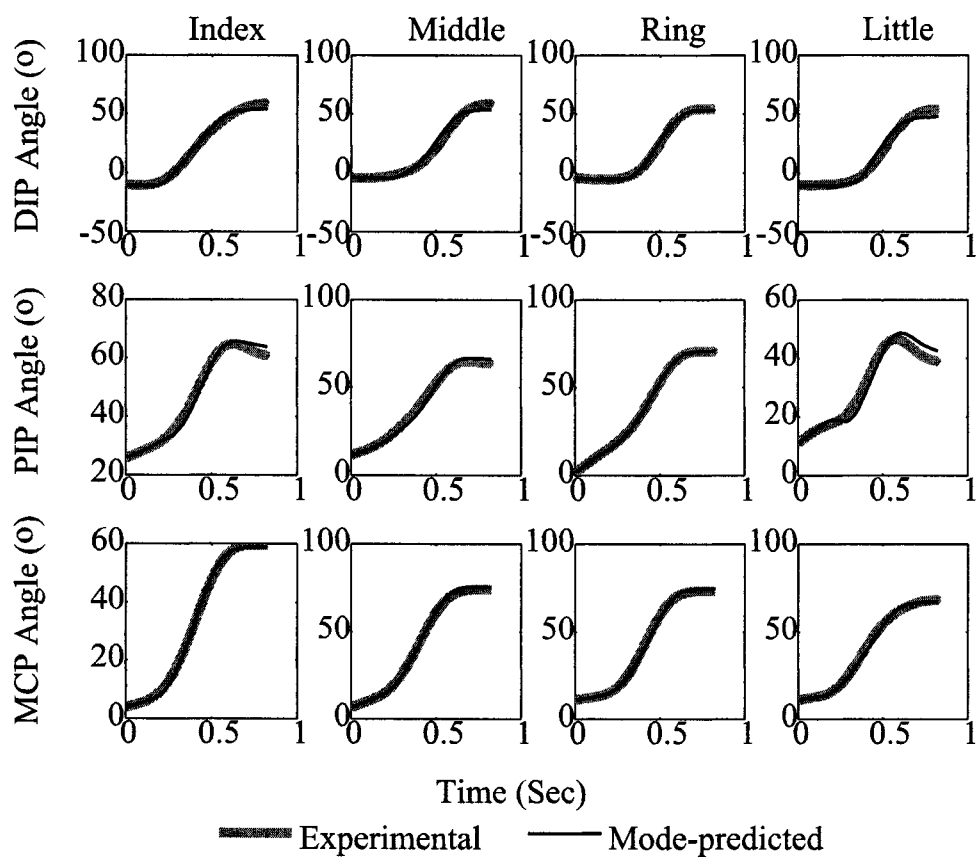
Fig. 3.1 (a) model-predicted and measured joint angle profiles at 12 joints for grasping
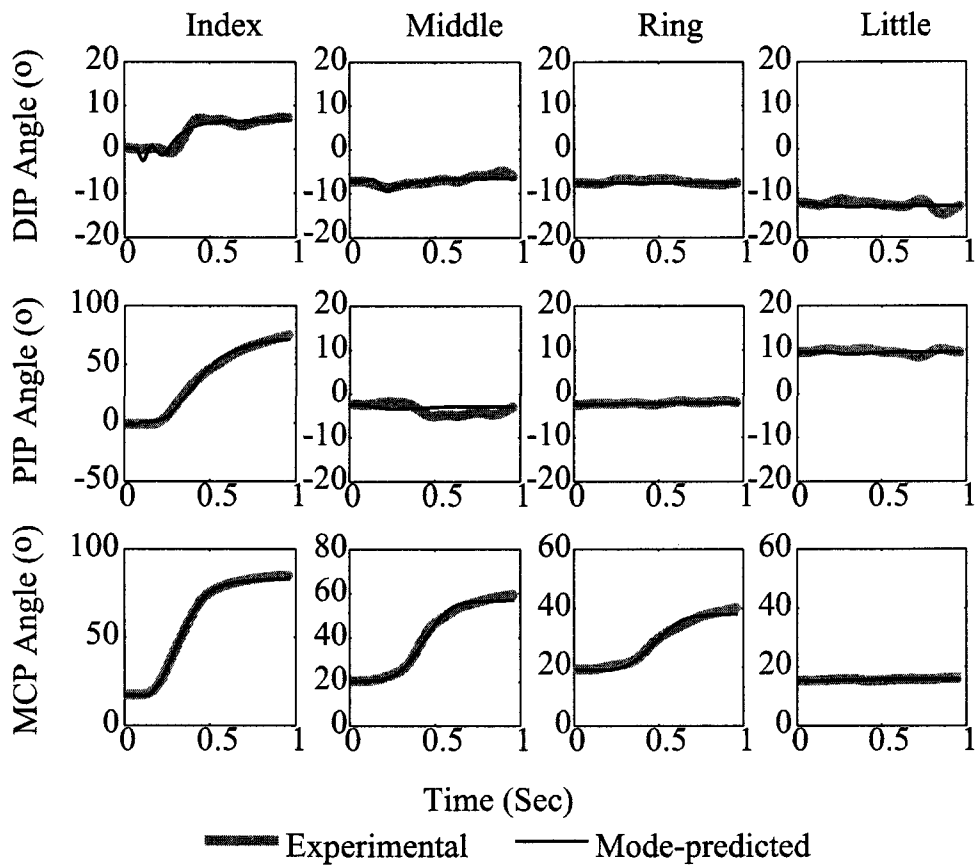
Fig. 3.1 (b) model-predicted and measured joint angle profiles at 12 joints for 'enslaving'

Fig. 3.1. A representative comparison of model-predicted (thick soild line) and measured (thin solid line) joint angle profiles at 12 joints for grasping (a) and 'enslaving' (b) movements.
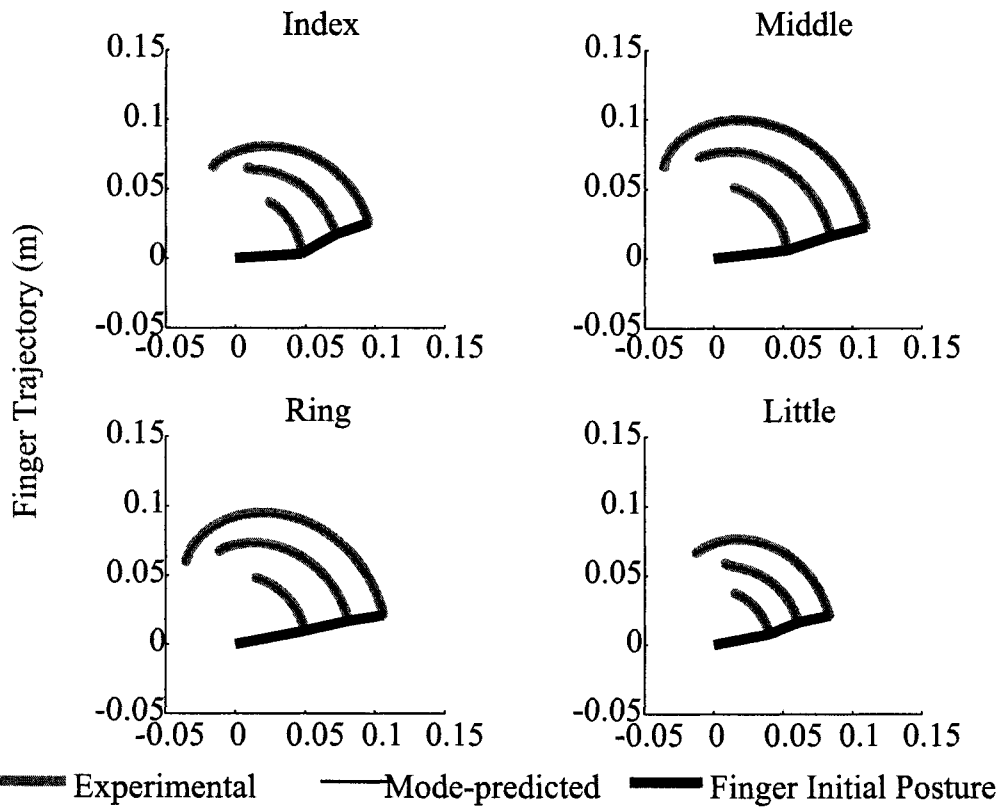
Fig. 3.2 (a) Model-predicted and measured finger trajectories for grasping
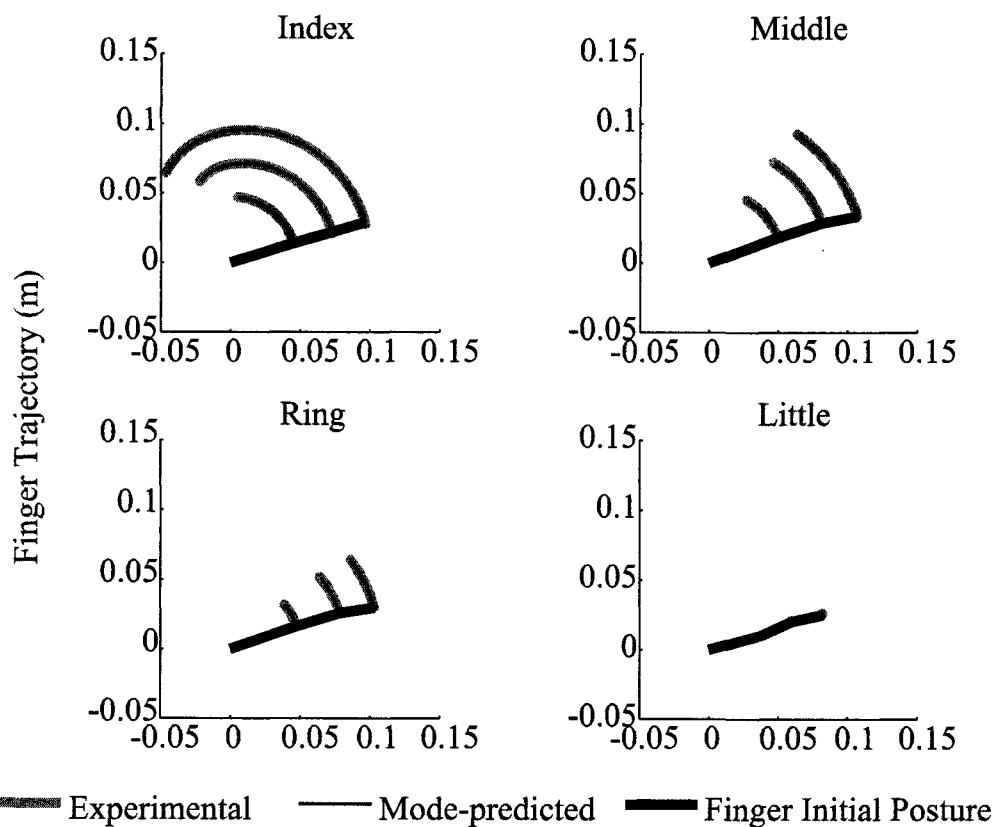
Fig. 3.2 (b) Model-predicted and measured finger trajectories for 'enslaving'

Fig. 3.2. Model-predicted (black thin line) and measured (grey thick line) finger trajectories in flexion-extension planes of digits 2-5 for grasping (a) and 'enslaving' (b) movements for the same representative case presented in Fig. 3.1. The three-segment linkage (black thick line) represents the initial finger posture with the origin being the MCP joint.
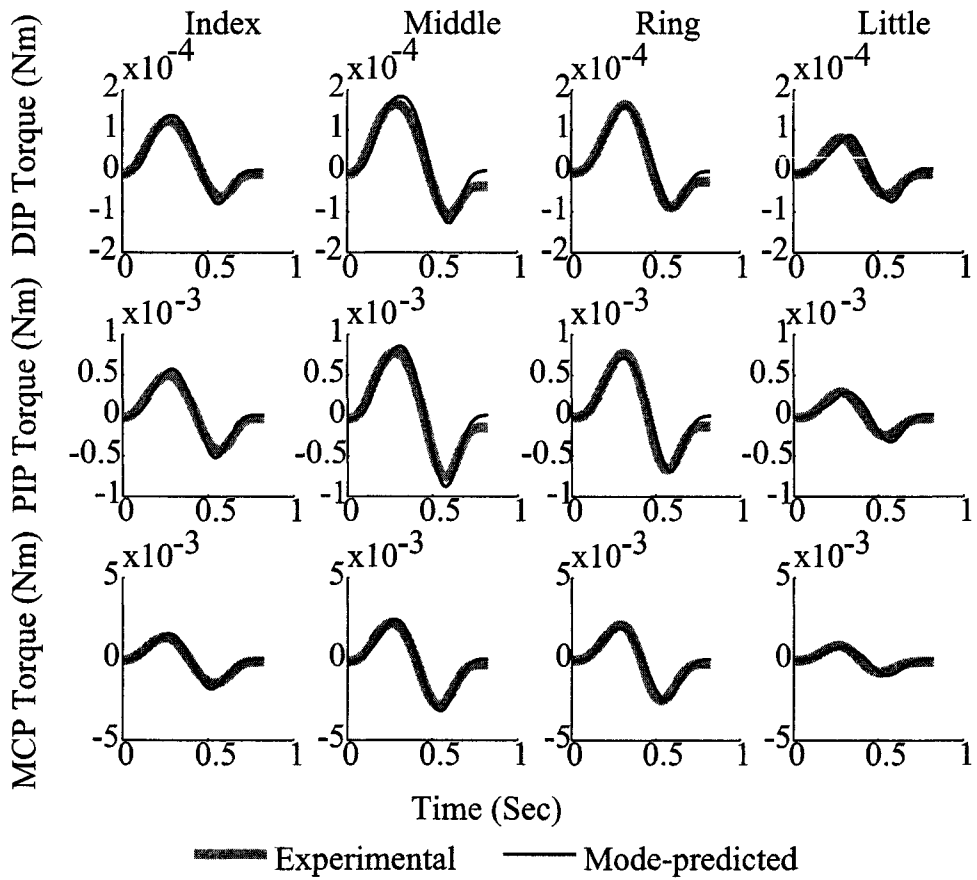
Fig. 3.3 (a) Model-predicted and inversely derived net joint torques for grasping
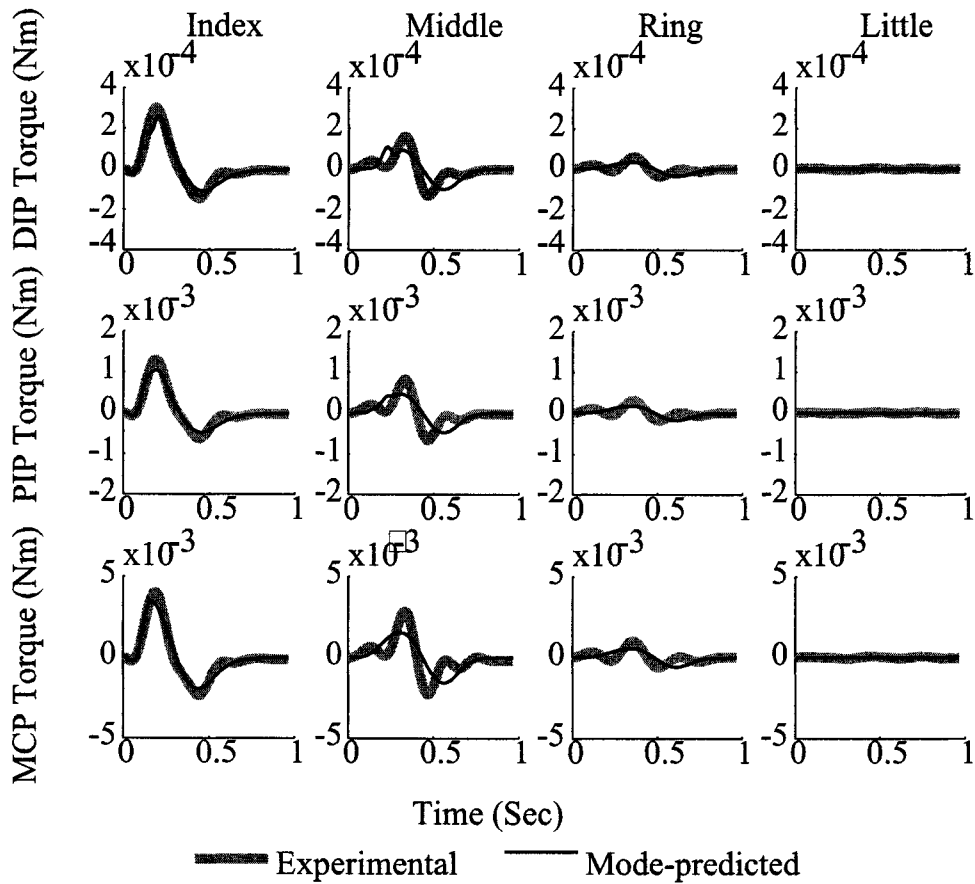
Fig. 3.3 (b) Model-predicted and inversely derived net joint torques for 'enslaving'

Fig. 3.3. Model-predicted and inversely derived net joint torques. Fig. 3.3a and 3.3b depict the model-predicted (black thin line) and inversely (measurement) derived net joint torques (grey thick line) at 12 joints as functions of time t for grasping (a) and 'enslaving' (b) movements for the same representative case presented in Fig. 1.
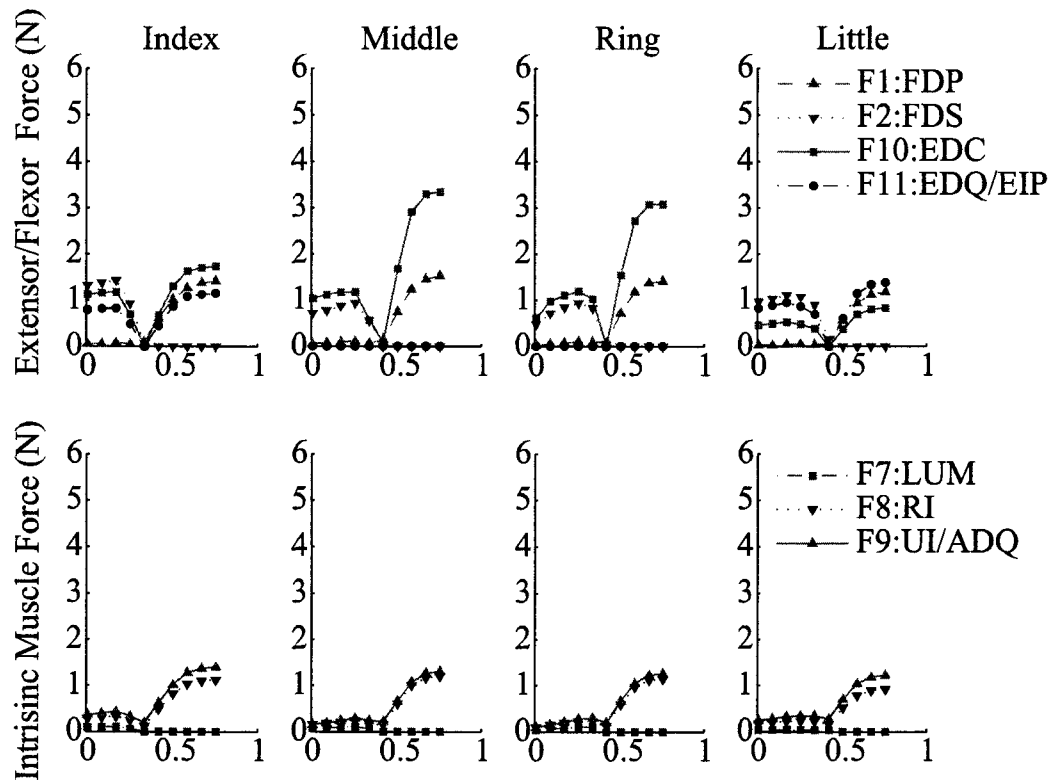
Fig. 3.4 (a) Muscle-tendon force profiles for grasping
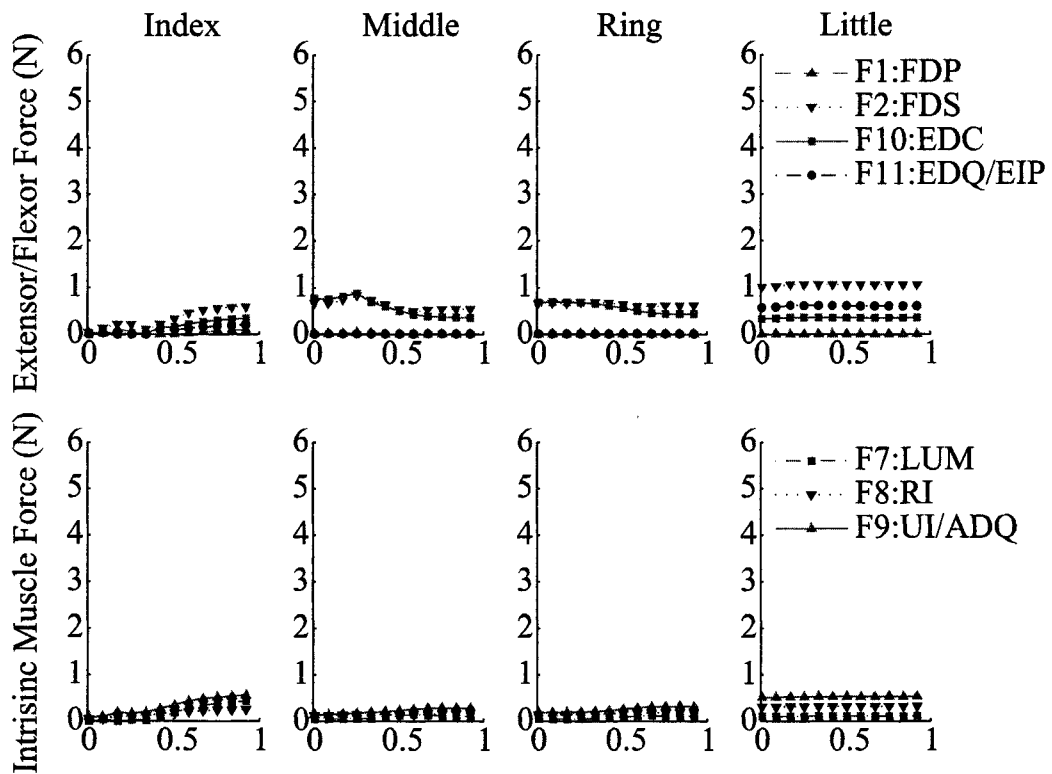
Fig. 3.4 (b) Muscle-tendon force profiles for 'enslaving'

Fig. 3.4. Muscle-tendon force profiles for grasping (a) and 'enslaving' (b) movements for the same representative case presented in Fig. 3.1. The FDP dominated grasping movements while the FDS dominated 'enslaving' movements.

The two "agonist-antagonist" components of torque actuators displayed stereotypical spatial-temporal patterns that were consistent across multiple joints, multiple fingers, and two types of movement (Fig. 3.5). These patterns, more in the temporal than in the spatial aspect, seem to resemble the activation patterns of the agonist and antagonist muscles during single joint movements (Gottlieb, 1998; Marconi et al., 2006).
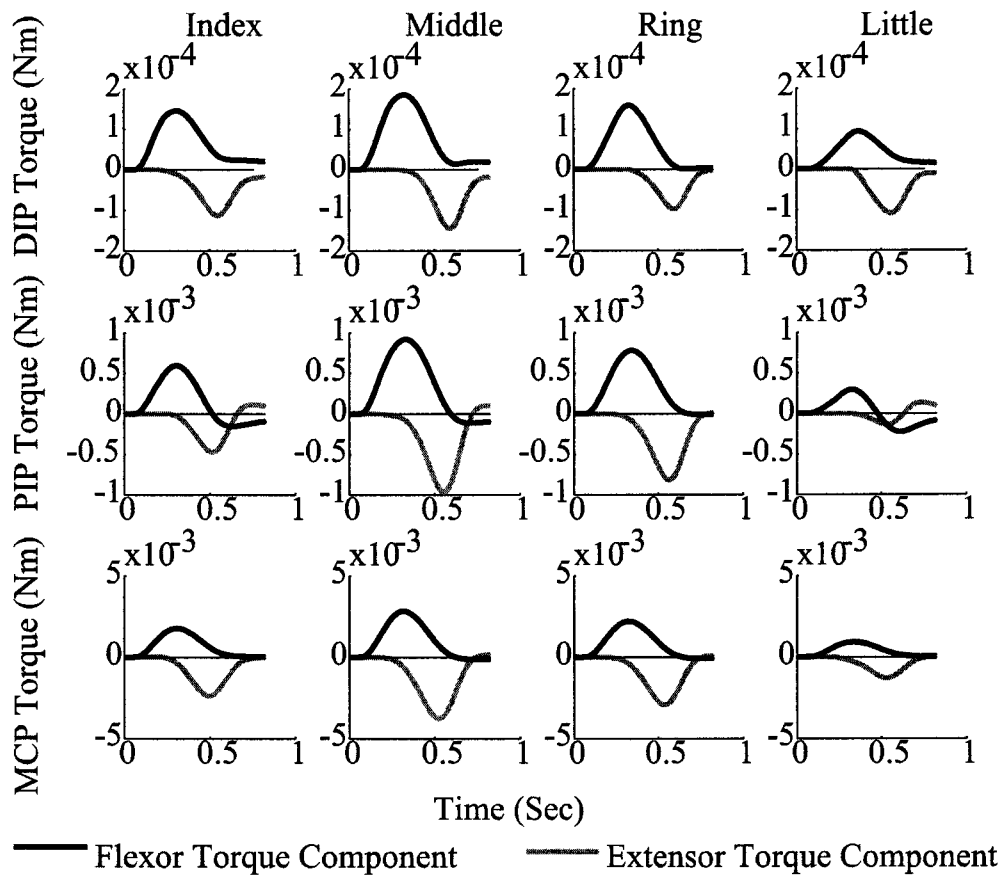
Fig. 3.5 (a) Torque components for grasping
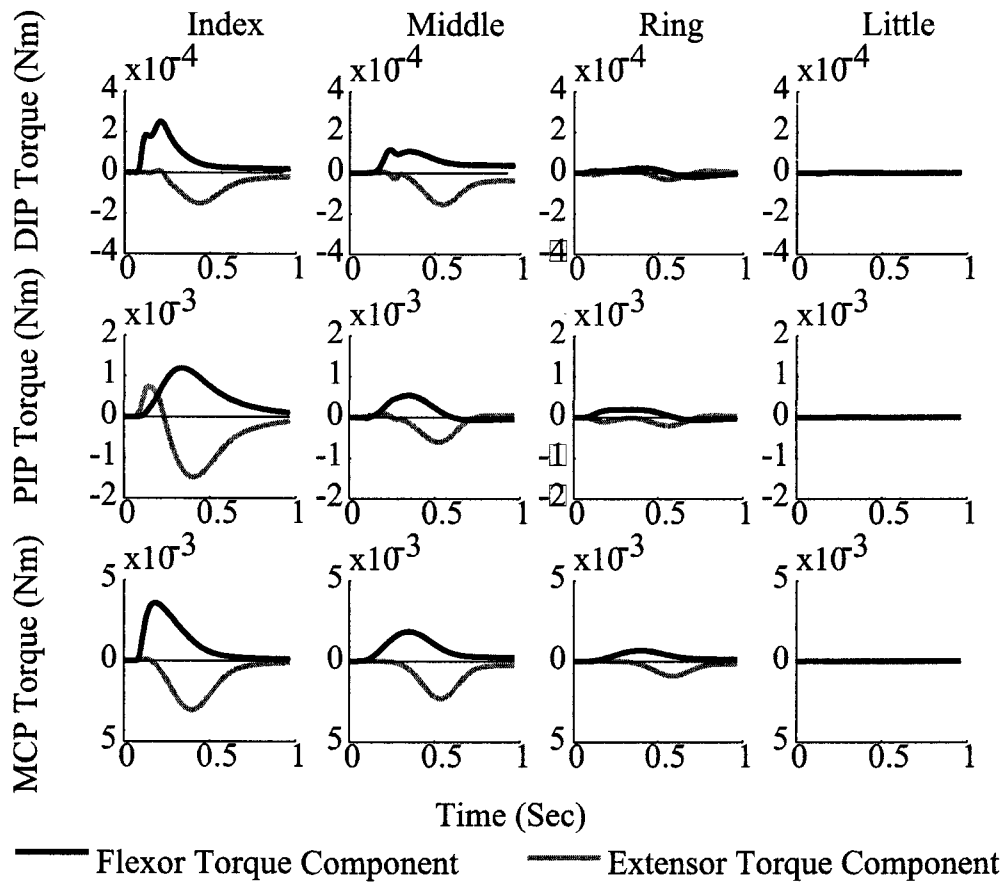
Fig. 3.5 (b) Torque components for 'enslaving'

Fig. 3.5. The torque components for the movements presented in Fig. 3.1a and 3.1b, respectively. The spatial-temporal pattern of the flexor (black line) and extensor (grey line) torque components for both movements were similar to the "agonist-antagonist" muscle activation patterns observed in single-joint movements. Note that the summations of the two components are the predicted net joint torque presented in Fig. 3.3a and 3.3b.

Subjects exhibited more coordinative behaviors across fingers during grasping movements than 'enslaving' movements. The mean ($\pm$SD) of the average absolute values of correlation coefficients across subjects of joint angle and muscle/tendon forces were 0.96($\pm$0.02) and 0.65($\pm$0.25), respectively, for grasping movements and only 0.48($\pm$0.29) and 0.27($\pm$0.22), for 'enslaving' movements.

The numbers of invariants or the functional degrees of freedom in the joint and

muscle-tendon dynamics, as revealed by the PCA, varied minimally between the two movements (Table 3.2). The distributions of the PAVF for two movements were almost same at the joint angle and muscle-tendon force levels (Fig. 3.6). The ANOVA did not identify any significant effect of movement type or subject on the number of invariants and PVAF (by the three leading PC's) for the joint angle and muscle-tendon forces. The three leading principal components accounted for at least 94% of the variance. The mean (±standard deviation) of the total PVAF (by the three leading PC's) were 99.88% (±0.14%) and 98.79% (±1.44%) at the joint and muscle-tendon force level, respectively.

Table 3.2

Mean and standard deviation of the number of invariants in the joint angle and muscle-tendon force for both grasping and 'enslaving' movements

Movement	Joint Angle	Muscle-tendon Force
grasping(n=11)	1(0)	3(1.61)
enslaving (n=11)	1.09(0.30)	3.09(1.45)
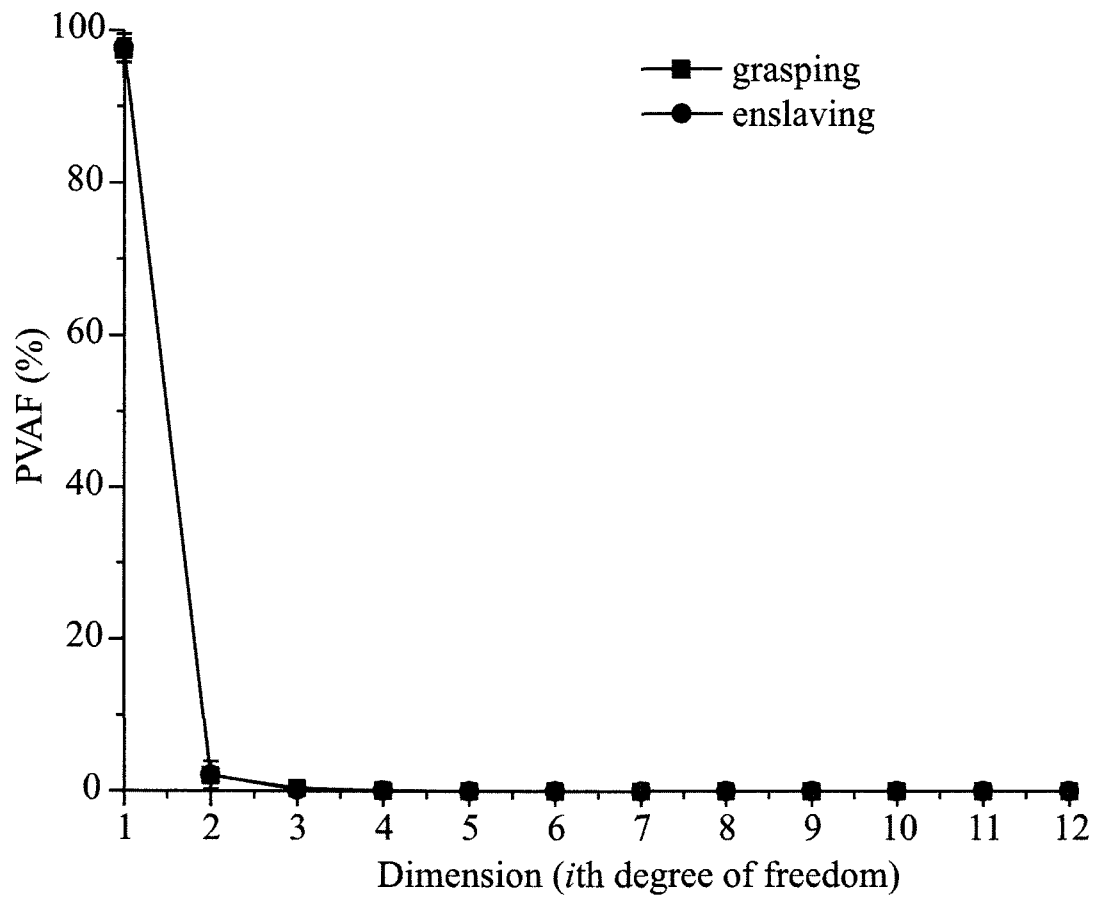
Fig. 3.6 (a) PVAF by each degree of freedom of joint angle
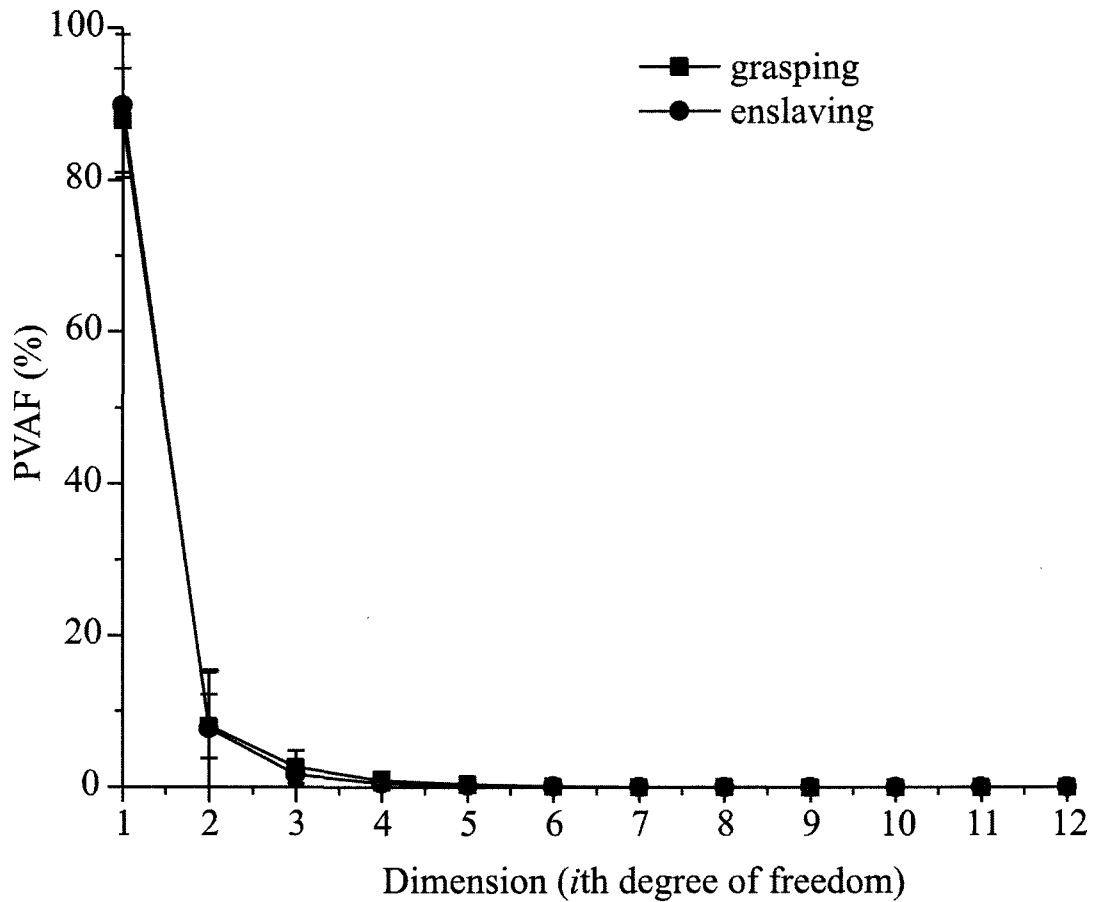
Fig. 3.6 (b) PVAF by each degree of freedom of muscle-tendon force

Fig. 3.6. PVAF by each degree of freedom of joint angle (a) and muscle-tendon force (b) for grasping and 'enslaving' movements.

3.5 Discussion

The current study investigated whether the mechanisms to control functionally different multi-finger movements remain consistent at the system control, joint and muscle-tendon dynamics levels. At the system control level, there appears to be a uniform scheme to control the two movements. Both movements were faithfully reproduced by the same forward dynamics model embedded with a unified control scheme. In addition, the response of each controller in the model displayed a consistent stereotyped pattern across movements: the generated torque components exhibited similar and physiologically plausible characteristics.

At the joint and muscle-tendon dynamics levels, evidence also emerged to support the stated hypothesis. The PCA showed that the joint angles and muscle-tendon forces of the two movements could be reconstructed by the same numbers of invariants, which were much smaller than the number of mechanical degrees of freedom possessed by the multiple fingers. The results also showed that the PVAF (by the three leading PC's) of the two movements had the same distributions and the three leading PC's dominated the variance.

A subtle difference in the role of the flexors was discerned in this study: the FDP served as the major flexor for cylinder-grasping, while the FDS served as the major flexor for 'enslaving' as the DIP joints exhibited minimal movements in the individuated flexions of the index finger. This difference seems to converge with the findings from neurophysiological studies (Butler et al., 2005; McIsaac and Fuglevand, 2007) suggesting that human beings have greater capacity in selectively activating the FDS than activating the FDP.

The observation that the movements actuated by different flexors had similar couplings and coordinative patterns may be a reflection of that the multi-fingered movements have hierarchical sources for dimensionality reduction. The multi-fingered movements are not only governed by the high level neuromotor synergies (Ishida et al., 2007) but also regulated by the 'non-neural somatic logic' (Valero-Cuevas et al., 2007) facilitated by the hand anatomical structure. Both of them could be a source for dimensionality reduction. The observed dimensionality reduction in muscle-tendon dynamics supported the postulation that a small set of neuromotor synergies could create most muscle activities of the finger (Ishida et al., 2007). The 'non-neural somatic logic' provided by the tendon network could further reduce the effective degree of freedom of observable human behaviors by limiting the possible control signals (Valero-Cuevas et al., 2007). These two sources for dimensionality reduction are cascaded in generating multi-fingered movements, as suggested by the findings that the number of invariants in the joint dynamics was smaller than that in the muscle-tendon dynamics and the mean correlation coefficient in the joint dynamics was larger than that in the muscle-tendon dynamics. When different flexors actuate the fingers through the same tendon network, the 'non-neural somatic logic' is activated and similar coupling and coordinative patterns

are generated.

The present study illustrated the use of a new methodology for a multi-level study of the invariants or synergies as control simplification mechanisms underlying complex human movement. Previous studies conducted at single discrete levels focused on only one aspect of synergy or one source of dimensionality reduction, and might produce misleading findings on, for example, where the reduction occurred. This study proposed a method to allow the dynamics and control of human movement to be investigated at multiple yet interconnected levels. It afforded more integrative insights into dimensional reduction behaviors and a differentiation of the sources for the reduction. Further investigation of the underlying mechanism of each individual source can thus be made possible.

The findings from this study can guide or inspire important applications. The study showed how different hyper-redundant multi-fingered movement acts can be controlled by a limited number of input commands. The knowledge gained could be applied to the design of the hand neuro-prosthetics and exoskeletons, which may be short of independent control sources or input commands (Weir, 2003).

It is acknowledged that the biomechanical model we used is deterministic in nature and could introduce artifacts into the model-derived solutions, particularly the musculo-tendon forces. The deterministic model relied on the assumption that the average values of musculoskeletal parameters represented the general population. The true inherent variability or relationship in muscle-tendon forces may thus be obscured. We expect that by taking into account the model parameter variability, more physically meaningful synergies can be identified in muscle-tendon dynamics.

3.6 References

Anderson, F.C., Pandy, M.G., 2001. Dynamic optimization of human walking. Journal of Biomechanical Engineering-Transactions of the ASME 123, 381-390.

Benjamin, M., Kaiser, E., Milz, S., 2008. Structure-function relationships in tendons: a review. Journal of Anatomy 212, 211-228.

Braido, P., Zhang, X., 2004. Quantitative analysis of finger motion coordination in hand manipulative and gestic acts. Human Movement Science 22, 661-678.

Brook, N., Mizrahi, J., Shoham, M., Dayan, J., 1995. A biomechanical model of index finger dyanmics. Medical Engineering & Physics 17, 54-63.

Butler, T.J., Kilbreath, S.L., Gorman, R.B., Gandevia, S.C., 2005. Selective recruitment of single motor units in human flexor digitorum superficialis muscle during flexion of individual fingers. Journal of Physiology 567, 301-309.

Chao, E.Y., An, K.N., 1978. Graphical interpretation of the solution to the redundant problem in biomechanics. Journal of Biomechanical Engineering 100, 159-167.

Cole, K.J., Abbs, J.H., 1987. Kinematic and electromyographic responses to perturbation of a rapid grasp. Journal of neurophysiology 57, 1498-1510.

Daffertshofer, A., Lamoth, C.J., Meijer, O.G, Beek, P.J., 2004. PCA in studying coordination and variability: a tutorial. Clin Biomech (Bristol, Avon) 19, 415-428.

Dennerlein, J.T., Diao, E., Mote, C.D., Rempel, D.M., 1999. In vivo finger flexor tendon force while tapping on a keyswitch. Journal of Orthopaedic Research 17, 178-184.

Dunteman, G.H. (1989). Principal components analysis. Newbury Park: Sage Publications.

Fish, J., Soechting, J.F., 1992. Synergistic finger movements in a skilled motor task. Experimental Brain Research 91, 327-334.

Gottlieb, G.L., 1998. Muscle activation patterns during two types of voluntary single-joint movement. Journal of Neurophysiology 80, 1860-1867.

Hager-Ross, C., Schieber, M., 2000. Quantifying the independence of human finger movements: Comparisons of digits, hands, and movement frequencies. Journal of Neuroscience 20, 8542-8550.

Ishida, F., Karatsua, K., Sakaguchi, Y., 2007. Muscle synergies extracted from human grasping movements. International Congress Series 1301, 110-113.

Kursa, K., Lattanza, L., Diao, E., Rempel, D., 2006. In vivo flexor tendon forces increase with finger and wrist flexion during active finger flexion and extension. Journal of Orthopaedic Research 24, 763-769.

Lee, S.W., Zhang, X., 2005. Development and evaluation of an optimization-based model for power-grip posture prediction. Journal of Biomechanics 38, 1591-1597.

Li, K., Zhang, X., 2008. A novel two-stage framework for musculoskeletal dynamic modeling: an application to multi-fingered hand movement. Sumbitted to IEEE Transactions on Biomedical Engineering.

Li, Z.M., 2006. Functional degrees of freedom. Motor Control 10, 301-310.

Li, Z.M., Dun, S.C., Harkness, D.A., Brininger, T.L., 2004. Motion enslaving among multiple fingers of the human hand. Motor Control 8, 1-15.

Marconi, N.F., Almeida, G.L., Gottlieb, G.L., 2006. Electromyographic and kinetic strategies to control movements. Revista Brasileira de Fisioterapia 10, 1-8.

Mason, C.R., Gomez, J.E., Ebner, T.J., 2001. Hand synergies during reach-to-grasp. J Neurophysiol 86, 2896-2910.

McIsaac, T.L., Fuglevand, A.J., 2007. Motor-unit synchrony within and across compartments of the human flexor digitorum superficialis. Journal of Neurophysiology 97, 550-556.

Menegaldo, L.L., Fleury, A.D., Weber, H.I., 2003. Biomechanical modeling and optimal control of human posture. Journal of Biomechanics 36, 1701-1712.

Menegaldo, L.L., Fleury, A.D., Weber, H.I., 2006. A 'cheap' optimal control approach to estimate muscle forces in musculoskeletal systems. Journal of Biomechanics 39, 1787-1795.

Nikanjam, M., Kursa, K., Lehman, S., Lattanza, L., Diao, E., Rempel, D., 2007. Finger flexor motor control patterns during active flexion: An in vivo tendon force study. Human Movement Science 26, 1-10.

Santello, M., Flanders, M., Soechting, J.F., 2002. Patterns of hand motion during grasping and the influence of sensory guidance. Journal of Neuroscience 22, 1426-1435.

Soechting, J.F., Flanders, M., 1997. Flexibility and repeatability of finger movements during typing: Analysis of multiple degrees of freedom. Journal of Computational Neuroscience 4, 29-46.

Thakur, P.H., Bastian, A.J., Hsiao, S.S., 2008. Multidigit movement synergies of the human hand in an unconstrained haptic exploration task. Journal of Neuroscience 28, 1271-1281.

Valero-Cuevas, F.J., Yi, J.W., Brown, D., McNamara III, R.V., Paul, C., Lipson, H., 2007. The tendon network of the fingers performs anatomical computation at a macroscopic scale. IEEE Transactions on Biomedical Engineering 54, 1161-1166.

Weir, R.F., 2003. The great divide - the human-machine interface: Issues in the control of prostheses, manipulators, and other human machine systems. In IEEE 29th Annual Northeast Bioengineering Conference.

Zhang, X., Lee, S.-W., Braido, P., 2003. Determining finger segmental centers of rotation in flexion-extension based on surface marker measurement. Journal of Biomechanics 36, 1097-1102.

CHAPTER IV
A PROBABILISTIC DYNAMIC MODEL FOR FINGER TENDON FORCE ESTIMATION CLARIFIES THE ROLES OF THE FLEXORS

4.1 Abstract

Previous deterministic finger biomechanical models predicted that the flexor digitorum superficialis (FDS) was silent whereas the flexor digitorum profundus (FDP) was the only active flexor during finger flexions. Experimental studies in vivo, however, recorded activities of both flexors. In this study, in an attempt to elucidate the roles of the flexors, a probabilistic biodynamic model of the index finger was constructed to estimate the muscle-tendon forces during an experimentally measured index finger flexion movement. Two thousand instantiations were simulated using a Monte Carlo method, with four model parameters, including moment arms, physiological cross sectional areas (PCSA), passive torques, and anthropometric measures as independent random variables. The muscle-tendon forces at each time point were determined using a nonlinear optimization technique. The model predicted that both FDS and FDP contributed to sustaining the movement and the FDS was not necessarily silent. The two distinct force patterns observed in vivo in previous studies were also corroborated by the simulations. The findings, contrary to previous deterministic models' predictions but in agreement with experimental measurements, clarified the controversy surrounding the roles of the flexors in finger movement dynamics.

4.2 Introduction

Assessment of the finger muscle-tendon forces is critical for understanding the functional anatomy of the hand and for designing prostheses and rehabilitation protocols (Chao et al., 1976; An et al., 1985). Several biomechanical models (Buchner et al., 1988; Brook et al., 1995; Sancho-Bru et al., 2001) have been proposed to estimate internal muscle-tendon forces of the fingers during hand movements. For example, Buchner et al. (1988) proposed a simplified planar dynamical finger model and estimated that the force of the flexor digitorum profundus (FDP) ranged from 2N to 6N during a hypothetical unloaded movement. Brook et al. (1995) reported that the estimated

61

extensor digitorum force was less than 10N in the free flexion motion and the FDP force was no more than 3N. A model proposed by Sancho-Bru et al. (2001) indicated much smaller tendon forces during a unloaded flexion/extension movement of the index finger; the estimated tendon forces were less than 4.5N and the FDP force ranged from 0N to 1.8N. All these models predicted no force in the flexor digitorum superficialis (FDS).

While the past studies provided important insights into the mechanics and production of coordinated hand movements, one significant shortcoming was that the models they employed were all deterministic. Such models use average values of musculoskeletal parameters for a group or population of varied size, which introduces artifacts into muscle-tendon force estimates and obscures the true inherent variability or relationship in muscle-tendon forces. Another limitation of the past model-based studies was that they used simulated finger movements that initiated all joint motions concurrently, contrary to experimental observations (Somia et al., 1998). The inaccurate kinematic input to biodynamic models, even only in the temporal aspect, can compromise the validity of estimated time-dependent muscle-tendon forces and lead to equivocal understanding of the function of a muscle or tendon.

Indeed, there have been inconsistencies between these model-predicted muscle-tendon force patterns and flexor forces measured in vivo or the electromyography (EMG) patterns (Darling et al., 1994; Dennerlein et al., 1999; Kuo et al., 2006; Nikanjam et al., 2007). Dennerlein et al. (1999) showed that the FDS force ranged from 0N to 4N before the fingertip touched the key during tapping. Kursa et al (2006) suggested both the FDS and FDP muscles were active during the index finger flexion. They reported that mean FDS tendon forces ranged from 1.3N to 8.5N respectively. Nikanjam et al. (2007) reported that the FDS force ranged from -0.8N to 4.0N at 0 degree wrist flexion. These experimental observations about the FDS activities contradicted the predictions from previous models (e.g., An et al., 1979; An et al., 1983; Buchner et al., 1988; Brook et al., 1995). The disparity suggested that the muscle-tendon force relationships in fingers might not be well described by deterministic models with simulated unrealistic kinematic input. These limitations have impeded further understanding of muscle-tendon force relationships during hand movements.

Recent applications of stochastic methods in a few biomechanical modeling

endeavors (Mirka and Marras, 1993; Hughes and An, 1997; Chang et al., 2000; McLean et al., 2003; Davidson et al., 2004; McLean et al., 2004; Langenderfer et al., 2006) have demonstrated the power of stochastic methods in predicting the population behaviors. The success encouraged us to incorporate stochasticity to a biomechanical hand model and, by taking into account the variability of the finger muscle-tendon geometry, to seek a mechanistic clarification of the role of the flexors in index finger coordination.

In the present study, we propose a probabilistic model for estimating the muscle-tendon forces in the index finger during flexion. We incorporate stochasticity into musculoskeletal parameters of a biodynamical model, and use Monte-Carlo simulation method to capture the parameter variability. Our hypothesis was that accommodating variability of musculoskeletal parameters in the model would result in better population-based predictions of the muscle-tendon forces, and specifically would clarify the roles of the flexors (FDP and FDS) in finger movement production and control.

4.3 Methods

Biomechanical Model

The index finger is modeled as an open chain of three segments-distal phanlanx (DP), middle phanlanx (MP), and proxiamal phalanx (PP), connected by three 1-DOF revolute joints—distal interphalangeal (DIP), proximal interphalangeal (PIP) and metacarpophalangeal (MCP) joints. The segments are simplified as conical cylinders with a density of $1.1 g/cm^3$ (Dempster, 1955); the mass and moment of inertia of each segment are functions of the length and thickness of the segment.

The three-segment dynamic system is actuated through an intricate network of extrinsic and intrinsic muscles (Brand and Hollister, 1999; Gonzalez et al., 2005). The extrinsic muscles include two flexors, the FDP and FDS, inserting at the bases of DP and MP, respectively, and two extensors, the extensor digitorum communis (EDC) and extensor indicis proprius (EIP), inserting on the dorsal side of the PP. The tendon of EDC trifurcates over PP into extensor slip (ES) and two lateral bands (LB and UB); the former inserts onto the MP while the latter two re-connect and merge into the terminal tensor (TE) inserting onto DP. The intrinsic muscles include the lumbrical (LUM) and interosseous muscle and form the extensor hood mechanism with the extensor tendons.

The LUM originates from the tendon of the FDP and inserts on the lateral bands of extensor. The interosseous muscles, radial or ulnar, originate from the lateral aspects of the MCP and insert on either side of the extensor hood.

The dynamics of this index finger biomechanical system without considering the gravity at time t can be represented by the following equations of motion:

$$M(\theta(t))\ddot{\theta}(t) = V(\theta(t), \dot{\theta}(t)) + \tau(t), \tag{4.1}$$

where $\theta(t) \in \mathfrak{R}^{3\times1}$ is the angle vector, $M(\theta(t)) \in \mathfrak{R}^{3\times3}$ is a positive definite mass matrix, $V(\theta(t), \dot{\theta}(t)) \in \mathfrak{R}^{3\times1}$ represents the centrifugal (square of joint velocity) and Coriolis forces, $\tau(t) \in \mathfrak{R}^{3\times1}$ is the torque vector at the joints. Given a finger motion, $\theta(t)$, the net joint torque at each joint $\tau(t)$ can be calculated from Equation 4.1.

This biomechanical system is subject to the moment equilibrium conditions, which can be described by the following equation when taking into account the passive torque:

$$\tau = M \cdot F + \tau_{passive} \tag{4.2}$$

where

$$\tau = [\tau_1 \ \tau_2 \ \tau_3]^T, \quad F = [F_1 \ F_2 \ ... \ F_{11}]^T, M = \begin{bmatrix} m_{11} & 0 & m_{13} & & & & & & & & \\ m_{21} & m_{22} & & m_{24} & m_{25} & m_{26} & & & & & \\ m_{31} & m_{32} & & & & & m_{37} & m_{38} & m_{39} & m_{3,10} & m_{3,11} \end{bmatrix},$$

$\tau_{passive} = \begin{bmatrix} \tau_1^p & \tau_2^p & \tau_3^p \end{bmatrix}$; m_{jk} is moment arm of muscle/tendon force k with respect to joint j, $\tau_{passive}$ is the passive torque. It is assumed that the passive torque was effective only at the MCP joint and followed a third-order polynomial torque-angle relationship (Kamper et al., 2002). The passive torque was therefore expressed as:

$$\tau_{passive} = \begin{bmatrix} 0 & 0 & a\theta_3^3 + b\theta_3^2 + c\theta_3 + d \end{bmatrix} \tag{4.3}$$

where a, b, c, and d, are the coefficients of the polynomial. It is also assumed that no abduction-adduction occurs in the MCP joint during finger flexion-extension. Therefore, another moment equilibrium equation can be obtained:

$$M_4 \cdot F = 0 \tag{4.4}$$

where $M_4 = [m_{41} \ m_{42} \ 0 \ 0 \ 0 \ 0 \ m_{47} \ m_{48} \ m_{49} \ m_{4,10} \ m_{4,11}]$ and m_{4k} is the moment arm of muscle-tendon force k with respect to the MCP joint for abduction and

adduction movements.

Four force constraints reflecting the interconnected nature of multiple finger tendons are included in the model as suggested by Brook et al. (1995):

$$F_3 = \chi_{RB} F_6 + \chi_{UB} F_5 \tag{4.5}$$

$$F_4 = (1 - \alpha_{UI}) F_9 + (1 - \alpha_{LUM}) F_7 + (1 - 2\alpha_{LE}) F_{10} + K(\varepsilon_{UB} + \varepsilon_{RB}) \tag{4.6}$$

$$F_5 = \alpha_{LE} (F_{10} + F_{11}) + \alpha_{LUM} F_7 - K\varepsilon_{UB} \tag{4.7}$$

$$F_6 = \alpha_{LE} (F_{10} + F_{11}) + \alpha_{LUM} F_7 - K\varepsilon_{RB} \tag{4.8}$$

where χ_{RB} and χ_{UB} are two cosine terms, which account for the convergence angles of the RB and UB onto the TE; ε_{RB} and ε_{UB} account for the relative motion between the ES and the RB and UB, respectively. The α coefficients are additional unknowns, which are determined in the subsequent nonlinear optimization; K is the tendon elasticity coefficient.

Given that the moment arm values in M are known, the moment equilibrium system contains 11 unknown muscle/tendon forces and 3 unknown α coefficients in 8 equations. The muscle/tendon forces could be estimated by solving a nonlinear optimization problem with the objective function of minimizing the muscle stress. Here the muscle stress is defined as the quotient of the muscle force divided by its physiological cross sectional area (PCSA) and thus the objective function is expressed as:

$$J = \sum_{i \in A} \left(\frac{F_i}{PCSA_i} \right)^2 , \quad A = \{1, 2, 7, 8, 9, 11\} \tag{4.9}$$

where i is the index of the muscles.

Monte Carlo Simulation of Model Parameters

Force predictions by the biomechanical model depend on model parameters including the moment arms, PCSAs, and passive torques. In previous deterministic models, parameters such as moment arms of extensors and PCSA values are assumed constant across subjects for the entire range of motion (Fig 4.1a); parameters such as moment arms of flexors and passive torques are assumed constant across subjects for a given posture (Fig 4.1b). The current model recognizes the variability in these parameters and models the parameters as random variables using Monte-Carlo methods (Fig 4.1c and

65

4.1d).
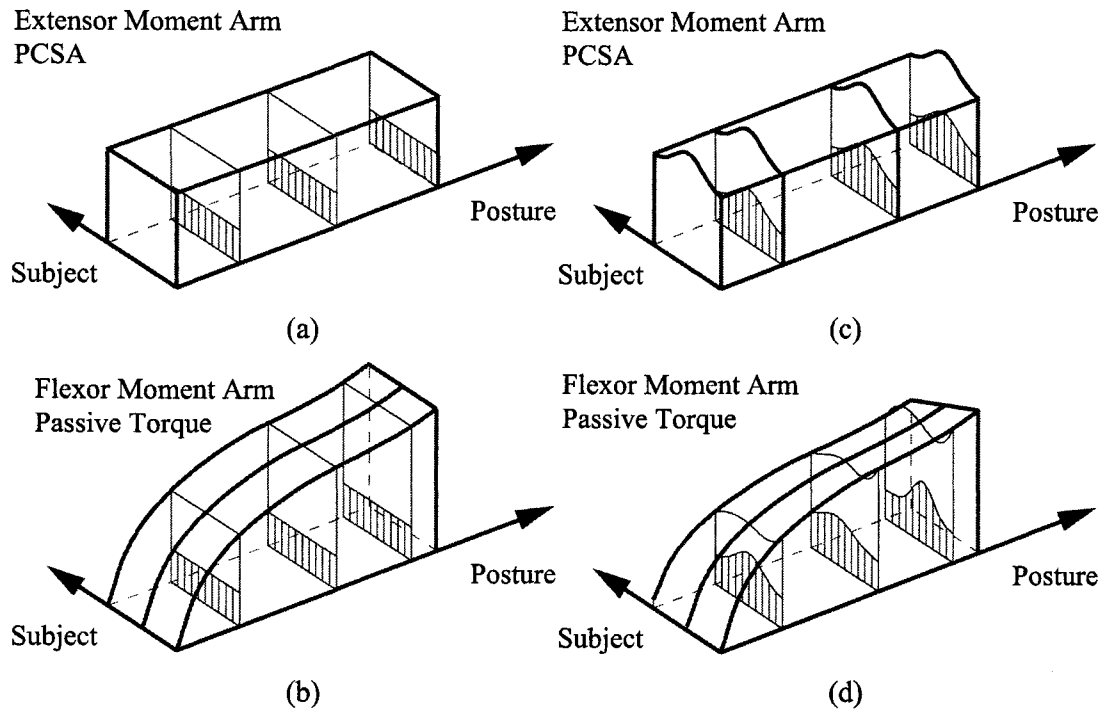
Fig. 4.1. Uniform, posture-independent (a) and posture-dependent (b) distributions of musculoskeletal parameters most commonly used in conventional deterministic models; more realistic posture-independent (c) and posture-dependent (d) distributions in the proposed stochastic model.

The first set of the random variables are the moment arms of the two flexors (FDS and FDP) and two extensor tendons (ES and TE).   These moment arms are usually estimated using tendon excursion based models (An et al., 1983).   The flexor tendon excursions at the DIP, PIP, and MCP joints can be estimated by the equation:

$$E = \theta d + 2y\left(1 - \frac{\theta/2}{\tan(\theta/2)}\right) \tag{4.10}$$

where d is the distance between long axis of the bone and the tendon, y is the distance from the joint center to sheath, θ is the joint angle in radians, and E is the excursion. The extensor tendon excursions can be estimated as

$$E = r\theta \tag{4.11}$$

where r is the radius of the articular surface. The associated moment arms are derived by differentiating the excursion, that is, $m = \dfrac{dE}{d\theta}$. Therefore, the moment arms of the extensor tendons are

$$m = r \tag{4.12}$$

and the moment arms of the flexors are

$$m = d + y \cdot g(\theta) \tag{4.13}$$

where $g(\theta)$ is a function of θ.

Unlike previous deterministic models in which the parameters r, d, and y were modeled as constants across subjects for a population, these parameters are modeled as independent random variables following a normal distribution in this study (2 parameters per joint for each flexor and 1 for each extensor tendons, 12 in total). The means of these parameters, $\mu_{mr} = (\mu_1, \ldots, \mu_{12})'$, are from Brook et al. (1995) and the variances are assumed to be 0.1μ.

Similarly, the PCSA values of the two flexors are modeled as random variables following normal distributions with the means from An et al (1983). In addition, the four coefficients of passive torque, a, b, c and d, also follow normal distributions with the means from Kamper et al. (2002). All the variances of the parameters are chosen to be one-tenth of their means. The variability of general anthropometry was also taken into account. The length and thickness of each segment are also modeled as the random variables with the mean and standard deviation derived were from a database previously established in our laboratory (Braido and Zhang, 2004).

Implementation and Test

Two thousand samples were generated for each of the random variables using the statistics toolbox in Matlab 7.5 (Mathworks, Natick, MA) and served as the input to the biomechanical model described in the preceding section. Note that parameters of other muscle-tendon units in this model were calculated based on the methods from Brook et al. (1995), which were constant across subjects or functions of the above described random

variables.

The proposed probabilistic model was tested on an experimentally measured index finger movement, which was randomly taken from a pre-established database (Braido and Zhang, 2004). Identical joint kinematic data were used in all instantiations of the simulation (Fig. 4.2a), which allowed us to isolate the effects of the variability in musculoskeletal parameters in the investigation.

(a)   (b)
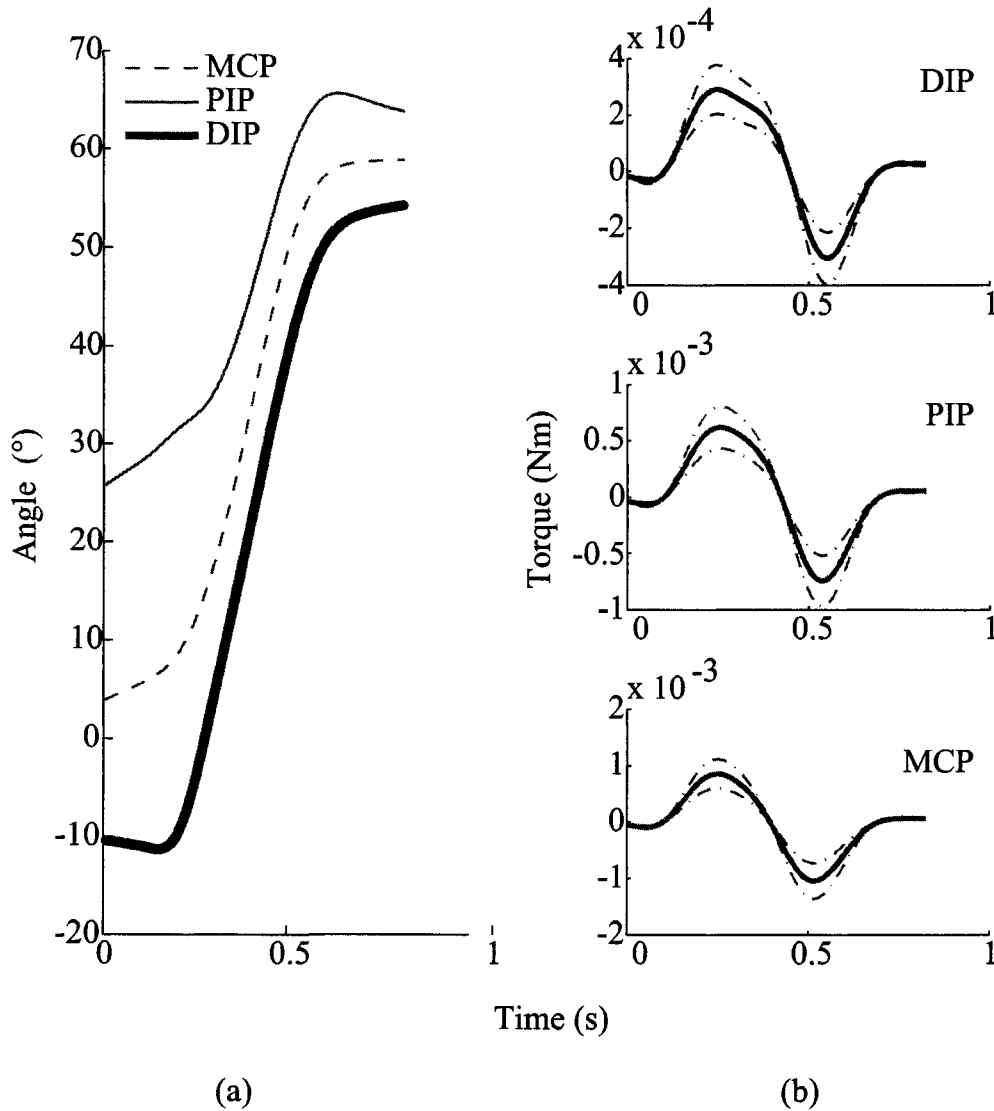
Fig. 4.2.   The measured index finger kinematics input (left) and the simulated torque profiles (right) with the time-varying mean (solid line) and ±1 standard deviation (the two dash-dot lines).   The sequence of the joint movement is PIP-DIP/MCP.

4.4 Results

The resulting torques at the three finger joints (Fig. 4.2b) had similar sinusoidal profiles, and the dispersion across the instantiations simulating anthropometric variability increased with the torque magnitudes. The model parameters generated by Monte Carlo simulations formed plausible population representations. The simulated moment arms followed the normal distributions at any given posture (Fig. 4.3) and the flexor moment arms exhibited multimodal or skew distributions through the entire movement (Fig. 4.4). The ranges of the simulated moment arms (Table 4.1) generally agreed with the experimental data (An et al., 1983).

Table 4.1

Simulated moment arms summarized over the entire movement (unit: mm)

Joint	FDP	FDS	TE	ES
DIP (N=2000)	3.04(0.29)		1.88(0.19)	
PIP (N=2000)	7.05(1.12)	5.27(0.95)		2.92(0.29)
MCP (N=2000)	10.56(1.32)	11.78(1.38)		
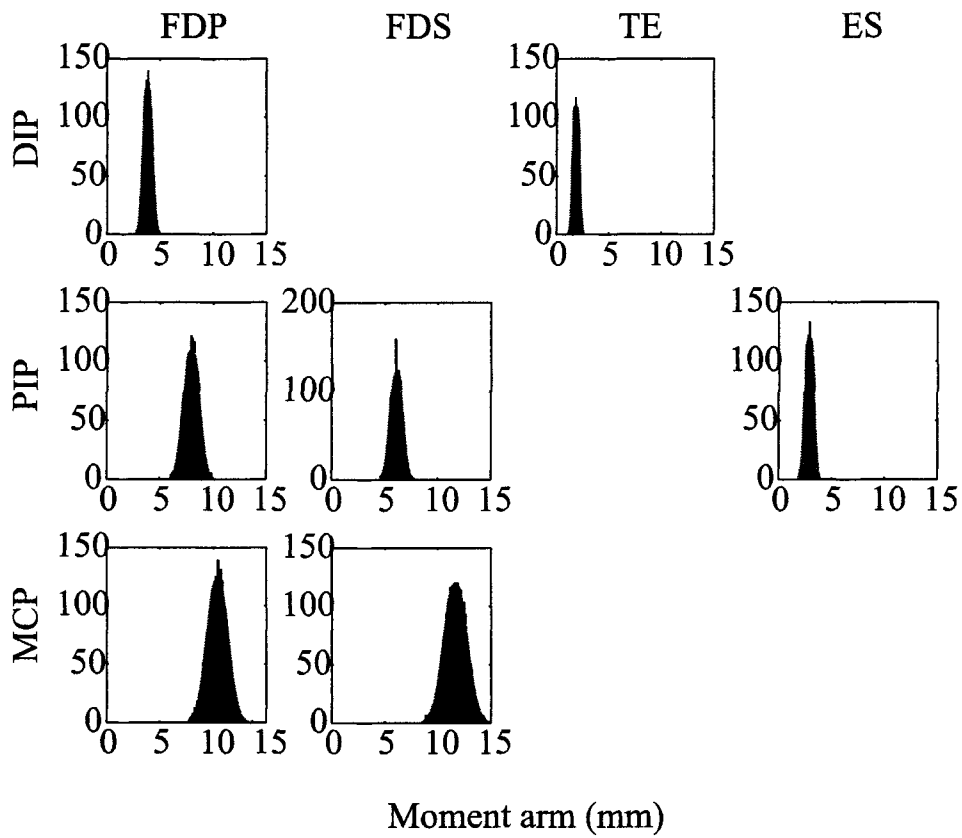
Fig. 4.3. Histograms of the simulated moment arms of the flexors and extensor tendons at MCP, PIP and DIP joints for a given posture. The red lines are the fitted normal distributions.
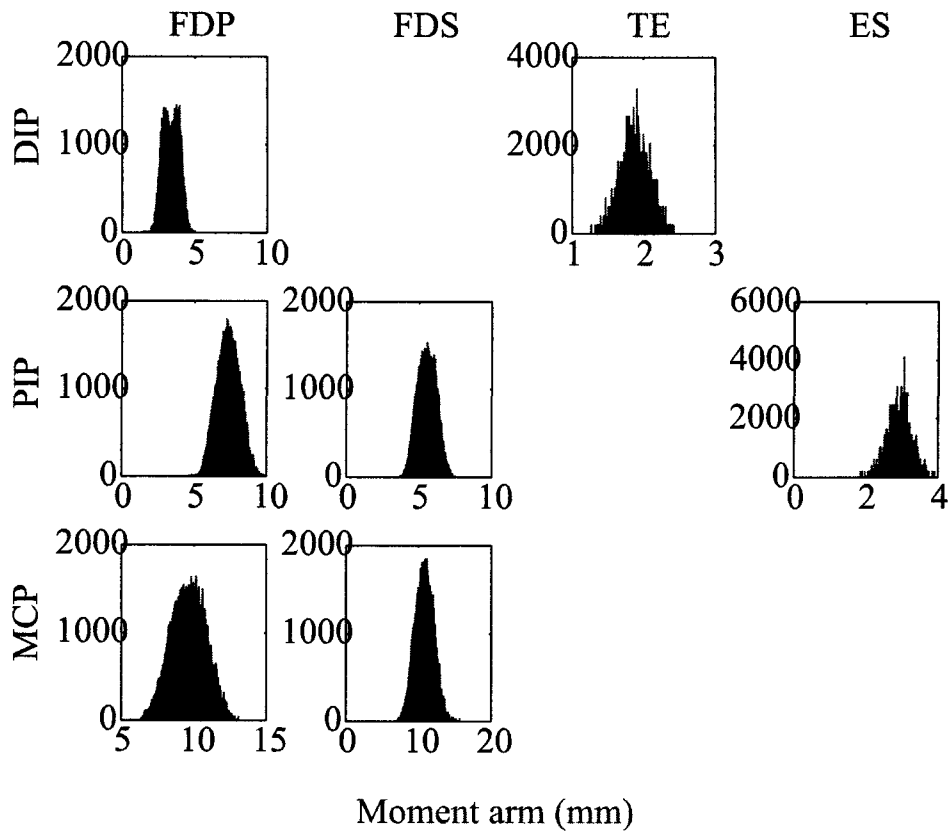
Fig. 4.4.   Histograms of the simulated moment arms of the flexors and extensor tendons at MCP, PIP and DIP joints through the entire movement.   The moment arms of the FDP at the DIP exhibit a bi-modal distribution while the moment arms of the FDP at the MCP exhibit skewed distributions.

The flexor forces (Fig. 4.5) predicted based on the simulated model parameters displayed a pattern that qualitatively agrees with what was recorded in a in-vivo study by Nikanjarn et al. (2007).   The predicted FDP force declined in the initial phase of the movement (the first 0.4s) and then increased to sustain the motion and dominated the movement after the initial phase.   The FDP force ranged from 0~4.72 N.   The mean (±SD) of the maximum FDP was 1.22 (±0.97) N during the initial phases and 1.41 (±0.60) N after.   The FDS dominated the movement in the initial phase and decreased significantly before the FDP dominated the movement.   The FDS force ranged from 0~5.98 N.   The mean (±SD) of the max FDS was 1.74(±0.93) N during the initial phase and 0.17(±0.29) N after.   This FDS force-time pattern in the initial phase also agreed

with what was observed by Dennerlein et al. (1999). An inspection of the individual flexor force profiles also revealed that another type of force pattern reported by Nikanjam et al. (2007) could be simulated. In those cases, the FDP dominated the entire movements and the FDS force was consistently smaller than FDP force.
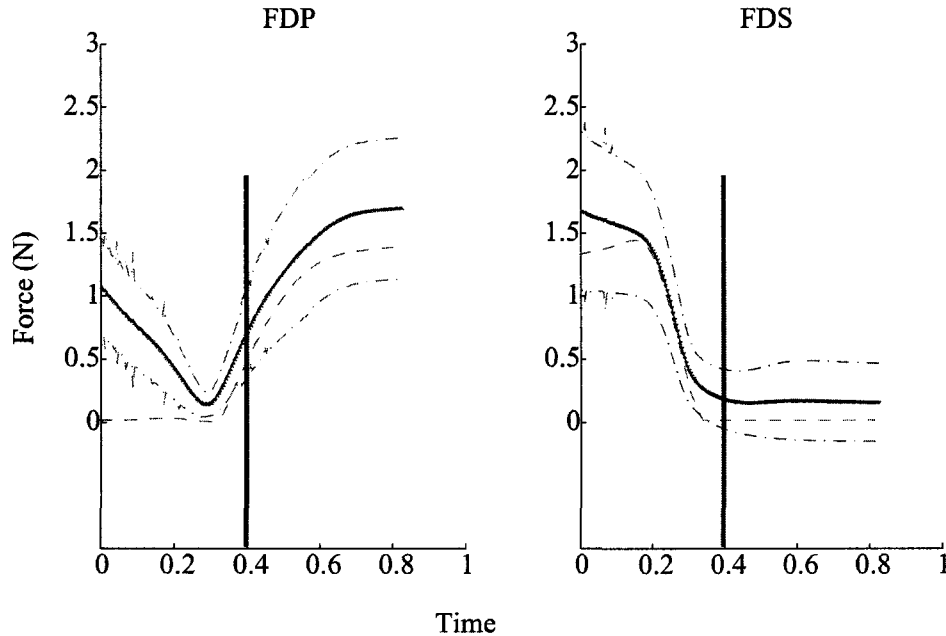
Fig. 4.5. The predicted FDP and FDS force distributions during the movement: the time-varying mean (solid line) and ±1 standard deviation (between the two dash-dot lines). The vertical solid lines denote the time point before which the FDS dominated the movement and after which the FDP dominated the movement. The dashed line is the force profile predicted by a deterministic model.

When the passive torque was not taken into consideration, the general patterns of the flexor forces did not change but the total flexor forces decreased. The range of FDP force reduced to 0~4.74 N. The mean (±SD) of the maximum FDP was 0.56 (±0.30) N during the initial phases and 1.48(±0.55) N when the FDP became the major flexor. The range of FDS force reduced to 0~4.03 N. The mean (±SD) of the maximum FDS was 1.39(±0.4) N during the initial phase and 0.05(±0.03) N after.

Both the FDP and FDS forces formed gamma distributions at a given time or posture (Fig 4.6). When the FDP dominated the movement, the FDS was no longer silent, in

contrary to the prediction by a deterministic model (Fig 4.5). The probability for FDS not being silent (FDS force >0. 01N) ranged from 36.4%~56.7% when the passive torque was taken into account, and 0.15%~2.8% when not.

a)   b)

c)   d)
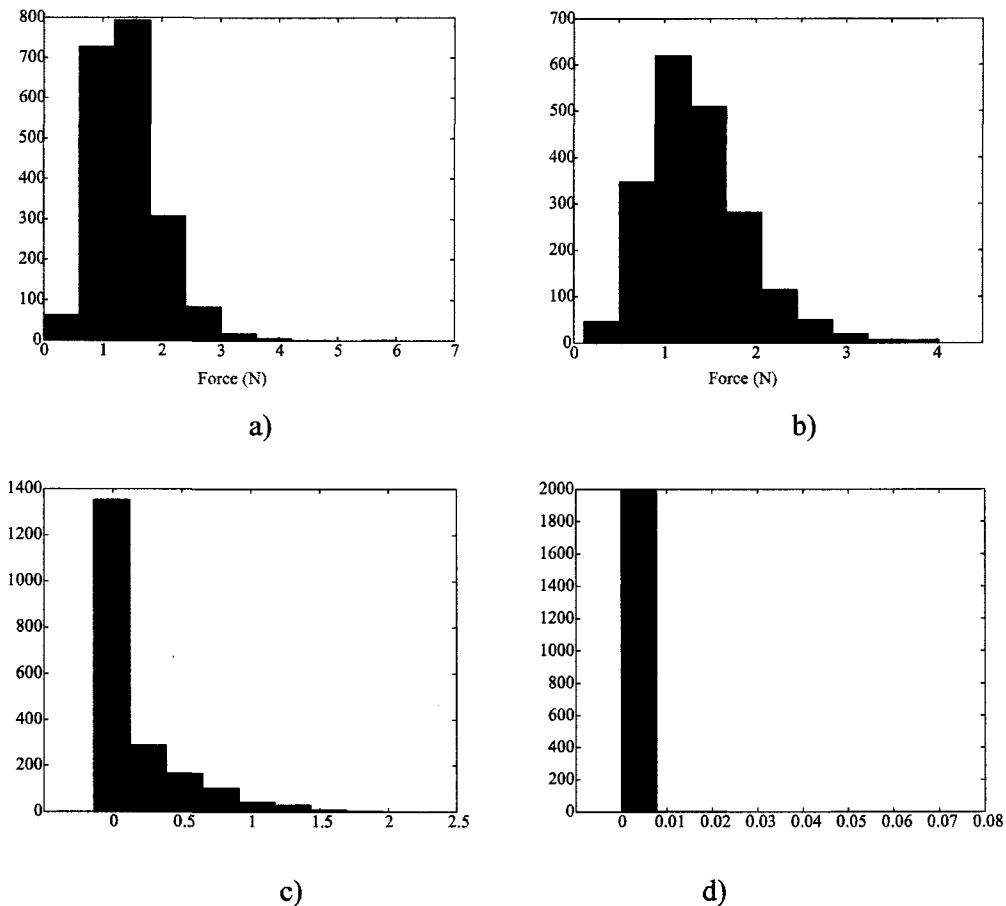
Fig. 4.6. The FDP (with the passive torque (a) vs. without the passive torque (b)) and FDS (with the passive torque (c) vs. without the passive torque (d)) force distributions at a randomly selected posture when the FDP was the major flexor. The FDP exhibited gamma distributions.

4.5 Discussion

The current study developed a probabilistic model incorporating musculoskeletal parameter variability for estimating the time-dependent muscle-tendon forces in the index finger during flexion. The model was able to unveil and delineate the active, intricate roles of the FDP and FDS during finger flexion, which previous deterministic models

failed to show (Buchner et al., 1988; Brook et al., 1995; Sancho-Bru et al., 2001) but were indicated in experimental studies (Darling et al., 1994; Dennerlein et al., 1999; Kuo et al., 2006; Nikanjam et al., 2007). Two experimentally observed distinct force patterns have also been corroborated by the simulations. These results clarified the controversy surrounding the roles of the flexors in finger movement dynamics and demonstrated the efficacy of probabilistic models in predicting more realistic muscle-tendon forces for a population.

There are several reasons why the FDS is not necessarily silent during finger flexion, all of which in fact were evidenced in the computational process of our work. First, since the FDS is the only flexor inserting onto the MP, it has to be activated when the PIP motion is initiated prior to the DIP and MCP motions. Second, the FDS must also exert force to balance the pass force generated in the ES which inserts onto the opposite (dorsal) aspect of the MP. Third, the FDS could be activated in order to reduce the total muscle stress. It was not mechanically advantageous to activate the movement by the FDP solely when the passive moments resisted the finger movement or when the PCSA value of the FDS was much greater than that of FDP.

Compared to previous stochastic biomechanical modeling work (Hughes and An, 1997; Langenderfer et al., 2006), this study featured a novel method to capture both the inter-person and movement-dependent variabilities of musculoskeletal parameter. It thus allowed the implementation of stochasticity in dynamical modeling. The previous models directly treated the moment arms as random variables and neglected the fact that the moment arms are both posture-dependent and subject-specific. Such an approach is only adequate in static biomechanical modeling and for studies of static tasks.

This study also demonstrated the feasibility of using stochastic methods to explore the function of anatomical structures that are not well understood. Accuracies in both model topology and parameters are critical for understanding the function of the biomechanical systems with model-based approaches (Valero-Cuevas et al., 2007). Yet, creating a pool of the candidate topologies for modeling movement is difficult. For example, it was known that the joint stiffness was an important property at finger joints and the joint passive torque of the finger could be caused by a number of factors (Li et al., 2006); however, little has been incorporated into the model topology in the previous

74

finger models (Buchner et al., 1988; Brook et al., 1995). In this study, the passive moment at MCP was modeled as a random variable, whose mean followed the experimentally established data (Kamper et al., 2002). In doing that, the model topology was probed by the Monte-Carlo simulations and the effect of passive torque on the muscle-tendon forces was examined.

It is acknowledged that this study excluded variability of many other parameters, aspects, and the covariance between the parameters. Future endeavors will focus on expanding the parameter space to cover more variability, acquiring the covariance structures between parameters, and conducting more systematic experimental validation.

4.6 References

An, K.N., Ueba, Y., Chao, E.Y., Cooney, W.P., Linscheid, R.L., 1983. Tendon excursion and moment arm of index finger muscles. Journal of Biomechanics 16, 419-425.

Braido, P., Zhang, X., 2004. Quantitative analysis of finger motion coordination in hand manipulative and gestic acts. Human Movement Science 22, 661-678.

Brand, P.W., Hollister, A.M. (1999). Clinical mechanics of the hand (3rd ed.). St. Louis, MO: Mosby-Year Book, Inc.

Brook, N., Mizrahi, J., Shoham, M., Dayan, J., 1995. A biomechanical model of index finger dyanmics. Medical Engineering & Physics 17, 54-63.

Buchner, H.J., Hines, M.J., Hemami, H., 1988. A dynamical model for finger interphalangeal coordination. Journal of Biomechanics 21, 459-468.

Chang, Y.W., Hughes, R.E., Su, F.C., Itoi, E., An, K.N., 2000. Prediction of muscle force involved in shoulder internal rotation. Journal of Shoulder and Elbow Surgery 9, 188-195.

Darling, W.G., Cole, K.J., Miller, G.F., 1994. Coordination of index finger movements. Journal of Biomechanics 27, 479-491.

Davidson, P.L., Chalmers, D.J., Wilson, B.D., 2004. Stochastic-rheological simulation of free-fall arm impact in children: application to playground injuries. Computer Methods in Biomechanics and Biomedical Engineering 7, 63-71.

Dempster, W.T. (1955). Space requirements of the seated operator (No. WADC-TR-55-159). Wright-patterson Air Force Base, OH: Aerospace Medical Research Laboratories.

Dennerlein, J.T., Diao, E., Mote, C.D., Rempel, D.M., 1999. In vivo finger flexor tendon force while tapping on a keyswitch. Journal of Orthopaedic Research 17, 178-184.

Gonzalez, M., Mohan, V., Elhassan, B., Amirouche, F., 2005. Biomechanics of the digit. Journal of the American Society for Surgery of the Hand 5, 48-60.

Hughes, R.E., An, K.N., 1997. Monte Carlo simulation of a planar shoulder model. Medical & Biological Engineering & Computing 35, 544-548.

Kamper, D.G., George Hornby, T., Rymer, W.Z., 2002. Extrinsic flexor muscles generate concurrent flexion of all three finger joints. Journal of Biomechanics 35, 1581-1589.

Kuo, P.L., Lee, D.L., Jindrich, D.L., Dennerlein, J.T., 2006. Finger joint coordination during tapping. Journal of Biomechanics 39, 2934-2942.

Kursa, K., Lattanza, L., Diao, E., Rempel, D., 2006. In vivo flexor tendon forces increase with finger and wrist flexion during active finger flexion and extension. Journal of Orthopaedic Research 24, 763-769.

Langenderfer, J.E., Carpenter, J.E., Johnson, M.E., An, K.N., Hughes, R.E., 2006. A probabilistic model of glenohumeral external rotation strength for healthy normals and rotator cuff tear cases. Annals of Biomedical Engineering 34, 465-476.

Li, Z.M., Davis, G., Gustafson, N.P., Goitz, R.J., 2006. A robot-assisted study of intrinsic muscle regulation on proximal interphalangeal joint stiffness by varying metacarpophalangeal joint position. J Orthop Res 24, 407-415.

McLean, S.G., Huang, X., Su, A., Van Den Bogert, A.J., 2004. Sagittal plane biomechanics cannot injure the ACL during sidestep cutting. Clinical Biomechanics (Bristol, Avon) 19, 828-838.

McLean, S.G., Su, A., van den Bogert, A.J., 2003. Development and validation of a 3-D model to predict knee joint loading during dynamic movement. Journal of Biomechanical Engineering 125, 864-874.

Mirka, G.A., Marras, W.S., 1993. A stochastic model of trunk muscle coactivation during trunk bending. Spine 18, 1396-1409.

Nikanjarn, M., Kursa, K., Lehman, S., Lattanza, L., Diao, E., Rempel, D., 2007. Finger flexor motor control patterns during active flexion: An in vivo tendon force study. Human Movement Science 26, 1-10.

Sancho-Bru, J.L., Perez-Gonzalez, A., Vergara-Monedero, M., Giurintano, D., 2001. A 3-D dynamic model of human finger for studying free movements. Journal of Biomechanics 34, 1491-1500.

Somia, N., Rash, G.S., Wachowiak, M., Gupta, A., 1998. The initiation and sequence of digital joint motion. A three-dimensional motion analysis. Journal of Hand

Surgery:Journal of the British Society for Surgery of the Hand 23, 792-795.

Valero-Cuevas, F.J., Anand, V.V., Saxena, A., Lipson, H., 2007. Beyond parameter estimation: Extending biomechanical modeling by the explicit exploration of model topology. Ieee Transactions on Biomedical Engineering 54, 1951-1964.

CHAPTER V
SUMMARY AND RECOMMENDATIONS

5.1 Overview

The three coherent studies integrated in this dissertation center on the development of a minimum-input biodynamical model for multi-fingered hand movements.

The key component of this dissertation is a two-stage computational framework for biodynamic modeling of human movement proposed in the first study, which addresses two major limitations that has been plaguing musculoskeletal biodynamical modeling: (1) the trade-off between model realism and computational efficiency, and (2) the irreconcilability of the inverse and forward solutions. This framework creates a benchmark for studying the multi-fingered hand movements from three levels, system control, joint and muscle-tendon dynamics, and enables the examination of a central claim of the second study that common mechanisms are deployed to control different multi-fingered movements. In the second study, we demonstrate that the two types of multi-fingered hand movements, cylinder-grasping and individuated flexion of the index finger ('enslaving'), could be predicted by the same forward dynamic model embedded with a common physiologically stereotyped control scheme. We also show that the predicted movements have consistent numbers of invariants in the joint and muscle-tendon dynamics as well as consistent underlying dynamical couplings and coordination patterns. This study thus provides evidence to support the commonality of control mechanisms underlying different multi-finger movements. The third study is an exploratory study. It is an attempt to address the limitations of previous deterministic finger biomechanical models, in particular, their inability to predict experimentally measured flexor digitorum superficialis activities. A probabilistic biodynamic model is proposed to elucidate the roles of the flexors and clarifies the controversy surrounding the roles of the flexors in finger movement dynamics. Taken together, these three studies build a unique biomechanical science foundation for a minimum-input biodynamical model that identifies important applications, including design of next-generation hand prostheses or hand rehabilitation strategies, and advancement of digital human simulation and virtual reality technologies.

This chapter summarizes the principal contributions made by this dissertation

research and provides recommendations for future work.

5.2 Principal contributions

1) Establishment of a physiologically based control scheme for controlling multi-fingered hand movements

A novel stereotyped control scheme is established for controlling multi-fingered movements (Chapter II).   In this control scheme, the torque actuator of each joint has two components: one represents the flexor action and the other represents the extensor action.   Both torque actuators are controlled by proportional-derivative (PD) controllers and modulated by distribution functions that emulate muscle contractile mechanics. This control scheme overcomes the difficulties in generating realistic kinetics in forward dynamics simulation.   The hypothesized two-component torque actuator originates from the observation that the agonist and antagonist muscles exhibit different spatial-temporal patterns as recorded by electromyography (EMG) during single-joint movements (Gottlieb, 1998; Marconi et al., 2006).   The responses of the controllers in applications of modeling multi-fingered movements display spatial-temporal patterns similar to the experimentally observed EMG patterns.

2) Introduction of an open-structure modeling framework addressing two major limitations hindering the advancement of biodynamical modeling and applications

A two-stage modeling framework (Chapter II) is proposed to address two major limitations plaguing musculoskeletal biodynamical modeling: the realism-efficiency trade-off and the irreconcilability of the inverse and forward solutions.   This framework has an open architecture allowing various control schemes or distribution functions to be hypothesized and empirically tested.   By incorporating the physiologically based control scheme described in Chapter II, it addresses the two limitations as demonstrated by an application of this framework to cylinder-grasping movement.   The model achieves biomechanical realism at a relatively low computational cost.   It faithfully reproduces the kinetics (joint torque), suggesting that it provides a solution to alleviate the inverse dynamics failure problem.

3) Establishment of a method for studying human movement control and dynamic at multiple yet interconnected levels

A method is established to allow the dynamics and control of human movement to be investigated at multiple yet interconnected levels (Chapter III). This method uses the two-stage modeling framework to connect the information at three levels—the system control, joint and muscle-tendon dynamics. The analyses based on the information from multiple levels could provide integrative insights into dimensional reduction behaviors.

4) Demonstration of common mechanisms to control functionally different multi-fingered movements

Although previous investigations have shown that all the joints and fingers of the hand are not completely independent, the findings from these investigations are contradictory on issues such as at which levels or to what extent at each level the control simplification or dimensionality reduction occurs. The current work (Chapter III) demonstrates that the mechanisms to control two types of multi-fingered movement, cylinder-grasping and individuated flexion of the index finger ('enslaving'), are generally consistent in the system control, joint and muscle-tendon dynamics. It also shows that these coordinative multi-fingered movements have multiple sources for dimensionality reduction in the control. Insights gained from the study can guide or inspire applications including the design of next-generation hand neuro-prosthetics and exoskeletons or hand rehabilitation strategies.

5) Development and validation of a probabilistic finger biodynamical model

A probabilistic biodynamic model is proposed to predict the population-based muscle-tendon forces in the index finger during flexion (Chapter IV). In this model, a novel approach is introduced to allow the implementation of stochasticity in dynamical modeling. Previous stochastic biomechanical modeling work (Hughes and An, 1997; Langenderfer et al., 2006) directly treated moment arms as random variables, which was not adequate for studies dynamic tasks. We model the parameters determining moment arms and passive torques as random variables and capture both the inter-person and movement-dependent variabilities of musculoskeletal parameter in a dynamic model. This is a unique methodological contribution to biodynamical modeling of the musculoskeletal systems.

This probabilistic model is tested on an experimentally measured index finger movement. The predicted flexor force patterns qualitatively agree with what were

recorded in two in-vivo studies (Dennerlein et al., 1998; Nikanjam et al., 2007), which gives support to the validity of this model. The findings also clarify the controversy surrounding the roles of the flexors in finger movement dynamics.

5.3 Recommendations for future work

The dissertation has indicated several research directions for future work.

1) Examination of alternative distribution functions and control scheme for movement prediction

The gamma and beta distribution functions proposed for simulating the initial torque profiles of agonist and antagonist and antagonist latency are chosen somewhat arbitrarily although they performed well in modeling the kinetics of the finger flexions. Plamondon and his colleague (Plamondon et al., 1993; Plamondon, 1995b; 1995a; 1998; Plamondon et al., 2003) proposed a kinematic theory for analyzing rapid human movements and proved that the impulse response of agonist or antagonist converges toward a lognormal function using the Central Limit Theorem. Their success inspires us to think whether there are some rationales behind the gamma and beta distribution functions and whether any other distributions could be used for substituting these distribution functions with solid physiological and theoretical bases.

Therefore, a thorough search of alternative distribution functions will not only create a database of control scheme for movement prediction but also yield insights into underlying mechanisms of the generation and modulation of muscle torque during movement.

2) Application of the proposed modeling framework to other types of hand movement and other multi-segmental body movements

Although the proposed modeling framework has been only tested with two types of multi-finger movements (Chapter II&III), the modeling framework is expected to be applicable for other types of hand movement and other multi-segmental body movements since the proposed modeling framework has an open structure for allowing us to incorporate various control schemes or distribution functions. By applying the modeling framework to other movements, we will have an opportunity to examine whether human motor control strategies are joint-dependent. Moreover, if we

demonstrate that other multi-segmental body movements can be modeled by this modeling framework, we should be able to create a comprehensive model to simulate all the human movements efficiently.

3) Development of a biodynamical model with a centralized control mechanism driving digits 2-5 simultaneously

Although the multi-fingered movements are successfully predicted by the current forward dynamic model (Chapter II & III), the current model uses a decentralized control mechanism to drive the forward simulations. The four fingers are modeled as four uncorrelated three-segment biomechanical systems. Independent torque actuators are used to generate the net joint torques of the joints for each finger. The decentralized control mechanism has two drawbacks. First, a large set of parameters is requested to parameterize the control mechanism (6 parameters per joint). Second, the decentralized control mechanism cannot be able to predict the inter-digit coupling mechanisms since the fingers are modeled separately. We can develop a biodynamical model with a centralized control mechanism driving digits 2-5 simultaneously, The control parameters of all the torque actuator can be created from a small set of parameters through certain transformations given that the multi-fingered hand movement are highly synergic and the functional degree of freedom is much less than the mechanical degree of freedom. The biodynamical model only requires a minimum number of input commands.

4) Refinement of the muscle-tendon biomechanical model by including ignored mechanisms

The finger biomechanical model used to estimate the muscle-tendon force (Chapter II, III) is based on a conceptual model of finger anatomy (Valero-Cuevas et al., 2007). The model topology of the hand may be far away from reality in that the anatomical extensor mechanism may be over simplified (Valero-Cuevas et al., 2007; Lee et al., 2008). Therefore, a refined model is desired with these currently disregarded mechanisms or elements, such as crossover tendons, frictional forces, and soft tissues. We expect that consideration of such mechanisms will improve the accuracy of muscle-tendon force estimation. The enhancement of the accuracy model topology could significantly affect the current understanding of the roles of the muscle-tendon units in finger movement and

control and advance our understanding of the functions of each muscle-tendon units.

5) Refinement of the developed probabilistic model to achieve better matches between model predictions and experiment observations

Although the current work (Chapter IV) can predict flexor forces whose patterns qualitatively agreed with the experimental observations, a more comprehensive model is desired to further improve the predictive accuracy. Some of the musculoskeletal parameters of the current model are assumed constant and all the parameters are chosen to follow independent normal distributions, which may not accurately reflect the reality.

The current probabilistic model can be improved in two steps. In the first step, the parameter space of the model can be expanded to cover more variability. Variability of all the muscle-tendon units including intrinsic muscles, the extensor digitorum communis (EDC) and extensor indicis proprius (EIP) can be taken into consideration. In the second step, the realistic distributions of these parameters and the covariance structures between parameters will be acquired and the musculoskeletal parameters will be modeled based on the acquired more realistic information. The complexity of the current probabilistic model will significantly increase. The refined model is expected to achieve better matches between model predictions and experiment observations.

5.4 References

Alexander, R.M., 2002. Tendon elasticity and muscle function. Comparative Biochemistry and Physiology 133, 1001-1011.

Clewley, R.H., Guckenheimer, J.A., Valero-Cuevas, F.J., 2008. Estimating effective degrees of freedom in motor systems. IEEE Transactions on Biomedical Engineering 55, 430-442.

Dennerlein, J.T., Diao, E., Mote, C.D., Rempel, D.M., 1998. Tensions of the flexor digitorum superficialis are higher than a current model predicts. Journal of Biomechanics 31, 295-301.

Gentner, R., Classen, J., 2006. Modular organization of finger movements by the human central nervous system. Neuron 52, 731-742.

Gottlieb, G.L., 1998. Muscle activation patterns during two types of voluntary single-joint movement. Journal of Neurophysiology 80, 1860-1867.

Hughes, R.E., An, K.N., 1997. Monte Carlo simulation of a planar shoulder model.

Medical & Biological Engineering & Computing 35, 544-548.

Langenderfer, J.E., Carpenter, J.E., Johnson, M.E., An, K.N., Hughes, R.E., 2006. A probabilistic model of glenohumeral external rotation strength for healthy normals and rotator cuff tear cases. Annals of Biomedical Engineering 34, 465-476.

Lee, S.W., Chen, H., Towles, J.D., Kamper, D.G., 2008. Estimation of the effective static moment arms of the tendons in the index finger extensor mechanism. Journal of Biomechanics 41, 1567-1573.

Lee, S.W., Zhang, X., 2007. Biodynamic modeling, system identification, and variability of multi-finger movements. Journal of biomechanics 40, 3215-3222.

Li, Z.M., 2006. Functional degrees of freedom. Motor Control 10, 301-310.

Marconi, N.F., Almeida, G.L., Gottlieb, G.L., 2006. Electromyographic and kinetic strategies to control movements. Revista Brasileira de Fisioterapia 10, 1-8.

Nikanjam, M., Kursa, K., Lehman, S., Lattanza, L., Diao, E., Rempel, D., 2007. Finger flexor motor control patterns during active flexion: An in vivo tendon force study. Human Movement Science 26, 1-10.

Plamondon, R., 1995a. A kinematic theory of rapid human movements. Part I. Movement representation and generation. Biological Cybernetics 72, 295-307.

Plamondon, R., 1995b. A kinematic theory of rapid human movements. Part II. Movement time and control. Biological Cybernetics 72, 309-320.

Plamondon, R., 1998. A kinematic theory of rapid human movements: Part III. Kinetic outcomes. Biological Cybernetics 78, 133-145.

Plamondon, R., Alimi, A.M., Yergeau, P., Leclerc, F., 1993. Modelling velocity profiles of rapid movements: a comparative study. Biological Cybernetics 69, 119-128.

Plamondon, R., Feng, C., Woch, A., 2003. A kinematic theory of rapid human movement. Part IV: a formal mathematical proof and new insights. Biol Cybern 89, 126-138.

Valero-Cuevas, F.J., Anand, V.V., Saxena, A., Lipson, H., 2007. Beyond parameter estimation: Extending biomechanical modeling by the explicit exploration of model topology. Ieee Transactions on Biomedical Engineering 54, 1951-1964.

APPENDIX
A.1 Algorithm and logic diagram for estimating the control parameters
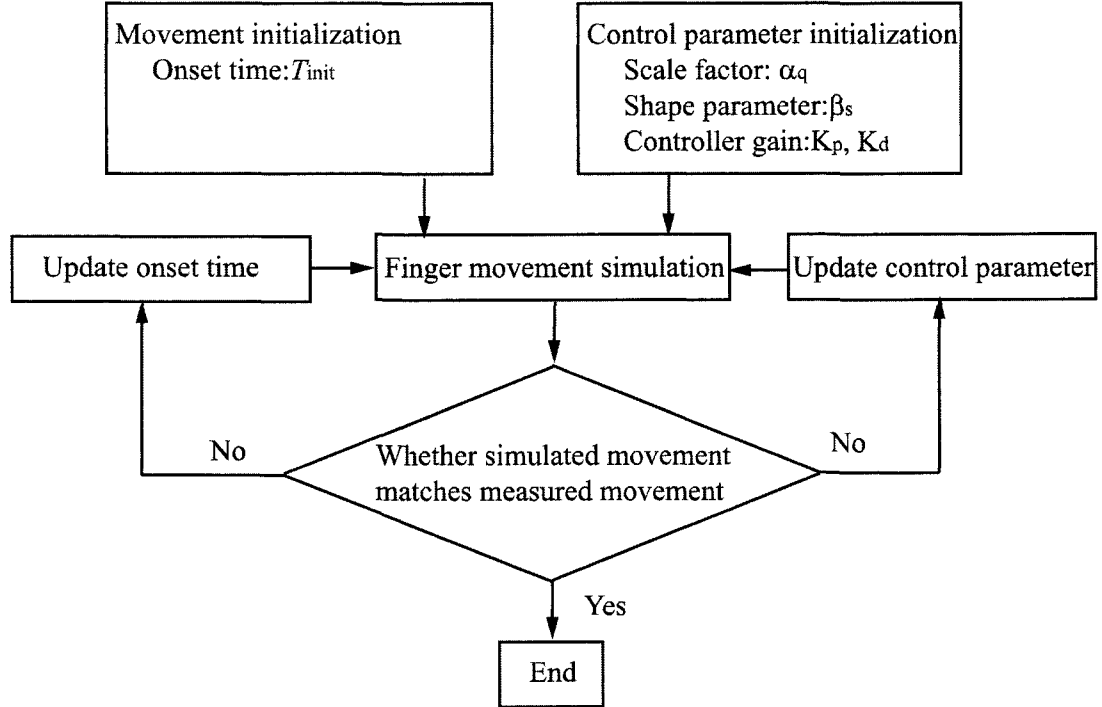
Figure A.1. A logic diagram of the search routine for estimating the parameters of the controller structure for a measured movement.

In Chapter I, we formulate an optimization problem to estimate the control parameters of the two-component torque actuator. This problem is essentially a simulation-based optimization problem (Kolda et al., 2003). It aims to find the time-independent values of $K^p_{flexor}, K^p_{extensor}$, K^d_{flexor}, $K^d_{extensor}$, α_q, and β_s so that the system (Equations 2.1-2.6) can replicate the given kinematics $\theta^*(t)$ and measurement-derived torque $\tau^*(t)$. To solve this problem, the first step is to determine the initial onset time of the movement. When the two-component torque actuator is used to generate the torque that drives the multi-linkage system to produce the movement, the generated joint torque starts from zero and increases gradually. However, the measured movement may not have zero starting joint torque due to noise or measurement errors. The inconsistent starting joint torque may cause a failure in replicating the measured kinematics or

85

kinetics in forward simulation. In this study, the initial onset time of the movement is estimated by finding a time point in the initial phase of the movement (before the torque reaches its peak) at which the joint torque and its first derivative are close to zero.

After determining the initial onset time of the movement, an iterative search routine is used to estimate these control parameters of the two-component torque actuator (Fig. A.1). Because of high dimensionality of the system model, the gradient and Hessian of the system are difficult to obtain or even to approximate, which may exclude the feasibility of using derivative-based methods in our study. We use the direct search (DS) (Torczon, 1997) method to solve this problem, which is able to find optimal solution not by computing derivatives but by evaluating function values. The major advantage of the DS method is that it is not movement-dependent and is easy to implement. It can be further generalized to the highly nonlinear and non-smooth constrained problems and other difficult optimization problems.

The method of implementing the DS follows a standard approach using the generalized pattern search (GPS) algorithm (Torczon, 1997) for bound constrained problems. The maximum iteration is selected to be 150. The parameter, *Complete poll*, is set to *on*, i.e. the algorithm polls all the mesh points at each iteration. The parameters, *tolerance on mesh size (TolMesh), tolerance on function (TolFun), tolerance on variable (TolX)*, and *tolerance on constraints (TolCon)*, are all set to be 1e-6. For all the trials, we use the same initial guess of control parameter, pre-determined by a trial-by-error process. The lower bounds of all the gains are selected to be 1e-6 and the upper bounds are 0.01. The lower bounds of α_q, and β_s are 1 and the upper bounds are 50.

In each iteration, we compare the generated movement with the measured movement. This search process continues until the L2-norm of the RMSE values of all the angular profiles becomes less than the threshold value (4°) or the solution does not exhibit any improvement. Then we check the normalized mean-square difference between measured and model-predicted torque profiles. If the differences of the torque profiles are large than 10%, we adjust the onset time of the movement and re-run the direct search method until the solution does not exhibit any improvement. Otherwise, the entire search process terminates.

A.2 Pseudo code for control parameter estimation and forward simulation

%===

% ParameterEstimationbyDS: Estimate the control parameters using the Direct Search

%   Input:

%   Anthropometric Variable: Segment Mass, Length and Inertia and Position of

%   Center of Mass

%   Measured Kinematics: Experimental Angle

%   Measured Derived Joint Torque: NetJointTorque

%   Output:

%   Controller gain: Kp_flexor,   Kp_extensor, Kd_flexor, Kd_exensor.

%   Distribution function parameter: alpha_q and beta_s

%===

function [Kp_flexor, Kp_extensor, Kd_flexor, Kd_exensor, alpha_q,

beta_s]=ParameterEstimationbyDS (NetJointTorque, ExperimentalAngle, SegmentMass,

SegmentInertia, SegmentLength, CenterofMassPosition)

Call GetInitialParameter   % Get the initial guess of the parameter

Call SetupOptimizationOption   % Set up the optimization parameters for the Direct

Search Method

Call DirectSearch   % Use the Direct Search method to get the control

parameter.

Return Kp_flexor, Kp_extensor, Kd_flexor, Kd_exensor, alpha_q, beta_s

%===

% SetupOptimizationOption   : Set up the optimization parameters for the DS method

%   Output: the optimization parameter

%===

% Here we will directly create the optimization parameter using the function

psoptimset % routine provided by Matlab.

% The typical code is shown as follows

% options

= %psoptimset('PlotFcns',{@psplotbestf,@psplotfuncount,@psplotmeshsize,@psplotbest

x%} , 'MaxIter',150, 'TolMesh',1e-6,'TolCon',1e-6, 'TolX', 1e-6,'TolFun',1e-6,

% 'CompletePoll', 'on', 'SearchMethod','GPSPositiveBasisNp1',

'MeshAccelerator', %'On','Cache', 'On', 'MeshRotate', 'On');

%==

% DirectSearch: Estimate the control parameter using DS

%   Input:

%   Objective function: objfun:

%   Measured Kinematics: Experimental Angle

%   Measured Derived Joint Torque:NetJointTorque

%   Lower Bound: LBX

%   Upper Bound: UBX

%   Optimization Parameter: optimizationoptions

%   Initial parameter: x0

%   Output:

%   estimated control parameter: x

%==

function [x]= DirectSearch ((@(x)objfun(x, ExperimentalAngle,NetJointTorque), x0,

LBX,UBX,optimizationoptions)

% Here we will directly apply the directresearch routine provided by Matlab to estimate

the parameter

% The typical code is shown as follows

%[x] = patternsearch(@(x)objfun(x, ExperimentalAngle,NetJointTorque),

%x0 ,[],[],[],[],LBX,UBX, optimizationoptions);

Return x

%==

% objfun: the objective function of the optimization problem

%   Input:

%   Control parameter: x, a set of parameters including Kp_flexor, Kp_extensor,

%   Kd_flexor, Kd_exensor, alpha_q, beta_s

%   Measured Kinematics: ExperimentalAngle

%   Measured Derived Joint Torque: NetJointTorque

%   Output:

```
%      RMSEvalue:   the norm of the RMSE values of all the angular profiles.   :
%      MSETorquevalue: the normalized mean-square difference between measured and
%                      model-predicted  torque profiles
%========================================================================
function [RMSEvalue, MSETorquevalue]= objfun(x, ExperimentalAngle,
NetJointTorque)
[SimulatedTorque, SimulatedAngle]=ForwardSimulation (Mass, Initial, Length,
CenterofMassPosition, x); % generate a forward simulation with the given control
parameter
% Compare the movement and calculate the difference between simulated and
measured % movement
RMSEValue= Integral (ExperimentalAngle- SimulatedAngle)/Movement time
MSETorquevalue = Integral (SimulatedTorque - NetJointTorque)/ Integral
(NetJointTorque)
%========================================================================
% ForwardSimulation: forward simulation of hand movement
%      Input:
%      Anthropometric Variable:   Segment Mass, Length and Inertia and Position of
%                                 Center of Mass
%      Controller gain: Kp_flexor, Kp_extensor, Kd_flexor, Kd_exensor.
%      Distribution function parameter: alpha_q and beta_s
%      Target task: the joint angle theta_end and velocity theta_dot_end at the ending
time
%      Output:
%      SimulatedAngle: the simulated kinematics.   :
%      SimulatedTorque: the simulated joint torque
%========================================================================
function [SimulatedTorque, SimulatedAngle]= ForwardSimulation (SegmentMass,
SegmentInertia, SegmentLength, CenterofMassPosition, x, theta_end, theta_dot_end );
OdeOptions = odeset( 'RelTol',1e-3, 'AbsTol', 1e-3, 'MaxStep',1/120.0 ); %optimization
parameter
```

```
Time =0;    % initial time
StopSimulation = 0;
StateDerivatives(Time,statevariables,0);
CurrentStatus=[];    % the current status
while 1,
    if( T_end>=0 & Time+0.1*1/120.0>=T_end ) StopSimulation = -1; end
    if(StopSimulation <= 0.01 ),
        CurrentStatus (i,:)=[ statevariables T1 T2 T3];
        if(StopSimulation == -1 ) break; end
        StopSimulation = 1;
    end
[TimeArray,StatevariableArray] = ode45(@StateDerivatives, [Time T+1/120.0],
statevariables, OdeOptions );
    T = TimeArray(length(size(TimeArray,1) ));;
    statevariables = StatevariableArray ( size(StatevariableArray ,1),: );
    StopSimulation = StopSimulation - 1;
end
SimulatedAngle = CurrentStatus (1:3);
SimulatedTorque= CurrentStatus (7:9);
%=========================================================
% StateDerivatives: Calculates the derivatives of the states
%    Input:
%       The current state variables:    statevariables
%    Output:
%       The state variables after one step: state.    :
%=========================================================
function state = StateDerivatives(Time, statevariables)
% Here we will solve the following equations of motion and compute the state variables
after one step based on the current state variables.
%   M(\theta(t))\ddot{\theta}(t) = V(\theta(t),\dot{\theta}(t)) + \tau(t)
Return state
```

90

A.3 References

Kolda, T.G., Lewis, R.M., Torczon, V., 2003. Optimization by direct search: New
perspectives on some classical and modern methods. Siam Review 45, 385-482.

Torczon, V., 1997. On the convergence of pattern search algorithms. Siam Journal on
Optimization 7, 1-25.

AUTHOR'S BIOGRAPHY

Kang Li was born on November 16, 1976 in Zhijiang, a small town in Hunan, China. He graduated from Tsinghua University in 1999 with a Bachelor of Science degree in Mechanical Engineering. In 2003, he went to Mississippi State, Mississippi, to pursue graduate study in Industrial Engineering. He completed a Master of Science in Industrial Engineering from Mississippi State University in December 2004.

In the fall of 2004, Kang relocated to Champaign, Illinois and enrolled in the Mechanical and Industrial Engineering at the University of Illinois at Urbana-Champaign, beginning his doctoral studies in the Ergonomics and Biomechanics fields under the guidance of Professor Xudong Zhang. Since Fall 2007, he has been a visiting student at the Orthopedic Research laboratories of the University of Pittsburgh. He has published two journal articles and completed five manuscripts that are currently in review. He has also presented at national and international conferences including the North American Congress on Biomechanics and the First International Conference on Digital Human Modeling where he chaired a session. Following the completion of his Ph.D., Kang plans to be a postdoctoral research associate at the University of Pittsburgh.